TRANSPORTATION RESEARCH RECORD 884

Piling 1982

TRANSPORTATION RESEARCH BOARD

NATIONAL RESEARCH COUNCIL

NATIONAL ACADEMY OF SCIENCES
WASHINGTON, D.C. 1982

Transportation Research Record 884
Price $8.60
Edited for TRB by Scott C. Herman

modes
1 highway transportation
3 rail transportation

subject area
63 soil and rock mechanics

Library of Congress Cataloging in Publication Data
National Research Council. Transportation Research Board.
Piling, 1982.

(Transportation research record; 884)
1. Piling (Civil engineering)–Addresses, essays, lectures. I. National Research Council (U.S.). Transportation Research Board. II. Series.
TE7.H5 no. 884 380.5s [624.1'54] 83-6254
[TA780]
ISBN 0-309-03471-X ISSN 0361-1981

Sponsorship of the Papers in This Transportation Research Record

GROUP 2–DESIGN AND CONSTRUCTION OF TRANSPORTATION FACILITIES
R.V. LeClerc, consultant, Olympia, Washington, chairman

Soil Mechanics Section
Lyndon H. Moore, New York State Department of Transportation, chairman

Committee on Foundations of Bridges and Other Structures
Bernard E. Butler, Reinforced Earth Company, chairman
Arnold Aronowitz, Michael Bozozuk, W. Dale Carney, Harry M. Coyle, Albert F. DiMillio, Bengt H. Fellenius, Frank M. Fuller, G.G. Goblè, Richard J. Goettle III, James S. Graham, Hal W. Hunt, Gay D. Jones, Jr., Philip Keene, Hugh S. Lacy, Clyde N. Laughter, Robert M. Leary, G.A. Leonards, Richard P. Long, Lyle K. Moulton, Michael Wayne O'Neill, Alex Rutka, Aleksandar S. Vesic, Harvey E. Wahls, John L. Walkinshaw, James Doyle Webb

John W. Guinnee, Transportation Research Board staff

The organizational units, officers, and members are as of December 31, 1981.

Contents

Authors of the Papers in This Record

Cochran, David, Materials and Testing Division, Nevada State Highway Department, 1263 S. Stewart Street, Carson City, NV 89710
Das, Braja M., Civil Engineering Department, University of Texas at El Paso, El Paso, TX 79968
Fellenius, Bengt H., Department of Civil Engineering, University of Ottawa, 735 Ludgate Court, Ottawa, Ontario, Canada K1J 8K8
Goble, G.G., Department of Civil, Environmental, and Architectural Engineering, University of Colorado, Boulder, CO 80309
Hawkins, Richard A., Raymond Technical Facilities, Inc., 5065 Westheimer, Houston, TX 77027
Jones, Andrew D., Civil Engineering Department, University of Texas at El Paso, El Paso, TX 79968
Keen, Philip, Soils and Foundations Engineer, 34 Home Avenue, Middletown, CT 06457
Laughter, Clyde N., Wisconsin Department of Transportation, 3502 Kinsman Boulevard, Madison, WI 53704
Loftus, William F., William F. Loftus Associates, Inc., 120 Charlotte Place, Englewood Cliffs, NJ 07632
Marcucci, Floyd, Bridge Design Division, Nevada State Highway Department, 1263 S. Stewart Street, Carson City, NV 89710
Merjan, Stanley, Underpinning & Foundation Constructors, Inc., 55-14 48th Street, Maspeth, NY 11378
Moore, Bruce H., Foundations and Materials Branch, U.S. Army Corps of Engineers, 210 Tucker Boulevard, St. Louis, MO 63101
O'Brien, Arthur J., CH2M Hill, 1500 114th Avenue, S.E., Bellevue, WA 98004
O'Neill, Michael W., Department of Civil Engineering, University of Houston, Houston, TX 77004
Pita, Frank W., CH2M Hill, 1500 114th Avenue, S.E., Bellevue, WA 98004
Whited, Gary C., Wisconsin Department of Transportation, 3502 Kinsman Boulevard, Madison, WI 53704
Wu, Ming-Jiun, Shannon & Wilson, Inc., 1105 North 38th Street, Seattle, WA 98103
Yamane, George, Shannon & Wilson, Inc., 1105 North 38th Street, Seattle, WA 98103

Pile-Head Behavior of Rigidly Capped Pile Group

MICHAEL W. O'NEILL AND RICHARD A. HAWKINS

The results of a series of vertical load tests on a full-scale group of nine rigidly capped piles and two control piles driven into stiff, saturated clay are described. The scope of the paper is limited primarily to a description of the performance of the piles at their heads; that is, load-settlement and load-distribution behavior and apparent mode of failure. Results from the study that are of practical engineering significance, including group efficiency, settlement ratio, and distribution of loads among the piles, are described, followed by a discussion of test procedures and magnitudes of inherent test errors.

It is generally understood that installing several piles in close proximity to one another alters the stress state and fabric of the supporting soil in a manner different from that produced by installing a single pile, where its synthesized or measured load-settlement response often forms the basis for prediction of foundation performance. Stress overlaps that result from loading the group of piles (mechanical interaction) further tends to produce differences in group and single pile behavior.

Model tests have been used extensively in the past to investigate the relative effects of spacing, penetration, soil properties, and other parameters on the behavior of pile groups. However, physical models fail to replicate effective stress states in the soil that impact on efficiency, settlement, and distribution of load among piles. Full-scale testing eliminates this problem, but the obvious expense of full-scale tests makes them a generally impractical means of conducting parameter studies. Therefore, it is important that maximum use be made of the limited body of full-scale data that does exist. This paper is presented for the purpose of adding to these data.

In the past, full-scale tests have been employed on a limited basis to investigate the effects on group performance of sand density and pile spacing (1), disturbance of sensitive clays (2), pile spacing and group size in soft clays (3,4), combined loads (5), and other phenomena. A recent study sponsored by the Federal Highway Administration (FHWA) (6) undertook the investigation of the behavior of a vertically loaded full-scale group of nominally vertical piles in stiff, insensitive, strain-softening, overconsolidated clay in southeastern Houston, Texas, that contained zones of slickensides, fissures, and sand partings. This paper describes the overall results of load tests on a nine-pile (3x3x3-diameter spacing) group. The test piles were 264-mm (10.75-in) outside diameter by 9.27-mm (0.365-in) wall thickness steel pipes, which were all instrumented and driven closed-ended to a depth of 13.1 m (43 ft) with flush boot plates. Subgroups of five (center and middle edge) and four (middle edge only) piles within the main group (6) were also tested after testing the main group. The piles were connected by a rigid cap suspended off the soil.

Three sets of tests were conducted to failure on the nine-pile group at 20, 82, and 110 days after the piles were driven. These tests were preceded (four or five days) by tests on two single control piles near the test group, which served as references for assessing group efficiency and settlement ratio. Details of the soil profile and testing procedures will be found later in the paper.

LOAD-SETTLEMENT BEHAVIOR: CONTROL PILES AND NINE-PILE GROUP

Load tests were first conducted on the two control piles (piles 1 and 11) 15 days after they were driven. These piles exhibited similar apparent load-settlement behavior, both at the butts and the tips, as shown in Figure 1, except that pile 11 failed suddenly at a lower load than pile 1. The term "apparent" refers to the fact that the tip loads were assumed to be zero prior to loading for purposes of plotting Figure 1. The piles were largely, but not exclusively, friction piles, and sudden plunging occurred after near-linear response.

All of the test piles in the study were driven in 200-mm (8-in) diameter pilot holes 3.1 m (10 ft) deep to assist in maintaining alignment. The pilot hole for pile 1 was dry at the time of driving, while that for pile 11 was partly filled with water. Piezometers on pile 1 indicated that essentially all excess pore-water pressure generated by driving had dissipated by the time of the first load test. Pile 11 had no piezometers, but it is speculated that its low capacity may have been due to undissipated pore pressures associated with driving the pile in a wet hole. Three piles of the main group were also driven in wet holes, so that the average performance of the two control piles is believed to be an appropriate reference for assessing group efficiency and settlement ratio.

By the second test, pile 11 had developed a capacity nearly equal to that of pile 1, which had also developed a slightly higher capacity. The apparent setup between tests 1 and 2 for pile 1 was due almost entirely to an increased tip capacity brought about by the effects of load cycling and of residual tip loads remaining after removal of the earlier test load. Freeze (increased shaft capacity due to pore-pressure dissipation) apparently occurred in the time interval between tests 1 and 2 in pile 11. No further freeze occurred, however, as revealed by uplift testing conducted after completion of compression testing (6).

The strain-softening nature of the soil (relaxation of load during plunging) is evident in Figure 1, as loads, which were reduced after each pile, were pushed beyond the settlement at which peak resistance occurred.

The pile numbering scheme and alignments for the piles in the nine-pile group are shown in Figure 2. (The pile tops were located at the top of the cap.)

Load-settlement behavior of the group during the first load test is shown in Figure 3. This figure does not include the dead weight of the pile cap [254 kN (57 kips)] that was supported by the piles prior to the test. It is observed from Figure 3 that

1. Load-settlement curves based on data taken 5, 30, and 55 min after application of a load increment are essentially linear and coincident to approximately 75 percent of the maximum load, which indicates very low creep rates at working load levels;
2. Settlement across the pile cap was essentially uniform up to about 60 percent of the maximum load, whereafter considerable tilting occurred; and
3. The load-settlement curve, unlike the curves for the control piles, plunged without relaxing.

Item 2 is further illustrated by Figure 4, which shows the measured attitude of the cap at the maximum load as measured by triaxial dial gages mounted at the lower corners of the cap. These instruments confirmed rigid cap behavior. The cap pitched toward the north as the articulated beams used as a

jacking reaction for the test translated slightly in that direction during the course of the test. The northeastward batter of piles 8 and 9 also caused a clockwise yaw to develop. The pitching was magnified by the fact that pile 8, which by virtue of its position in the laterally translating group and its slight batter attracting more than the average pile load, failed one load increment before the other piles failed.

Figure 1. Butt and tip load-settlement curves for control piles (test 1).

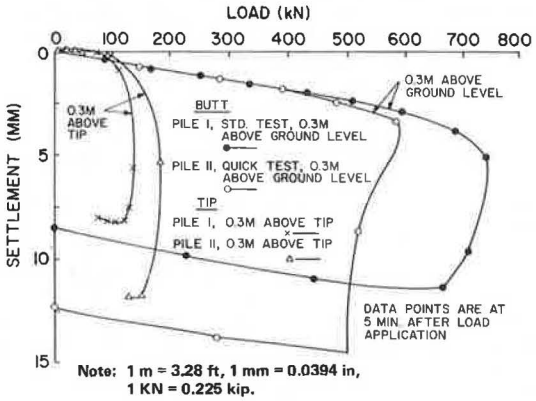

Note: 1 m = 3.28 ft, 1 mm = 0.0394 in, 1 KN = 0.225 kip.

Figure 2. Pile numbering and alignment.

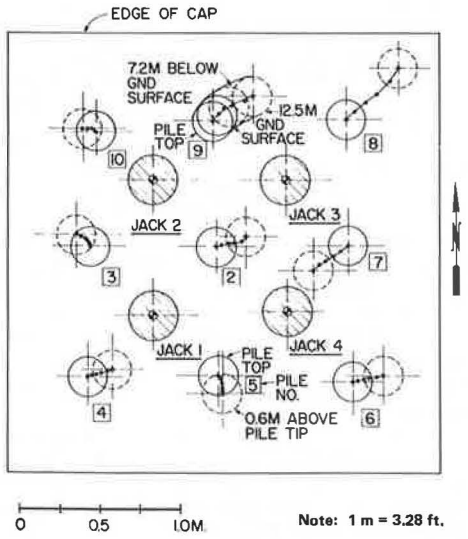

Note: 1 m = 3.28 ft.

Figure 3. Load-settlement relations for nine-pile group (test 1).

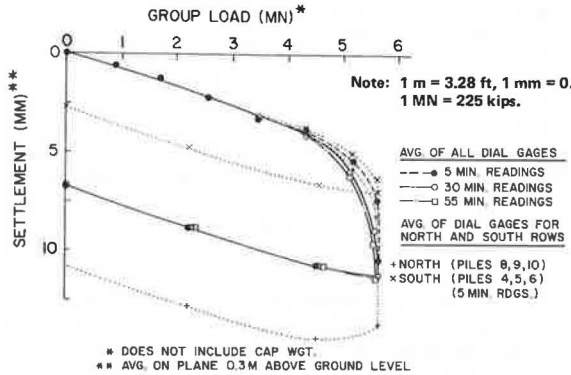

Note: 1 m = 3.28 ft, 1 mm = 0.0394 in, 1 MN = 225 kips.

Item 3 can be explained qualitatively by considering the load-settlement curves of the individual piles in the group; typical curves are shown in Figure 5. First, all of the group piles had about the same distribution of side and end loads at failure as the control piles and, like the control piles, failed by plunging. No block action was observed (6). Second, because of the rotation of the cap, the piles on the north row plunged prior to those on the center or south rows. The north row piles then relaxed as the remaining piles continued to attract load; the net effect was that the overall group load-settlement curve became vertical. Piles 4 and 5 did not plunge during this test. Loading was stopped before those piles plunged because the group itself had plunged and because flexural stresses at the pile heads had reached allowable values. These observations are of practical significance because group failure in a strain-softening soil appears to be associated with the load at which the first pile fails and hence with both the symmetry of the piles in the system and the concentricity of the applied load.

Figure 4. Displacement of cap at maximum load (nine-pile group, test 1).

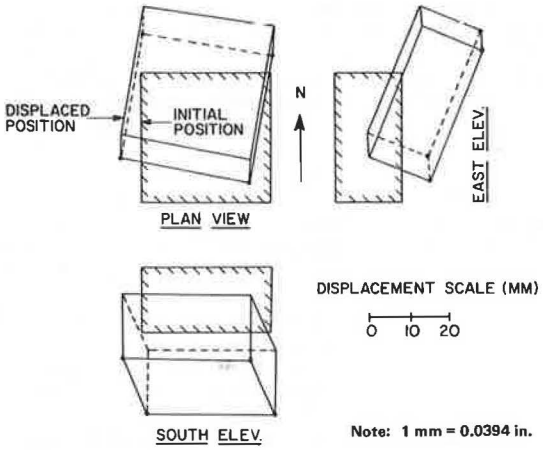

Note: 1 mm = 0.0394 in.

Figure 5. Load-settlement curves for north row of piles.

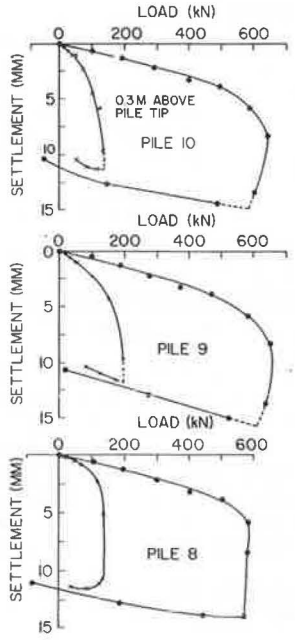

Note: 1 m = 3.28 ft, 1 mm = 0.0394 in, 1 KN = 0.225 kip.

A more fundamental representation of failure can be seen in Figure 6, in which failed zones along each pile are shown by vertical bars at various loads. In addition to the early failure of pile 8, Figure 6 also shows the manner in which failure (development of peak side load transfer) began and progressed along each of the piles. Progression of failure downward from the surface began at load 5 (83 percent of maximum group load) in most piles, and failure progressing upward from the tips began at loads 6 or 7 (92 or 99 percent of maximum group load). Downward-progressing failure is due to the flexibility of the piles relative to the soil, which causes maximum load transfer to be achieved at the pile tops first. Upward-progressing failure is produced by a shear stress concentration at the pile tips, followed by relaxation of that shear stress as further movement occurs. It is our hypothesis that the point of onset of upward-progressing failure in the first pile (pile 8) marks the limit of the load that could be sustained indefinitely by the group without plunging failure in the strain-softening soil. This load (load 6) is 92 percent of the short-term plunging capacity for this test. Side failure patterns in the control piles were similar to those shown in Figure 6.

The group appeared to gain capacity between tests. This phenomenon, which was also observed for the control piles, was primarily due to increased tip capacity produced by cycling the tip load and not to side resistance setup, as demonstrated by pore-pressure measurements and by tension tests conducted after the compression test (6). Essentially all excess pore-water pressures produced by installation had been dissipated against group piles 2, 3, 4, and 5 (those instrumented for this effect) and in the soil mass around those piles prior to test 1, and load testing produced insignificant pore pressures both in the soil and at the pile and soil interfaces.

INTERPRETATION OF FAILURE

At this point it is appropriate to address the subject of interpreting failure in tests on groups of piles. Several methods of assessing failure loads are illustrated in Figure 7. Curve 1 represents a group that plunges, the vertical tangent to which is the plunging load (P). This load may be an appropriate definition of failure in soils of the type described here if sufficient load can be applied in a test to affect plunging. Curve 2 represents the type of failure that might be expected for piles in granular soils. Plunging is not achieved, but a point is reached on the gross load-settlement curve beyond which a terminally linear branch is observed. This point (TL) can be interpreted as failure in such soils (1).

A rational method that is suggested if neither plunging nor terminal linearity is achieved is construction leading to the group offset (GO) load shown in the upper part of Figure 7. This construction is similar to that suggested for single piles by Davisson (7) but includes a tacit postulation that settlement of pile tips in a group is equal to the square root of the ratio of the width of the group to the width of a single pile times the tip settlement for a single pile. In Figure 7, $\zeta = 0.6$ for a friction pile group and 1.0 for an end-bearing group. The latter term is not a part of the original method proposed by Davisson. Failure of groups may also be defined by traditional methods, such as the point at which 13-mm (0.50-in) net settlement (NS) is realized (curve 3), since group settlements in excess of the settlement of a single pile under the same average load may be largely elastic.

The plunging and group offset loads are identical for this test, and they represent the short-term capacity of the group. Because plunging followed by relaxation occurred, the terminal-linearity method is inappropriate for this test. Load was not cycled, so the net settlement failure load was not obtained. By the former criteria (taking into account the cap weight), the efficiency of the group was 0.98.

An additional method that may be of use in groups of the type tested, in which progressive failure occurs both along and among piles in the group, is to define failure as the load at the accelerated creep point (C) shown in Figure 8, which was proposed by Housel (8) for single piles. Creep settlement (settlement in the last half of each load increment) versus load for test 1 on the nine-pile group is shown in Figure 8. The accelerated creep point falls at 92 percent of the plunging load, which (from Figure 6) is the load at which upward-progressive failure began.

Figure 6. Progressive failure in individual piles (nine-pile group, test 1).

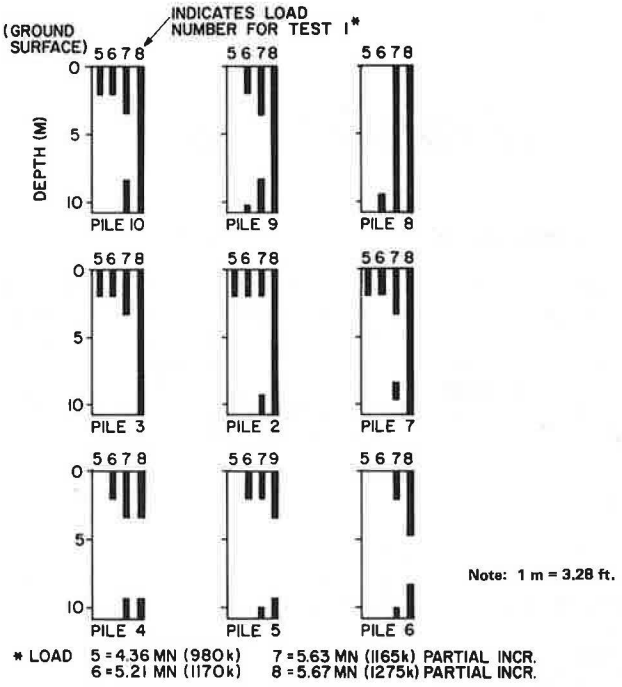

Figure 7. Methods of interpreting group failure.

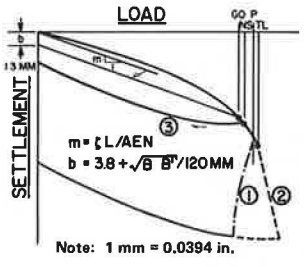

L = Pile length
A = Pile cross sectional area
E = Pile modulus of elasticity
N = No. of Piles in group
B = Diameter of piletips
B' = Width of group
ζ = Side resistance factor

Figure 8. Failure load of nine-pile group (test 1) by creep method.

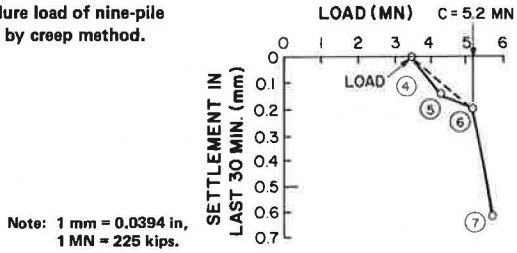

Figure 9. Load-settlement curves for subgroup tests.

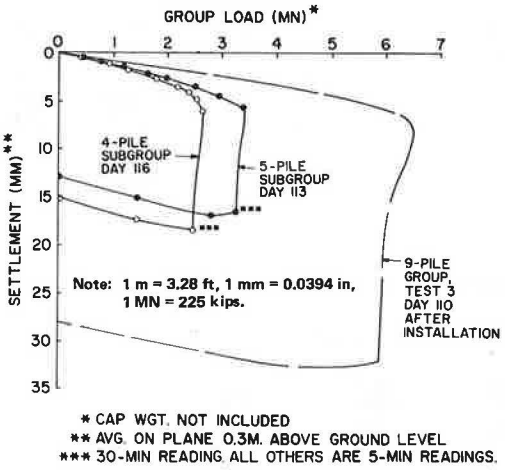

LOAD-SETTLEMENT BEHAVIOR: SUBGROUPS

Immediately following the third load test on the nine-pile group, the subgroup tests were conducted. The load-settlement curves for the final nine-pile test and the two subgroup tests are shown in Figure 9. The average capacity per pile varied little among the various tests, which is evidence that the failure mode was by plunging of individual piles in all tests.

SETTLEMENT RATIOS

The ratios of settlement of the pile group to average settlement of the control piles at a common average load per pile are shown in Figure 10. Figure 10 also shows settlement ratios for these groups, as computed by methods proposed by Poulos and Davis (9) [halfspace and rigid boundary at the top of a layer of very dense silt 20.5 m (67 ft) below grade] and by Banerjee and Davies (10) for a Gibson soil (zero modulus at the surface increasing linearly with depth). These methods all overpredict the settlement ratio; the Gibson soil and rigid boundary models yield results closest to those measured. The differences in computed and observed settlement ratios are believed to be due to the inability of the mathematical models to consider the stiffening effect of the piles on the soil and, to a lesser extent, to errors associated with settlement measurements, which will be described later.

DISTRIBUTION OF LOADS TO PILES

Figure 11 shows the distribution of axial loads to the pile heads and the deflections of the piles at two values of applied load for the first nine-pile test. The pattern of relative load among piles at the subfailure load is basically as predicted by

Figure 10. Settlement ratios.

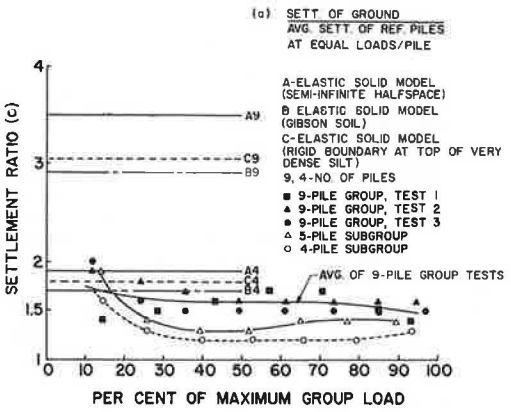

Figure 11. Distribution of loads to piles.

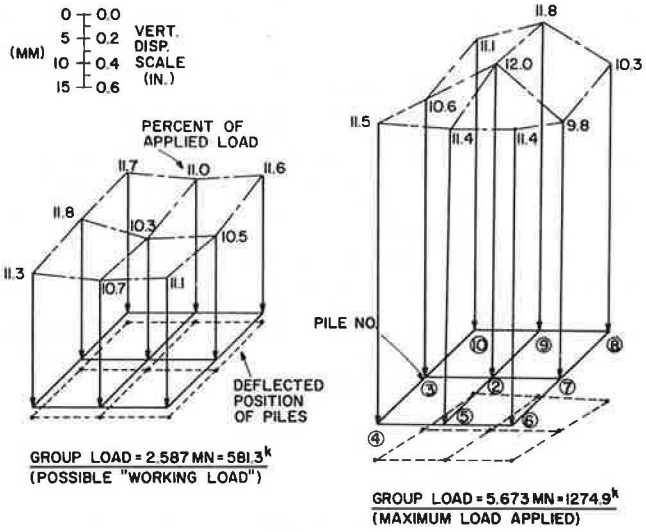

elastic theory (9,10): highest loads at the corners, next highest at the middle edge piles, and lowest at the center pile. However, the measured variation in load magnitude is much lower than predicted by such solutions. The pattern at the failure load is apparently reversed, but these load values do not necessarily represent failure loads for each pile, since the piles failed progressively (not simultaneously) and relaxed thereafter. Similar observations were made in the subgroup tests.

SOIL PROFILE AND TEST ARRANGEMENT

A section that shows the main pile group, soil properties, and reaction system is depicted in Figure 12. The soil properties listed are average undrained shear strength from UU triaxial compression tests (s_{uu}), average Young's modulus from a self-boring pressuremeter (E_{PM}), and Atterberg limits. Average standard penetration test values for the various layers (N_{AV}) are also tabulated. The soil had been overconsolidated by desiccation in the geologic past and then reinundated. The overconsolidation ratio ranged from about 7 at a depth of 5 m (16 ft) to about 4 at a depth of 15 m (48 ft).

Within the context of group action, the most significant soil properties are believed to be (a) increasing elastic stiffness with depth; (b) the presence of a secondary structure network in the strata

Figure 12. East-west section of test group, reaction system, and soil.

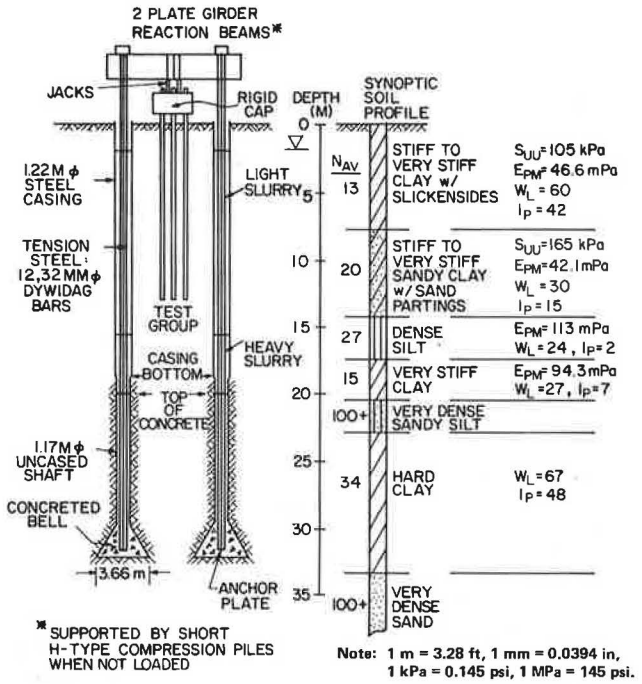

where the test piles were placed, thereby allowing rapid pore-pressure dissipation; and (c) soil insensitivity. The first property influenced settlement ratios, and the last two influenced efficiencies.

The cap that connected the group piles was a rigid concrete block 1.30 m (4.25 ft) thick and 2.75 m (9 ft) square in plan and was suspended 0.92 m (3.0 ft) off the ground. The test piles were instrumented at their tops for measurement of axial load and deflection with precalibrated strain-gage circuits and dial gages, respectively. The dial gages were suspended from steel reference beams supported on shallow piles 6.1 m (20 ft) from the center of the cap in a direction perpendicular to the section shown in Figure 12. In order to minimize thermally induced movements of the reference system, the test piles were covered by an opaque shroud. Independent measurements of cap deformations in three dimensions were made with 12 dial gages suspended from the reference beams and mounted in three orthogonal directions at the four lower corners of the cap and by microhead survey techniques that use a benchmark outside the zone of influence of the piles and the reaction anchor system.

The pile group was loaded by four hydraulic jacks (Figure 2) acting through load cells and reacting against a plate girder system that was anchored by two deep concrete caissons, each situated laterally approximately 3.66 m (12 ft) from the center of the group. The caissons consisted of 3.66-m-diameter bells and 1.17-m (3.83-ft) diameter shafts of concrete. The concrete was terminated 20 m (66 ft) below grade to restrict stresses produced by the anchor caissons in the zone of soil below the pile tips. The anchor holes were cased above that depth, except for a small gap that was provided to prevent the concrete from engaging the casings and producing shear stresses around the casings.

The caissons were connected to the reaction beams by means of tension bars placed through tubes in the concrete to prevent bonding and anchored at the bases of the bells to introduce load at the bottoms of the anchors. This detail further served to restrict anchor system stresses in the soil around the test group.

The jacks were positioned so their centroid was as near the anticipated center of reaction from the piles as possible, and the reaction beams were set over the jacks for the first load test. This caused the anchor bars to be slightly out of plumb (possibly due to minor misplacements of the anchor plates in the bells), so that when the group was loaded, the reaction beams tended to translate to the north, as described earlier.

The control piles were located about 4 m (13 ft) on either side (north and south) of the main group and were each loaded with single hydraulic jacks reacting against beams anchored by a system of four H-piles embedded 7.6 m (25 ft); each was situated 3.5 m (11.5 ft) symmetrically from the test pile. Settlements were measured, as with the group, by using the group reference system.

TESTING PROTOCOL

The testing program consisted of the following tests:

1. Simultaneous load tests of the two control piles 15 days after installation. Pile 1 was loaded by using the standard procedure described below. Pile 11 was loaded in increments of about 130 kN (29 kips) every 2.5 min until failure was achieved and then unloaded in two decrements.
2. Test of the nine-pile group 20 days after installation by using the standard procedure.
3. Simultaneous load tests of the two control piles 78 days after installation, followed in 4 days with a second test on the nine-pile group. Standard loading procedures were used in this and the following steps.
4. Repeat of 3 above at 105 and 110 days, respectively.
5. Test of the five piles, which consist of piles 2, 4, 6, 8, and 10 of the original group, after detaching the heads of the other piles from the cap, at 113 days after installation.
6. Test of the four piles, which consist of piles 4, 6, 8, and 10, after detaching pile 2 at 116 days after installation.

The standard procedure for loading consisted of the application of increments of about 12 percent of the anticipated failure load every hour until failure occurred, followed by a 1-h hold, followed by unloading in three decrements. Instruments were read at 5, 30, and 55 min after application of the load increment. All electronic strain-gage circuits and load cells were read and processed into engineering units in real time by a microcomputer data-acquisition system that was capable of scanning all circuits, including 99 circuits in the piles, in about 60 s. All dial gages and survey instruments were read manually.

SETTLEMENT ERROR ANALYSIS

The two primary sources of error in the measurement of settlement were thermally induced strains in the reference system and displacements of the test piles and reference beam supports produced by loading the anchors and the piles. The first problem was studied experimentally (6, Appendix E), and it was determined that the maximum displacement error excursion during the approximately 12-h period of a test was 0.13 mm (0.005 in). The use of the shroud over the test piles and the restriction of testing to low-temperature-differential overcast days helped to minimize this effect.

The effects of anchor and pile loads were ad-

Table 1. Summary of test results.

Test[a]	Failure Mode[b]	Plunging Load[c] (MN)	Efficiency			Settlement Ratio
			Shaft[d]	Tip[d]	Overall	
Control 1 (15 days)	P	0.747				
Control 11 (15 days)	P	0.591				
Nine pile (20 days)	PI	5.92	0.98	≈1.04	0.99	1.62
Control 1 (78 days)	P	0.831				
Control 11 (78 days)	P	0.756				
Nine pile (82 days)	PI	6.80	0.99	1.33	0.98	1.54
Control 1 (105 days)	P	0.787				
Control 11 (105 days)	P	0.804				
Nine pile (110 days)	PI	6.85	0.90	1.40	0.96	1.48
Five pile (113 days)	PI	3.70	0.89	1.15	0.93	1.31
Four pile (116 days)	PI	2.94	0.94	0.81	0.92	1.19

Note: 1 MN = 225 kips.
[a] After driving.
[b] P = plunging and PI = plunging of individual piles in groups (no block failure).
[c] Includes weight of cap and loading accessories.
[d] Apparent.

dressed analytically and experimentally (6, Appendix E). Four separate phenomena were considered analytically:

1. Upward movement of the pile tips (assumed equal to the movement of the pile tops) due to soil stresses produced by the group anchor reactions,
2. Upward movement of the reference beam supports [5-m (16.4-ft) deep H-piles 6.1 m (20 ft) north and south of the center of the test group] due to group anchor reactions,
3. Upward movement of the reference beam supports due to soil strains induced by H-pile anchors during the control pile tests, and
4. Downward movement of the reference anchors due to loads from the test piles themselves.

The first three phenomena were approached by using Mindlin's equation for the case of upward-directed point loads in a semi-infinite elastic mass (11). The mean depth of load transfer in the group anchors was assumed to be at 27.5 m (90 ft) below grade, the elastic modulus of the elastic mass (soil) was taken to be 103 MPa (15 000 psi) based on deep-seated pressuremeter test results, and the soil was assumed to be incompressible. Similar conditions were assumed for phenomenon 3, except that the mean depth of load transfer was assumed to be 4.6 m (15 ft) below grade in the H-pile anchors. The net effect of phenomena 1 and 2 yielded theoretical settlements of the piles with respect to the reference beams in the nine-pile group that were 6 percent low at one-half of the group plunging load.

Phenomenon 4 was approached by first computing the downward movement of the small piles that supported the reference beams by employing the elastic solid model proposed by Poulos and Davis (9), which uses the soil properties described above. (The same model was also used to compute the downward movements of the unloaded piles during the subgroup tests, which were measured relative to the displacements of the loaded piles.) The computed reference beam support settlements were then multiplied by the ratio of the observed to computed settlements of the unloaded piles to arrive at a corrected reference beam support settlement for both the group and control pile tests. This correction was considered necessary because the model that was used overpredicted the relative settlements of the unloaded piles in the subgroup tests.

The addition of the effect of phenomenon 4 to phenomena 1 and 2 for the group yielded a net error of 19 percent in settlement measurement in the nine-pile group (on the low side) at one-half of the maximum group load. Independent survey measurements made on the pile cap indicated an error of 9 percent on the low side with a statistical probable error of ±25 percent in the survey data. (The low quality of the survey data is associated with rainy weather conditions during the group load tests.)

The addition of phenomena 3 and 4 for the control pile tests resulted in essentially zero error for those piles. Therefore, it appears that the settlement ratios in the nine-pile group tests may actually be as much as about 20 percent higher than reported, with lesser errors for the subgroup tests.

CONCLUSIONS

Table 1 summarizes the test results in terms relevant to the designer, i.e., efficiencies and settlement ratios, the latter at one-half of the average plunging load for the control piles in a given test. Shaft and tip efficiencies for all tests are also given. Note that overall efficiencies are not weighted averages of shaft and tip efficiencies, since shaft and tip failure was not simultaneous.

The following observations are made:

1. The efficiencies of the group and subgroups were essentially 1.0. The most significant reasons for this fact are that the piles failed as individual piles (no block failure occurred) and that the soil was insensitive and contained a secondary structure network that allowed dissipation of excess pore pressures within a few days after the group piles were driven.
2. The settlement ratios were lower than those predicted by elastic theory, possibly because of the effect of pile reinforcement on the soil.
3. The distribution of load was generally uniform among the piles, although at about one-half of the maximum load interior piles carried slightly less load than the corner piles.
4. Failure was progressive. This fact suggests that long-term group capacity under concentric or eccentric loading can be evaluated from short-term tests by using the creep failure method suggested in Figure 7.

ACKNOWLEDGMENT

The study described in this paper was sponsored by the Office of Research, FHWA, U.S. Department of Transportation. Their support, and the assistance provided by Carl D. Ealy, FHWA contract manager for this project, is gratefully acknowledged.

REFERENCES

1. A.S. Vesić. Experiments with Instrumented Pile Groups in Sand. In Performance of Deep Founda-

tions, ASTM, Special Tech. Publ. 444, 1969, pp. 177-222.
2. Y. Koizumi and K. Ito. Field Tests with Regard to Pile Driving and Bearing Capacity of Piled Foundations. Soil and Foundation, Vol. 7, No. 3, Aug. 1967, pp. 30-53.
3. E.W. Brand, C. Muktabhant, and A. Taechthummarak. Load Tests on Small Foundations in Soft Clay. Proc., ASCE Specialty Conference on Performance of Earth and Earth-Supported Structures, Vol. 1, Part 2, 1972, pp. 903-928.
4. F.M. Masters. Timber Friction Pile Foundations. Trans., ASCE, Vol. 108, 1943, pp. 115-140.
5. J.B. Kim and R.J. Brungraber. Full-Scale Lateral Load Tests of Pile Groups. Journal of the Geotechnical Engineering Division, ASCE, Vol. 102, No. GT1, Jan. 1976, pp. 87-105.
6. M.W. O'Neill, R.A. Hawkins, and L.J. Mahar. Field Study of Pile Group Action, Final Report. FHWA, Rept. FHWA/RD-81/002, March 1981.
7. B.H. Fellenius. Test Loading of Piles and New Proof Testing Procedure. Journal of the Geotechnical Engineering Division, ASCE, Vol. 101, No. GT9, Sept. 1975, pp. 855-869.
8. W.S. Housel. Pile Load Capacity: Estimates and Test Results. Journal of the Soil Mechanics and Foundations Division, ASCE, Vol. 92, No. SM4, July 1966, pp. 1-30.
9. H.G. Poulos and E.H. Davis. Pile Foundation Analysis and Design. Wiley, New York, 1980.
10. P.K. Banerjee and T.G. Davies. Analysis of Pile Groups Embedded in Gibson Soil. Proc., Ninth International Conference on Soil Mechanics and Foundation Engineering, Tokyo, Vol. 1, 1977, pp. 381-386.
11. H.G. Poulos and E.H. Davis. Elastic Solutions for Soil and Rock Mechanics. Wiley, New York, 1974.

Pile Foundation—From Preliminary Borings to Production Driving

GARY C. WHITED AND CLYDE N. LAUGHTER

Foundation design for a major bridge structure requires extensive field and office investigation. The design process undertaken for the Arrowhead Bridge, which carries US-2 between Superior, Wisconsin, and Duluth, Minnesota, over the St. Louis Bay, is presented. Subsurface investigation results, geologic studies, pile load tests, wave-equation analysis, and dynamic pile testing are presented. Results of the geotechnical investigations allowed the use of high-capacity piles in soil for the bridge foundation. Subsurface conditions consisted of soft lacustrine and glacial clay deposits over dense glacial outwash sands. Depths to the underlying dense strata ranged from 130 to 260 ft (39.6-79.2 m) across the site. Six load tests were performed on steel H-piles and cast-in-place type piles. Maximum loads of 344 tons-force (3060 kN) were applied by using both maintained-load (ML) and constant-rate-of-penetration (CRP) methods. Load test results are presented by using five interpretative techniques, and comparisons between ML and CRP methods are shown. Wave-equation analyses were performed by using the WEAP computer program, and results are compared with driving records. Dynamic pile analysis was done by using the Goble-Case Western pile driving analyzer (PDA), and pile capacity predictions are compared with load test results. The PDA was also used on production piling, and experiences while analyzing the very long piles for capacity and damage are discussed.

The design of a foundation for a major bridge project requires a progression through various stages of literature review, field investigations, and office interpretation and evaluation. This paper presents details of the design process and resulting construction experience for the Arrowhead Bridge in Superior, Wisconsin.

The new Arrowhead Bridge is to be some 8400 ft (2.56 km) in length and will carry US-2 between Superior, Wisconsin, and Duluth, Minnesota. Located at the western tip of Lake Superior, the new high-level structure will span St. Louis Bay, the harbor shipping channel, a number of railroad tracks, and Interstate 35 in Duluth. The curved and skewed alignment, as shown in Figure 1, was necessary to provide navigational clearances for a harbor bend down channel yet meet desired connection points in Superior and Duluth. The bridge will provide a horizontal clearance of 500 ft (152.4 m) and a vertical clearance of 120 ft (36.6 m) at the channel.

The geotechnical investigation consisted of a literature review, three separate and progressive phases of subsurface investigation, and a pile load test program. The final foundation design was determined from results of these investigations, and construction was started. Foundation work on three of the four substructure contracts is essentially complete; so far, no major problems have developed.

SITE CONDITIONS

The foundation investigation for the structure began

Figure 1. Soil profile.

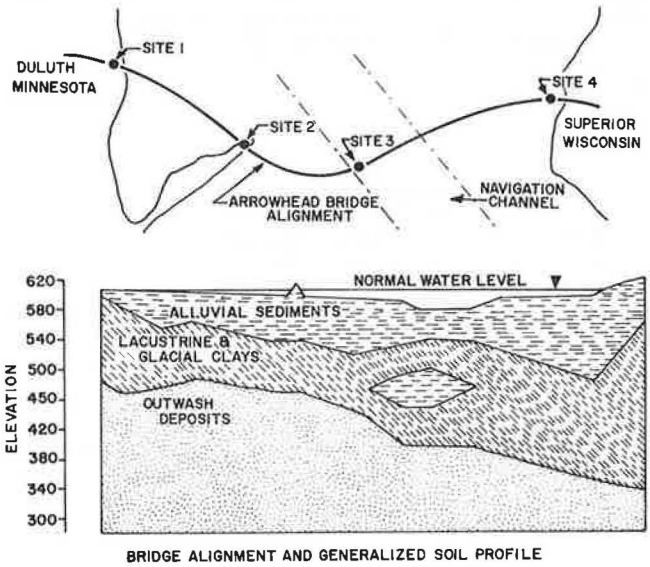

BRIDGE ALIGNMENT AND GENERALIZED SOIL PROFILE

in 1973 with an office review of available U.S. Geologic Survey reports, geologic maps, and well-drilling logs in the area. At the same time, a preliminary subsurface exploration program was initiated, which included making eight widely spaced borings along the proposed alignment. Results of these early investigations indicated a rather complex geologic section, involving alluvial stream deposits, lacustrine clays, glacial drift clays, and glacial outwash deposits. Bedrock was estimated to be at depths in excess of 600 ft (183 m) in what was assumed to be a preglacial bedrock valley of the St. Louis River. Water depths across the bay were generally less than 5 ft (1.5 m); depths in excess of 25 ft (7.6 m) were found in the channel area. A generalized stratigraphic section along the bridge alignment is shown in Figure 1.

The upper alluvial deposits were quite variable and consisted of very loose sands, silts, and often organics. Standard penetration test (SPT) N-values for these materials were generally less than 10. The lacustrine and glacial clays were classified as being soft to stiff; pocket penetrometer values ranged from 0.5 to 2.5 tons force/ft^2 (47.9-239.4 kN/m^2), and SPT N-values varied from 5 to 15. The underlying glacial outwash deposits were very dense silty sands; SPT N-values ranged from 50 to more than 100 for 6-in (15.2-cm) penetration. Depths to this dense foundation layer ranged from 130 ft (39.6 m) on the Minnesota side to 260 ft (79.2 m) on the Wisconsin side.

Based on the results of these preliminary investigations, it was apparent that a deep foundation would be required. The logical foundation choice was piling, based on experience of the local contractors and the type of bridge being proposed. A predesign pile load test program was initiated in 1977 to determine the most economical pile type, maximum pile load-carrying capabilities, probable tip elevations, and pile-driving characteristics (1). Four test locations were selected, as shown in Figure 1, and additional borings were made at each site to determine the soil conditions.

Two pile types were chosen for evaluation: a 16-in (406.4-mm) diameter concrete-filled cast-in-place pipe pile driven closed-end and a HP 14x73 (355.6-mm x 108.6-kg/m) steel H-pile. Selection of these two pile types for testing was based on anticipated loads, Wisconsin Department of Transportation's (DOT) past experience, and the experience of the local contractors. One H-pile was to be tested at each of the four sites; a cast-in-place (CIP) pile was to be tested at sites 1, 2, and 4. Piles were to be driven to minimum bearing of 172 tons-force (1530 kN) as determined by the Wisconsin (modified EN) driving formula (2):

$$P = 2WH/(S + 0.2) \quad (1)$$

where

P = bearing values (lb),
W = ram weight (lb),
H = height of ram fall (ft), and
S = penetration per blow (in).

Piles were also to be monitored during driving with the Goble-Case Western pile-driving analyzer (PDA).

PILE LOAD TEST

Contracts for the pile load test program were awarded to Johnson Bros. Corporation of Litchfield, Minnesota. (Johnson Bros. later became the major contractor for substructure construction.) All test pilings were driven with a Menck MRBS-500 single-acting air-steam hammer with an energy rating of 46 500 ft-lbf (63.0 kJ), which obtained the desired bearing when reaching the dense silty sand outwash deposits. Pilings were driven continuously with the exception of stops for splicing. The CIP piles were to have a 0.250-in (6.35-mm) minimum shell thickness, but the contractor opted to drive grade A52, 0.219-in (5.56-mm) shells due to the unavailability of the thicker shell. While driving the CIP piles at sites 2 and 4, the lighter shells buckled. A replacement pile with 0.250-in thickness was then driven at site 4, but this also buckled during driving. A second replacement pile that had a shell thickness of 0.320 in (8.13 mm) was finally driven successfully and load tested. Thus, three of the five shell piles driven for the program were damaged during driving. The H-piles drove with little difficulty at all four sites and essentially had the same driven lengths as the CIP piles at sites 1 and 4. The test pile at site 3, which was located in the deep channel water, was reinforced against buckling by welding 24x1.5-in (60.9x3.81-cm) steel plates across the flanges to a depth of 15 ft (4.6 m) below the mud line.

Six maintained-load (ML) type load tests were conducted on the four H-piles and two remaining CIP piles, essentially in accordance with ASTM D 1143, by using anchor piles for reactions. Four constant-rate-of-penetration (CRP) type load tests were conducted immediately after completion of the ML tests. Test loads were applied in three cycles; the test load was reduced to zero after each cycle to measure net set of the pile head. Test loadings for the respective cycles were cycle 1, 96 tons-force (854 kN); cycle 2, 128 tons-force (1139 kN); and cycle 3, 172 tons-force (1530 kN). These loadings were chosen to correspond to stresses of 9000, 12 000, and 16 000 psi (62, 82.8, and 110.3 MPa), respectively, in the steel for the HP 14x73 H-pile. Loads were applied in increments by using the following percentage of design cycle load and sequence: 0, 50, 100, 125, 150, 175, 200, 150, 100, 50, 0. Each load increment was maintained until the rate of settlement, or rebound, under that increment was less than 0.001 in (0.25 mm) in a 15-min period before proceeding to the next increment. The maximum cycle 3 load of 344 tons-force (3060 kN) was maintained for 24 h.

Applied loads were determined from calibrated hydraulic gauges. The instrumentation for measuring pile head movement consisted of three dial gauges spaced equally around the pile and two dial gauges mounted perpendicular to the pile to monitor horizontal movements. Secondary measurement systems of wire line and mirror and surveyor's level were also used. Telltales were not installed on any of the test piles.

LOAD TEST RESULTS

The load test results are summarized in the accompanying load versus displacement plots in Figures 2, 3, and 4. The H-pile at site 2 failed aboveground while placing the last increment of loading. The data point shown for the 344-ton-force loading was estimated from readings made during the loading. A maximum load of only 300 tons-force (2669 kN) could be maintained on a retest of cycle 3 for this pile due to excessive lateral pile movements. The load test for the H-pile at site 3 was terminated after reaching a 300-ton-force load on the third loading cycle as the pile was deflecting with no increase in load.

Ultimate pile capacities were predicted by using interpretive techniques suggested by Davisson, Mazurkiewicz, Shin, and the Swedish Pile Commission

Figure 2. Site 1: load versus displacement plots.

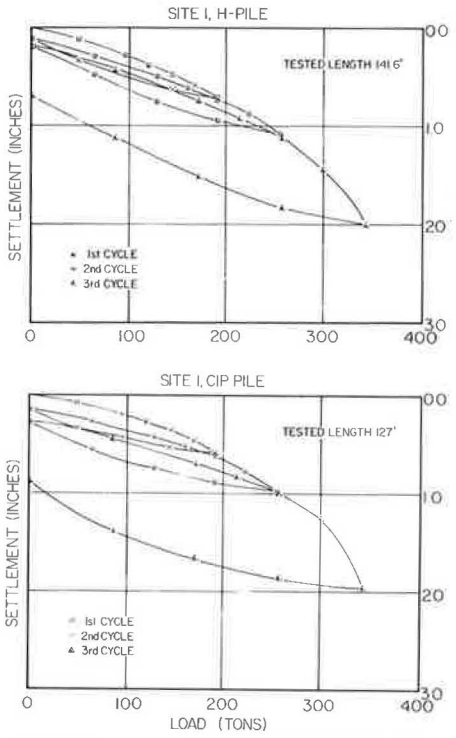

Note: 1 in = 1.83 cm, 1 ton-force = 8.896 kN, 1 ft = 0.3 m.

Figure 3. Sites 2 and 3: load versus displacement plots.

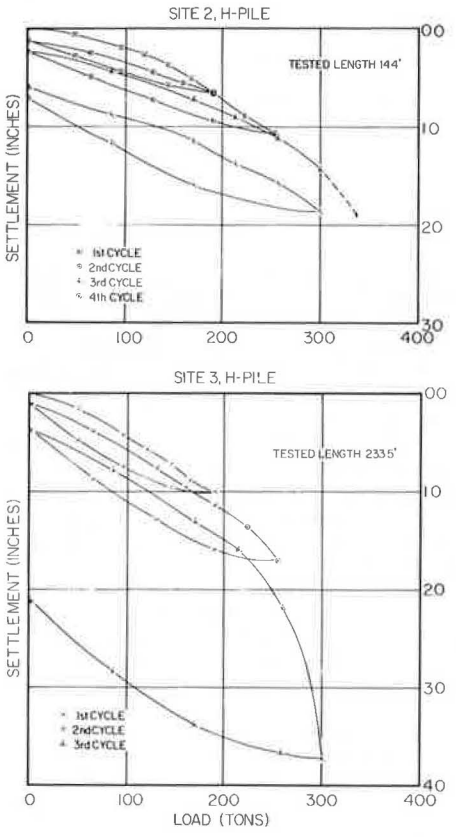

Note: 1 in = 1.83 cm, 1 ton-force = 8.896 kN, 1 ft = 0.3 m.

Figure 4. Site 4: load versus displacement plots.

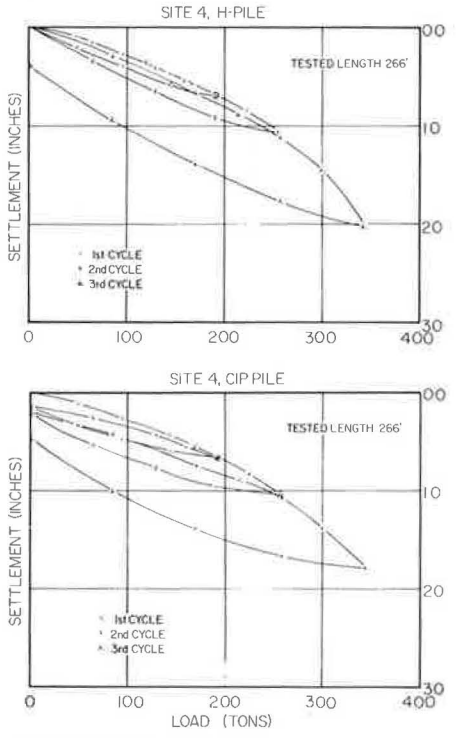

Note: 1 in = 1.83 cm, 1 ton-force = 8.896 kN, 1 ft = 0.3 m.

(90 percent criterion) (3). The general interpretation procedures and the American Association of State Highway and Transportation Officials (AASHTO) settlement criteria are shown in Figure 5 and summarized as follows:

1. Davisson: Davisson's method defines the failure load as the load that corresponds to the movement that exceeds the elastic compression of the pile, when considered as a free column, by a value of 0.15 in (3.81 mm) plus a factor depending on the diameter of the pile. For the 16-in (406.4-mm) CIP piles and HP 14x73 H-piles, this factor is approximately 0.1 in (2.54 mm). Thus, the pile reaches failure at a pile-head movement that exceeds the elastic compression by 0.25 in (6.35 mm).
2. Mazurkiewicz: The Mazurkiewicz technique involves arbitrarily choosing a set of equal pile-head movements and constructing from the intersection of these movement lines and the load-deflection curve a set of corresponding load lines. From the intersection of each load line with the load axis, a 45° line is drawn to intersect with the next load line. The intersections fall approximately on a straight line, from which the intersection with the load axis defines failure.
3. Chin: Chin proposes that the load-deflection curve can be approximated by a hyperbola. A plot of pile-head movement divided by load versus an abscissa of head movement gives a straight line, of which the inverse slope is the failure load.
4. Ninety percent criterion: The Swedish Pile Commission's 90 percent criterion defines failure as the load for which the pile-head movement is twice the movement obtained at a 10 percent smaller load.
5. AASHTO: The AASHTO specifications (4) define ultimate pile load as that load that, after a con-

Figure 5. Load test interpretative techniques.

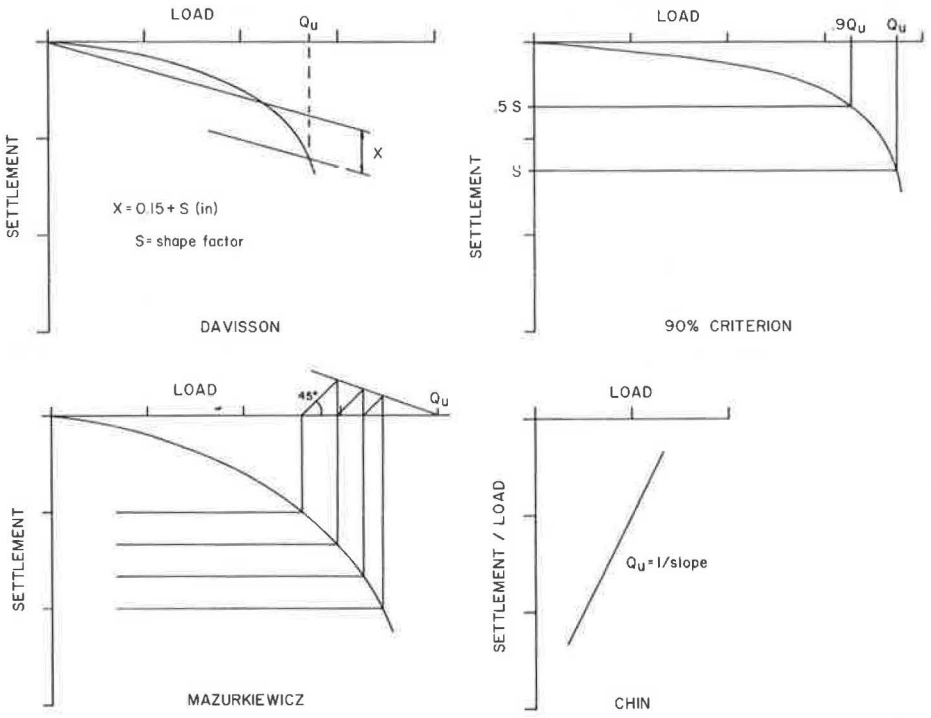

Table 1. Predicted ultimate loads from ML test data.

Item	Ultimate Load (tons-force)					
	Davisson	Mazur-kiewicz	Chin	90 Percent Criterion	AASHTO	Failure Load
Site 1						
H-pile	345	430	590	355	275	375[a]
CIP	300	370	510	360	250	
Site 2, H-pile	380	455	440	400	265	
Site 3, H-pile	295	315	580	300	235	300
Site 4						
H-pile	390	415	620	375+	325	380[a]
CIP	375+	455	630	375+	275	

Note: 1 ton-force = 8.896 kN.
[a]CRP test result.

tinuous application of 48 h, produces a permanent settlement not greater than 0.25 in.

A summary of the predicted ultimate failure loads obtained from the ML load test data is given in Table 1. Although the values obtained from the AASHTO criterion should be defined as a limiting load rather than an ultimate failure load, they are also listed, as this technique is typically used by state highway departments for determining maximum loads (5). Loads obtained by using this method were by far the most conservative capacities obtained. Chin's method, on the other hand, gave the highest values. It should be pointed out, however, that most of the predictions were based on extrapolations of the load-deflection curves. Of the interpretative techniques used, only Davisson's method takes into account the length and diameter of the pile (6). Although other investigators have reported the technique to be conservative, it was felt it represented the most rational approach and thus was used to define the ultimate pile capacity.

On completion of the ML load tests, CRP-type load tests were run on the piles at sites 1 and 4. Loading rates recommended by the New York State DOT were used (7). Results were very similar to those obtained with the ML tests, although the measured settlements were slightly less with the CRP tests. Figures 6 and 7 show a comparison of the CRP tests with a composite curve of the ML test results. The CRP test was run immediately after the ML test, but the data have been shifted to the zero settlement point to provide a comparison.

The Goble-Case Western PDA was used to monitor driving of the test piles at sites 1, 3, and 4. Testing was performed by the Soil Exploration Company of Minneapolis, Minnesota. Testing with the PDA involves making force and acceleration measurements at the top of the pile during driving. These measurements are then fed into a small field computer, and predictions of the pile's ultimate static capacity are made by using the Case method (8). A comparison of the PDA predictions made at the time of driving with the CRP load test results is given in Table 2.

The Case method of analysis was quite reliable in predicting ultimate capacity of the H-piles. Predictions for the CIP piles were, however, off by a factor of ±2. Reanalysis of the data by using the Case pile wave analysis program (CAPWAP) method of analysis did not improve the predictions. A possible explanation for the poor results on the CIP

Figure 6. Site 1: comparison of ML and CRP test results.

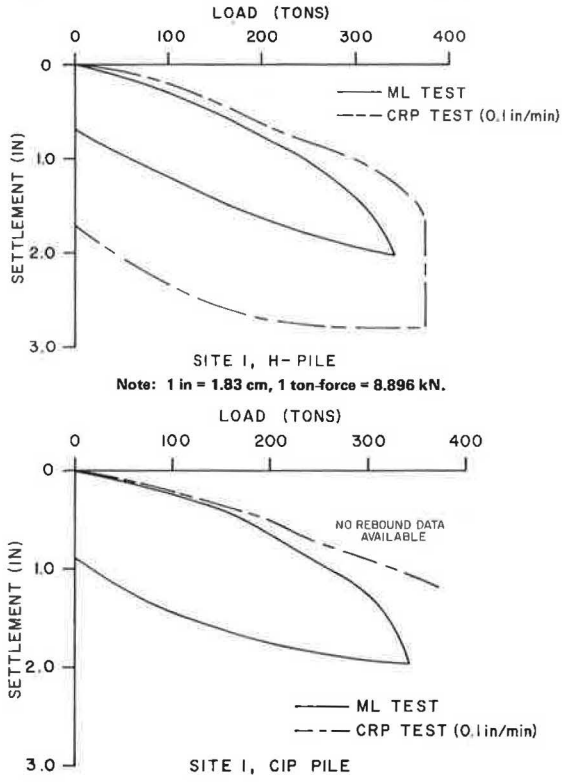

Figure 7. Site 4: comparison of ML and CRP test results.

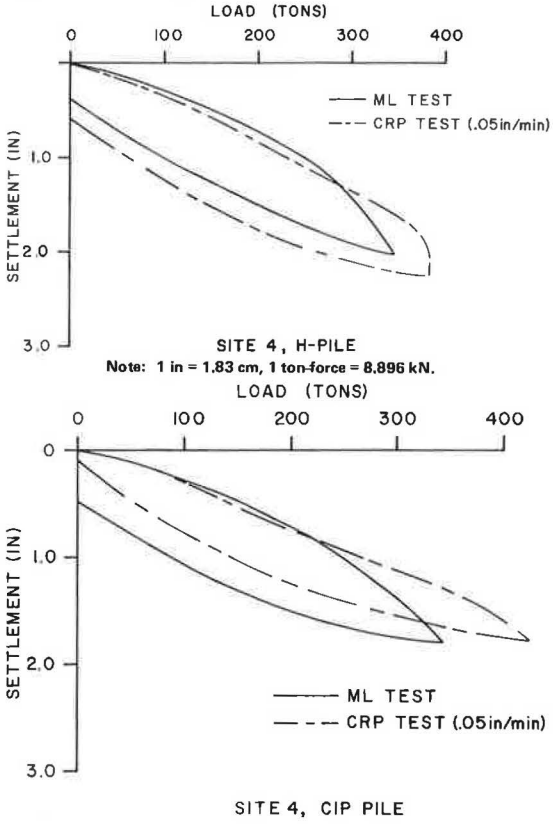

piles is that these piles were driven with an oversized end plate and probably experienced considerably more setup than did the H-piles during the time delay between driving and load testing. However, it was not possible to obtain restrike data after the load tests to confirm this.

On completion of the load test program, piles at sites 1 and 4 were analyzed by using the wave equation to evaluate the predictive capabilities of the method and how well it could model the pile-driving operation at this site. The analysis was performed independently by Federal Highway Administration (FHWA) personnel who used the WEAP computer program. Results of their analysis indicated that the piles could not have been driven to the capacities measured with the hammer used. A comparison of results from the WEAP analysis, PDA, and Wisconsin standard driving formula is shown in Figure 8. The wave equation gave the poorest correlation of the methods; thus, no further attempts were made to try and establish a driving criteria for field inspection with the wave equation.

Based on the poor driving experience of the CIP piles during the load test program, the HP 14x73 H-pile was selected for use on all substructure units. An ultimate load of 300 tons-force (2669 kN) that had a design load of 150 tons-force (1334 kN) was selected based on the load test results by using Davisson's technique. The piles were expected to drive to the dense granular layer; thus, no group reduction was felt necessary. With the very long piles and high capacities, it was decided to use the Goble-Case Western PDA for quality control on the project. Due to the poor results with the wave equation, driving criteria for production piles were established by using the Wisconson DOT standard driving formula.

FINAL SUBSURFACE INVESTIGATION

On completion of the preliminary bridge plan, a final subsurface investigation program was started in 1978. This program involved taking one SPT boring at each of the 45 substructure unit locations. Results of this investigation confirmed what had been found in the earlier studies, i.e., relatively soft sediments overlying a dense foundation zone. Driving records from the pile load test program indicated that the H-piles would penetrate the dense silty sand layer some 15 ft (4.6 m). Final bridge plans were prepared that required both a minimum tip elevation based on 15 ft of penetration into the dense silty sands and a minimum bearing of 150 tons-force as determined by the Wisconsin DOT standard driving formula.

Table 2. Comparison of PDA predictions with CRP load test results.

Item	Ultimate Load (tons-force)	
	PDA (Case method)	CRP Load Test
Site 1		
H-pile	380	375 (F)
CIP	180	360+
Site 3, H-pile	310[a]	300 (F)[b]
Site 4		
H-pile	330	380 (F)
CIP	230	425+

Notes: 1 ton-force = 8.896 kN.
(F) = actual failure load.

[a] Prediction at driven length of 199 ft (60.7 m).
[b] Failed under ML test with driven length of 255 ft (77.7 m).

CONSTRUCTION CONTROL

Bridge construction began in 1979, and the substructure was divided up into four separate construction contracts. Johnson Bros. obtained two of these con-

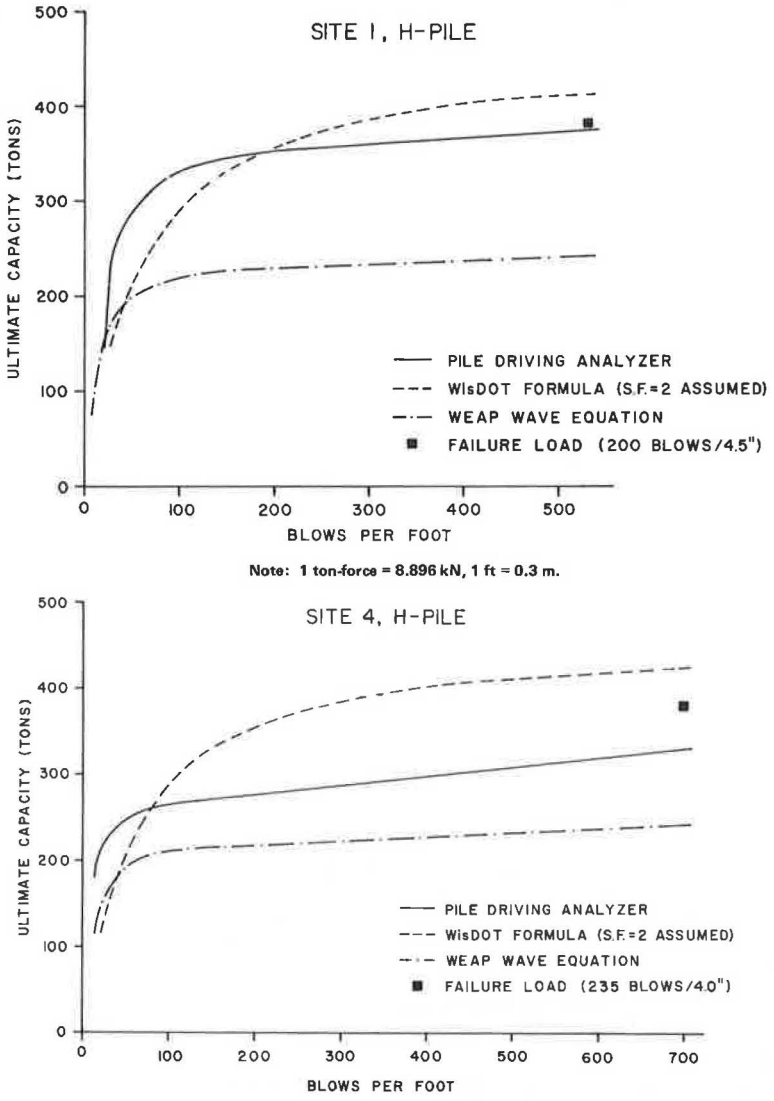

Figure 8. Wave-equation, PDA, and Wisconsin DOT driving analysis results.

tracts, Edward Kramer and Sons one, and the fourth is yet to be let. Estimates called for some 270 000 linear ft (82 296 m) of piling for the bridge. Pile driving on the first three contracts is essentially complete; approximately 185 000 ft (56 388 m) of piling have been driven.

Construction control for the job consists of using both the Wisconsin DOT driving formula and the PDA. A Wisconsin DOT pile inspector remains with the driver at all times, and blow count, height of ram fall, and calculated capacity are recorded for each foot of pile. Piles are required to be driven into the dense silty sand layer and obtain a minimum bearing of 150 tons-force by the formula. If penetration into the silty sand is not possible, a 200-ton-force (1780-kN) capacity by formula is required. The two impact hammers being used for production driving are a Delmag D-36 diesel hammer that has an energy rating of 83 100 ft-lbf (112.6 kJ) and a Conmaco 160 single-acting air-steam hammer that has a rating of 48 750 ft-lbf (66.1 kJ). These hammers are not the same as the driver used for the pile load test program, but the rated energies are in excess of that of the original hammer. With the higher energies and the verification with the PDA, it was felt that a requirement of identical hammers was not necessary.

One to two piles in each substructure unit are also tested with the PDA to verify that the hammer is performing satisfactorily and that desired bearing is being achieved. Testing with the PDA is accomplished by attaching reusable strain transducers and accelerometers to the pile. For each hammer blow, strain and acceleration signals are fed into the field computer for processing. An instantaneous printout of energy transmitted to the pile and forces developed in the pile is obtained. Due to the very long piles and high blow counts, the ultimate static capacity of the pile must be calculated by applying corrections for loading and unloading. The Conamaco 160 air-steam hammer being used by Johnson Bros. has produced such high accelerations that strain transducers were continually damaged during periods of prolonged driving. To minimize the occurrence of damage, piles are tested with the PDA only on a restrike basis after the pile has reached bearing by using the Wisconsin DOT formula. A summary of results obtained with the PDA is given below:

1. Length--maximum = 282 ft (86 m) and minimum = 180 ft (55 m);
2. Capacity--maximum = 500 tons-force (4448 kN) and minimum = 295 tons-force (2624 kN);

3. Stresses--maximum = 35 000 psi (241.4 MPa) and minimum = 21 700 psi (149.7 MPa); and
4. Energy--Delmag D-36, diesel: maximum = 36 000 ft-lbf (48.8 kJ) (51 percent) and minimum = 21 000 ft-lbf (28.5 kJ) (41 percent); and Conmaco 160, air-steam: maximum = 30 000 ft-lbf (40.7 kJ) (72 percent) and minimum = 21 000 ft-lbf (48 percent).

The energy percentages shown are hammer efficiencies that are based on the ratio of measured energy to the height of ram fall times the ram weight. The ultimate capacities being obtained are near or in excess of the capacities required for the job. Pile stresses and hammer energies were felt to be within an acceptable range.

CONSTRUCTION PROBLEMS

Construction problems have been minimal; the only major problem was associated with pile setup. The initial pile load test program required the test piles to be driven continuously; however, no such provision was included in the construction contracts. The contractor initially began driving in three substructure units, working from one to another. Piles that were in excess of 180 ft (55 m) and left for more than one day experienced difficulty on resumption of driving. Some could not be started again. With the foundation design based on penetrations of ±260 ft (79 m) to the dense granular layer, corrective measures were required or redesign would have been necessary. The problems were eventually resolved after negotiations with the contractor resulted in an agreement where only one substructure unit would be driven at a time, thereby reducing the times for development of setup. Time delays were reduced typically to one or two days, and the remainder of the piles have been driven down to the silty sand layer as planned.

The PDA has proved to be very useful in determining if a pile has been damaged during driving (9). Piles that experienced a dramatic decrease in blow counts or were significantly past plan tip elevation were tested with the PDA. A visual examination of the force and velocity wave traces allows immediate evaluation by the operator as to whether the pile is damaged and the location of the damage. Piles that were determined to be damaged are left in place and replaced by driving an additional pile adjacent to it. No load-carrying capacity is assigned to the damaged pile. To date, the project has experienced a damage rate of 2.3 percent; the majority of the damaged piles are battered.

CONCLUSIONS

From the various investigations, analyses, and later construction experiences, the following conclusions can be made:

1. The sequence of office studies, preliminary exploration program, load tests, and final subsurface investigation was necessary in progressing from initial project conception to final construction. Each step provided input for planning the next phase of the design process, which resulted in a more economical and efficient approach.
2. The pile load test phase proved to be a highly successful predesign program that (a) provided valuable information for selecting the most suitable pile type, (b) evaluated maximum design loads, and (c) determined pile tip elevations for final bridge design. The program also provided insight into the drivability of piles at the site, which aided contractors in preparing construction cost estimates.
3. Davisson's predictive method gave the most reliable results of the interpretative techniques tried. The ultimate capacity predictions from the ML test data were very close to those obtained during the CRP tests that were loaded to failure.
4. The CRP load tests appear to give essentially the same results as the ML tests in a much shorter time. The CRP test does result in less pile settlement and should be used with caution when a net settlement criterion is used for determining allowable load.
5. Results of the Goble-Case Western PDA were very positive in predicting ultimate capacity of the H-piles but were low by a factor of ±2 for the CIP piles. Restrike testing done closer to the time of load testing, though, may have improved the predictions for these piles.
6. The wave-equation analysis did not realistically model the pile driving at this site. However, it remains a powerful tool in the analysis of pile driving. There seems to be great potential for the technique, particularly if it is used in conjunction with PDA testing and CAPWAP analysis to refine the input soil parameters and correlated with static load tests.
7. The HP 14x73 H-pile with a design load of 150 tons-force and a ultimate load of 300 tons-force was selected for the bridge foundation based on the results of the pile load test program. This loading was a significant increase over the 96-ton-force (854-kN) design loading that would normally have been used for this pile in soil following AASHTO standard specifications. With pile driving for three of the substructure contracts essentially complete, construction experience has verified the choice of the pile type for the design loadings imposed. Piles drive to the dense silty sand zone and achieve bearing, as was anticipated. An overall pile damage rate of 2.3 percent has been observed so far.
8. The PDA has shown to be a very useful quality-control device. Due to a high equipment damage rate, however, only restrike data can be taken. Results of the testing verify that required capacities are being obtained and that the hammers are functioning properly. Measurement of hammer energy has been necessary, as the driving criterion is based on the Wisconsin DOT driving formula. Damage detection with the PDA has been an exceptionally useful part of the quality-assurance program.

REFERENCES

1. R.D. Darragh and R.A. Bell. Load Tests on Long Bearing Piles. In Performance of Deep Foundations, ASTM, Special Tech. Publ. 444, 1969.
2. Standard Specifications for Road and Bridge Construction. Wisconsin Department of Transportation, Madison, 1981.
3. B.H. Fellenius. Test Loading of Piles and New Proof Testing Procedure. Journal of the Geotechnical Engineering Division, ASCE, Vol. 101, No. GT9, Sept. 1975.
4. Standard Specifications for Highway Bridges, 12th ed. AASHTO, Washington, DC, 1977.
5. G.A. Leonards and D. Lovell. Interpretation of Load Tests of High-Capacity Driven Piles. In Behavior of Deep Foundations, ASTM, Special Tech. Publ. 670, 1979.
6. M.T. Davisson. High Capacity Piles. In Proc., Soil Mechanics Lecture Series--Innovations in Foundation Construction, Soil Mechanics and Foundation Division, ASCE (Illinois Section), 1973.
7. Soil Control Procedure SCP-4/77. In Static Piles Load Test Manual, Soil Mechanics Bureau,

New York State Department of Transportation, Albany, April 1977.
8. G.G. Goble, F. Rausche, and G. Likins. Bearing Capacity of Piles from Dynamic Measurements, Final Report. Ohio Department of Transportation, Columbus, and Department of Solid Mechanics, Structures, and Mechanical Design, Case Western Reserve Univ., Cleveland, Rept. OHIO-DOT-05-75, March 1975.
9. F. Rausche and G.G. Goble. Determination of Pile Damage by Top Measurements. In Behavior of Deep Foundations, ASTM, Special Tech. Publ. 670, 1979.

Notice: The Transportation Research Board does not endorse products or manufacturers. Trade and manufacturers' names appear in this paper because they are considered essential to its object.

Construction Control by Monitored Geotechnical Instrumentation for New Terminal 46, Port of Seattle

BENGT H. FELLENIUS, ARTHUR J. O'BRIEN, AND FRANK W. PITA

Geotechnical instrumentation was used to monitor and control construction pore pressures and soil movement during major modifications to an existing container terminal (old terminal 46) for the Port of Seattle. There was concern that the construction work, which consisted of dredging, filling, and pile driving, might disturb the confined and sloping (5H:1V) 25-ft-thick loose silt layer beneath the fill at the terminal. Construction control by monitored instrumentation was used because the topographic conditions at the site and the Port's economic and marine design parameters precluded conventional methods of preventing slope failure, such as total excavation of the silt and/or flattening the new fill slope. The instrumentation monitored the behavior of the confined silt layer to ensure that excess pore pressures and soil movements induced by the disturbance of the construction work were within acceptable limits. Two warning levels of observed excess pore pressure were established to control the construction sequence and rate. At the yellow level, extra caution and alertness were imposed. At the red level, construction was halted or relocated. The disturbance caused by dredging and filling operations was small. The disturbance from pile driving was limited to a zone that had a radius smaller than 30 ft. The pile-driving contractor was restricted to driving no more than 3 piles/day within 30 ft of each other. This posed little hardship for the contractor, and the construction was completed successfully.

This paper presents the background and results of the construction-control monitoring program implemented during the construction of new terminal 46, Port of Seattle, Washington. The preliminary design for the new terminal specified that an embankment be built on a confined, sloping layer of loose silt and that, afterward, displacement-type piles be driven through the embankment slope and silt layer into an underlying dense, glacial deposit. There was concern that implementation of these two construction procedures might cause embankment instability.

The preliminary design calculations for new terminal 46 indicated an unacceptably low margin of safety against slope failure if construction procedures caused loss of effective strength in the sloping silt layer. Such loss of strength could occur from increased pore pressures caused by rapid dumping of fill or by pile driving. However, the overall topographic conditions of the site and the marine design parameters were such that conventional solutions, such as complete removal of the silt layer or flattening of the new embankment slope, were not practical. Conventional solutions were also not economical because the cost difference between the use of instrumentation to implement the preliminary design concept and the use of conventional solutions was estimated to be more than $1 million. Therefore, the decision was made to implement the preliminary design with some minor modifications and to monitor the stability of the slope during construction by means of piezometers and slope inclinometers. If any excessive pore pressure or soil movements suggesting imminent risk of failure occurred, the construction would be halted until the risk had subsided.

Proper planning and use of the monitoring program would maintain the risk of embankment failure at an acceptably low level; however, too frequent construction halts and/or relocations could cause costly project delays. Nevertheless, the risk of costly delays was preferred over alternative conventional solutions.

SOUTHEAST HARBOR DEVELOPMENT PROJECT

The Port of Seattle implemented the Southeast Harbor Development Project to improve existing waterfront facilities and to provide new facilities for handling the growing volume of containerized cargo. Phases 1 and 2 of this project, which occurred between old pier 37 and old terminal 46, were completed in 1979. Phase 3, which consisted of a modification and lateral extension of old terminal 46, was completed in 1980. The completed facilities include 86 acres of a container storage and handling area; five container cranes will operate on 2740 ft of the pile-supported apron structure (Figure 1).

During the construction of phases 1, 2, and 3, pier 39 and portions of piers 37, 42, and 43 and old terminal 46 were removed (Figures 1 and 2). An earth-fill embankment was built at the outer edge of the old piers. A container storage area was then constructed by filling between the old piers and the new embankment. A pile-supported apron deck was constructed on the outer slope of the new embankment.

A variety of fill materials was used behind the embankment, including fine-grained organic dredge material from the Duwamish River, demolition rubble, riprap, and gravelly sand. The outer fill slope intersects the natural bottom of Elliott Bay, which descends at a slope of approximately 5H:1V at the site. The slopes were built in water at depths up to 90 ft in phase 1 and to 125 ft in phases 2 and 3.

The construction of new terminal 46 (phase 3)

Figure 1. Site plan, Southeast Harbor Development Project.

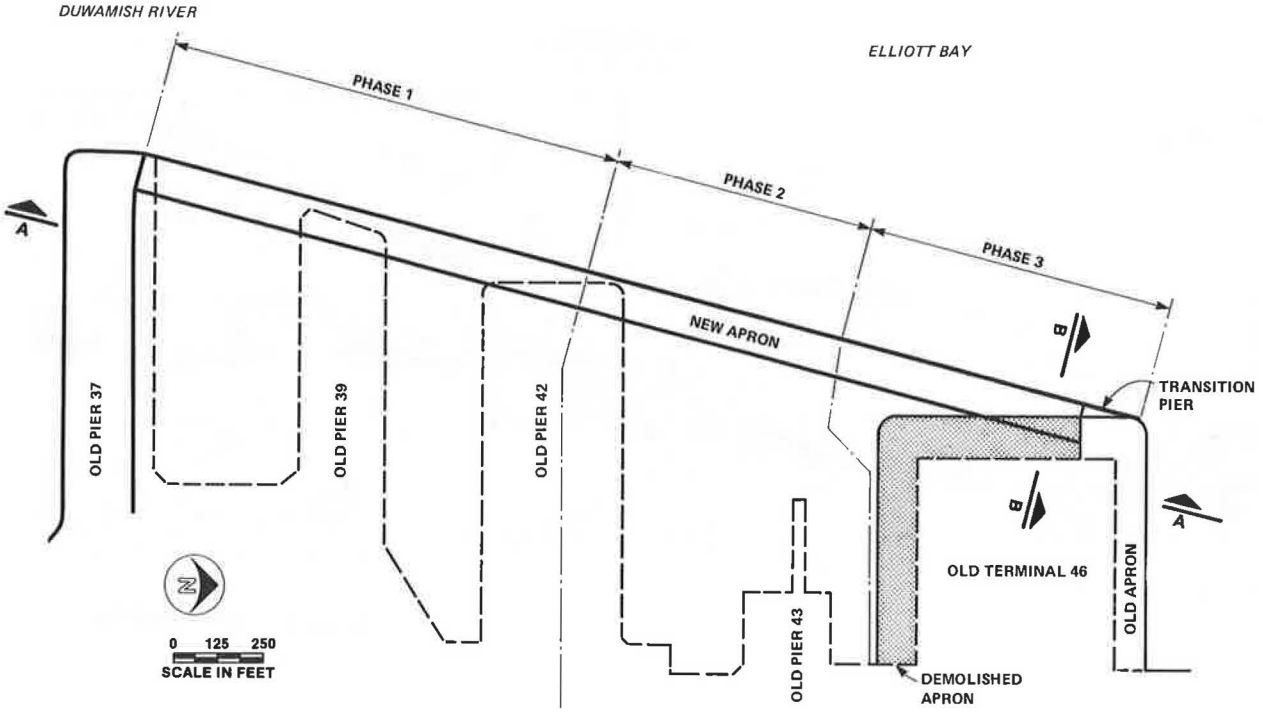

Figure 2. Section A-A of Figure 1.

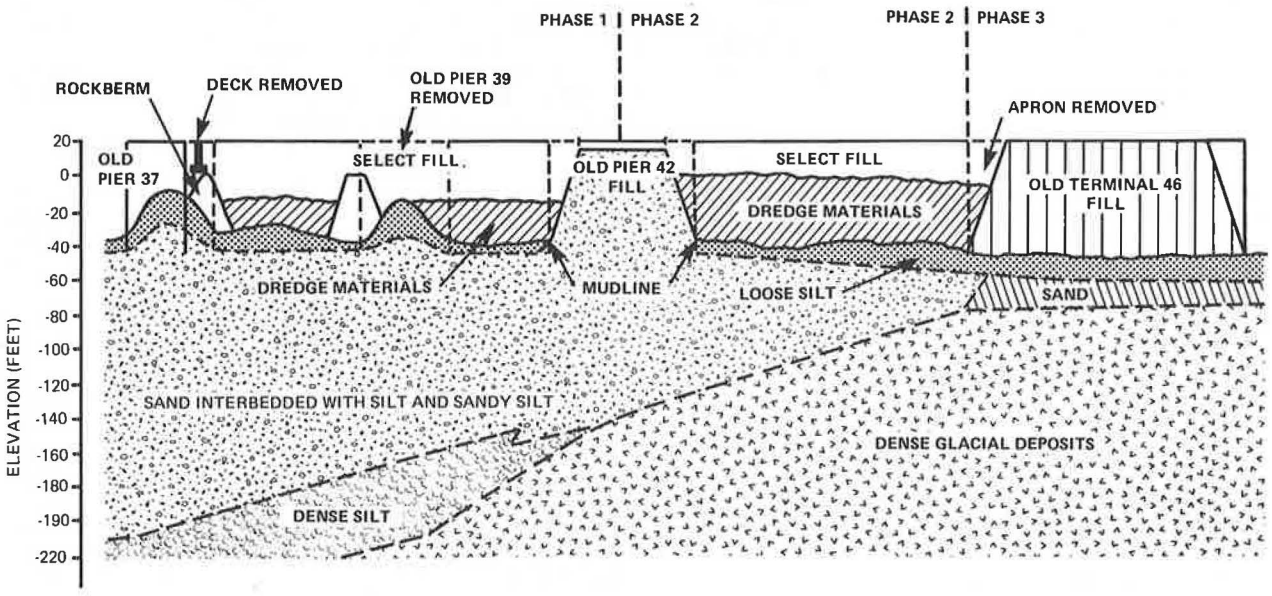

consisted of modifications to old terminal 46 (Figures 1 and 2). The major modifications included demolition of the south apron and approximately 630 ft of the west apron, placement of more fill to extend the embankment to the west, and construction of a new concrete apron that would connect to the previously constructed (phase 2) apron at the south. A transition section was constructed to connect the new and old terminal 46 aprons at the north.

The design criteria for the apron structure and embankment of new terminal 46 were provided by the Port of Seattle. They are summarized below:

1. Apron deck: dead load = 475 lb/ft² and live load = 1000 lb/ft²;
2. Yard, live load = 1000 lb/ft²;
3. Pseudostatic earthquake loading: seismic coefficient = 10 percent;
4. Piling = 16.5-in octagonal prestressed concrete piles;
5. Embankment slope = 1.75H:1.00V from elevation +7 ft at sheet pile wall to elevation -50 ft at edge of apron deck; and
6. Apron width = 101 ft.

Figure 3. Section B-B of Figure 1, old and new construction.

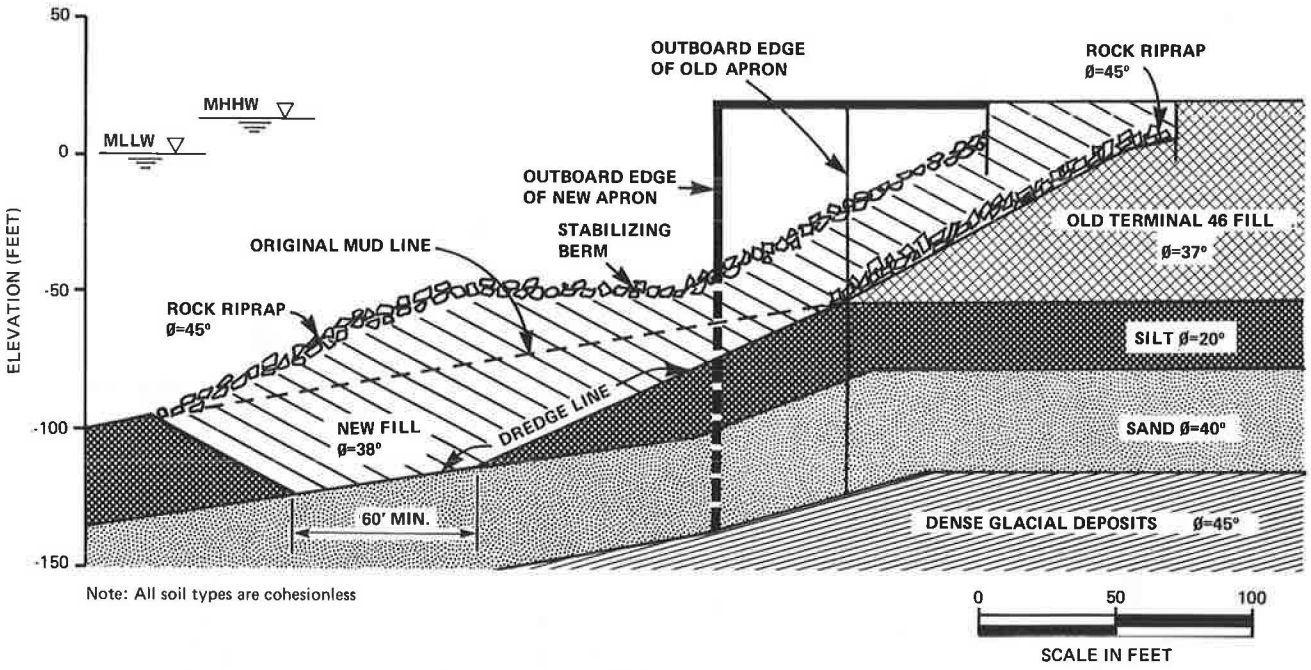

The material for the new embankment was to be clean, gravelly sand. To maintain sufficient draft at new terminal 46, the mud line at the outboard edge of the new apron had to be no higher than elevation -50 ft. Also, the apron was required to be 101 ft wide. These two conditions imposed an outer slope angle of 1.75H:1.00V. From elevation -50 ft, the embankment and/or the mud-line slope could vary, depending on stability requirements and existing conditions.

SOIL CONDITIONS

A geotechnical investigation that preceded the design was performed in early 1979. It consisted of test pits, test borings, and a static-cone penetrometer test. Disturbed samples were obtained from the test pits and split-spoon samples from the borings. Standard penetration tests (SPTs) and vane shear tests were performed. Shelby tube samples were attempted but not recovered.

Figure 3 (section B-B of Figure 1) presents a simplified vertical section across the site. Very dense glacial deposits underlie dense sand, which is covered by a layer of loose silt sloping toward the bay. The silt varies in depth and forms the base on which fill for old terminal 46 was placed. Ensuring the stability of the new fill with the presence of the loose sloping silt layer became the major concern in the geotechnical design.

In the silt, the sampling spoon and rods advanced ahead of the casing by their own weight, and the SPT values were mostly zero. In some places, however, SPT values as high as 17 were recorded. Also, the static-cone penetrometer showed some values equal to zero in the silt. The maximum cone resistance recorded in the silt was 20 kg/cm^2. The vane shear resistance in the silt was 250 lb/ft^2.

Grain-size analysis of the silt indicated 8-36 percent sand size and 92-64 percent fines (passing sieve No. 200). The clay-sized percentage was less than 10 percent. The organic content was small, about 2 percent.

Drained, direct shear tests on remolded samples of the silt indicated internal friction angles ranging from 26° through 36°. No cohesion intercept was found. The friction angle increased with the increasing density of the test specimen. The lowest density of the remolded test specimens was considered higher than the lowest in situ values. Based on the results of the field and laboratory testing and on engineering judgment, the design effective friction angle was designated as 20°.

In summary, the silt was found to be nonplastic and loose, and its primary strength of a frictional rather than a cohesive nature. Therefore, it was considered highly susceptible to excess pore pressure.

Based on results of the SPT and cone penetrometer tests, the effective friction angle for the dense sand underlying the silt was estimated at 40°. The effective friction angle of the new fill to be used for the embankment was estimated at 38°.

EMBANKMENT STABILITY

The stability of the embankment during construction (dredging, filling, and pile driving) and after construction (final conditions) was analyzed by using effective stresses. The analyses were made by using both cylindrical rotation slip surfaces (according to a modified Bishop method) and plane slip surfaces (wedge analysis). The cylindrical slip-surfaces analysis resulted in safety factors lower than the plane surfaces. Figure 3 shows the subsurface profile used in the stability analyses. The table below presents the results of the analyses:

Case	Safety Factor
During new embankment construction (after dredging outboard of old embankment)	1.07
Final conditions of new embankment	
No live loads	1.31
1000-lb/ft^2 live load	1.20
Seismic coefficient without stabilizing berm	0.92
Seismic coefficient with stabilizing berm	1.07

The subsurface profile shown in Figure 3 was used

to model the most critical section of the embankment. Because the new apron deck joins the existing apron at an angle, the relative locations of the new and old aprons change throughout the site. Figure 3 shows the profile at the intersection between the existing apron and embankment and the new apron and embankment. At the intersection, a limited amount of silt beneath the fill could be dredged without disturbing old terminal 46 fill, and a minimum thickness of new fill could be placed over the silt and still allow for the required draft clearance. Also shown in Figure 3 is a stabilizing berm outboard of the new embankment. The stability analysis indicated that this stabilizing berm must be included to attain acceptable stability for final conditions under earthquake loading.

Early in the design it became obvious that the behavior (pore pressures and lateral movements) of the loose silt layer during construction was critical to embankment stability. Pore-pressure increases during new embankment construction could critically decrease the stability of old terminal 46 fill. Also, the driving of displacement piles through the new embankment and into the loose silt layer would induce excess pore pressures that could critically decrease the safety of the new embankment. In order to proceed with the construction as designed, the decision was made to monitor the behavior of the silt layer and the embankment during the construction by means of geotechnical instrumentation.

To determine the effect of pore-pressure increases on embankment stability, two construction stages were analyzed: (a) building of the new embankment and (b) pile driving through the new embankment. During the analysis, excess pore pressures in the silt layer were imposed, which reduced the previously calculated safety factors.

Two warning levels (yellow and red) were established to help evaluate the observed excess pore pressure during each construction stage. The yellow warning level was defined as the excess pore pressure that decreased the safety factor to 1.0 when using an effective friction angle of 20° for the silt. The red warning level was defined as excess pore pressure that decreased the safety factor to 1.0 when using an effective friction angle of 26° (the lowest laboratory test result) for the silt. The excess pore pressures for these construction stages and warning levels are given in the table below:

	Pore Pressure (psi)	
Construction Stage	Yellow Level	Red Level
During new embankment construction	2.5	4.0
During pile driving	13.0	15.0

When excess pore pressure was below the yellow level, no extra caution was necessary in the construction procedure. Excess pressures between the yellow and red warning levels indicated use of cautionary measures, such as increasing the frequency of the monitoring of the instruments and the rigor of inspection and caution. Pressures above the red warning level required that the construction in that area be halted, or possibly relocated, until the pore pressures dissipated to below the red level.

In addition to pore-pressure measurements, lateral movements were monitored to aid the subjective judgment of the engineers. No specific limits were established for the observed lateral movements. If pore pressures were between the yellow and red levels but lateral movements did not occur, work continued. If lateral movements did occur, procedures for conditions above the red level were warranted, even if the pore pressures stayed between the yellow and red levels.

TYPES AND AMOUNT OF INSTRUMENTATION

Excess pore pressure was considered the most important factor contributing to possible embankment instability. Therefore, the piezometer was the main instrument for construction control. A piezometer, however, monitors the pore pressures at only one point and may not indicate pore pressures over the entire soil mass. For example, local zones of high values might not be representative of the whole, and important areas of excessive pore pressures might not be measured. Therefore, slope inclinometers were installed to provide information on the large-scale effect of construction procedures on the entire soil mass.

The piezometers used for the project were Petur Model P-102 Wellpoint. The inclinometers were Slope Indicator Company Model 50325 Digitilt. The instruments were installed in three phases during construction to accommodate the various conditions at the site. A total of 36 piezometers and 7 inclinometers was used. Figure 4 shows the location of the instruments. Figure 5 shows the approximate depths of the instruments in cross section.

In October 1979, 26 piezometers and 4 slope inclinometers were installed for phase A at old terminal 46 before its demolition. These instruments were used to monitor the embankment during the dredging operation and subsequent filling.

Figure 4. Instrument plan.

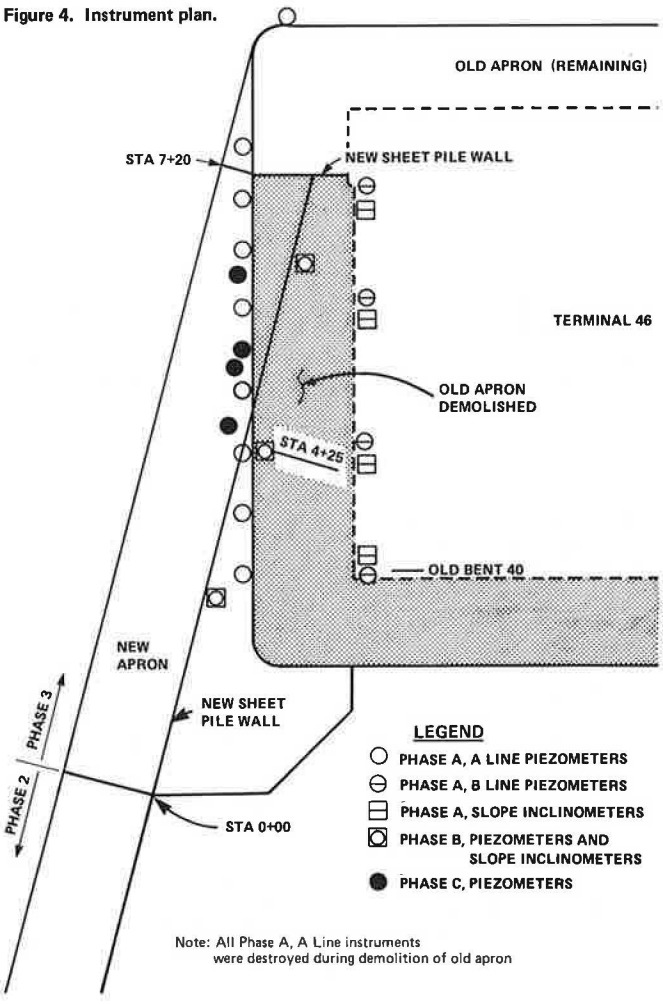

Figure 5. Instrumentation in profile.

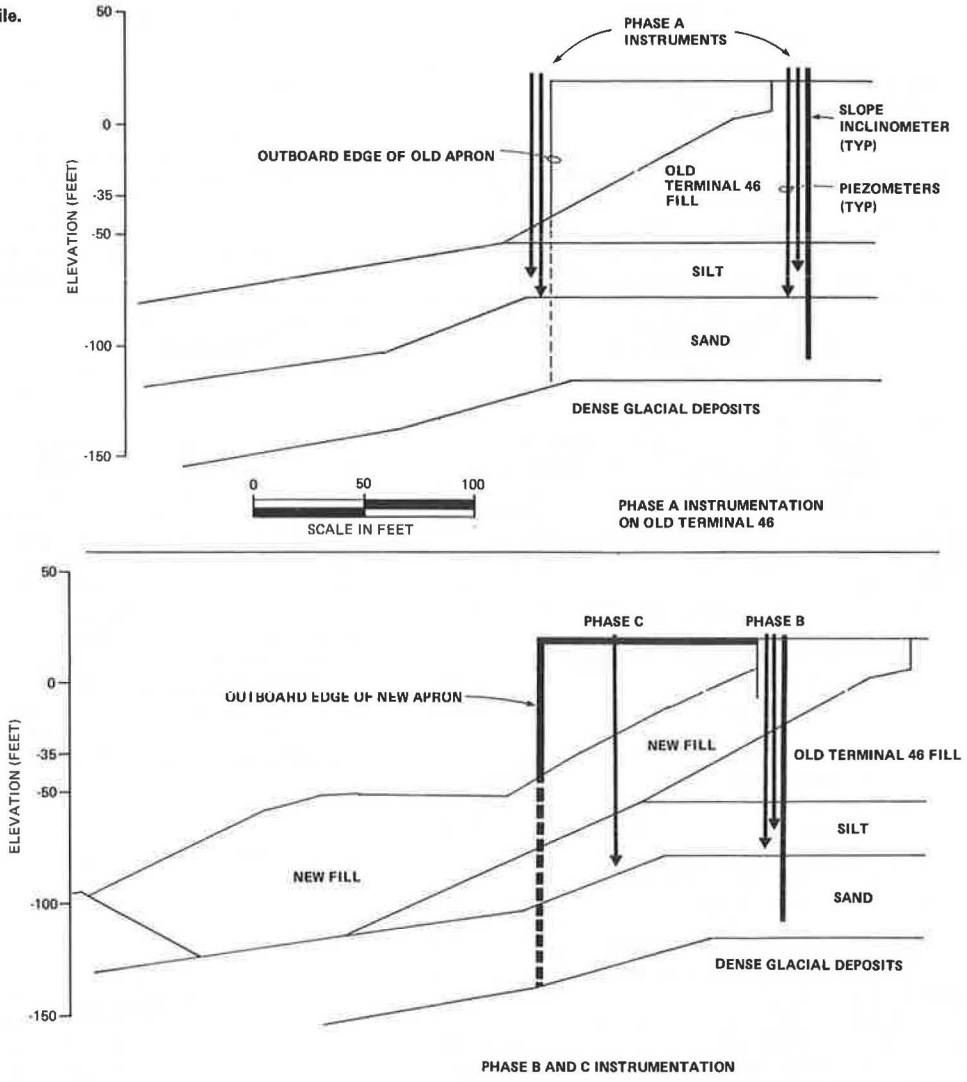

Phase B instrumentation, which was installed in March 1980, consisted of six piezometers and three slope inclinometers at three locations behind the new sheet pile wall. These instruments were installed at a distance greater than 30 ft from the nearest pile-driving area to monitor overall stability during pile driving.

Phase C instrumentation was installed in May 1980 and consisted of four piezometers. These instruments were installed adjacent to the pile-driving operation (each within 10 ft of a pile location) to monitor local pore-pressure increases during driving. Figure 6 shows the detailed location of phase C piezometers in relation to pile locations.

PRACTICAL PROBLEMS ASSOCIATED WITH USE OF GEOTECHNICAL INSTRUMENTATION

[Ed. note: This section is a general review of the problems of geotechnical instrumentation, which the authors felt was relevant not only to this project but also to any project in which instrumentation is needed.]

The practical problems of using geotechnical instrumentation must be considered early in the design process. The most important and easily overlooked problems are almost always associated with the people working on a project. The attitudes of owners, contractors, and field staff toward instrumentation are critical to proper operation and protection of the instruments.

Owners often think of instrumentation projects as research projects that have no direct cost benefits. Also, because they have been successful on other jobs without instrumentation, owners do not want to use it on their production-oriented projects. The designer must budget time and money to explain to the owner the technical reasons for, and cost-saving advantages of, instrumentation.

Contractors' opinions of instrumentation are often that it is a nuisance and a hindrance. Many times the contractor is indifferent to protection of the instruments from accidental destruction. Care must be taken to inform the contractor of the purpose and manner of use of the instrumentation to ensure his or her full cooperation and to show that the results can also be a benefit. In addition, strong wording must be included in the contract documents to provide an incentive for protection. Replacement clauses must be enforced from the start of the job. Even with a strongly worded contract, the design must provide for redundant instruments so that, when some of the instruments are destroyed or malfunction, enough remain to do the job.

Finally, the method of data gathering and reporting must be thoroughly planned and tested before the start of the project so that the data can be used

quickly and efficiently. It is most important to have field staff who are willing, alert, and competent.

RESULTS OF PORE-PRESSURE MONITORING

Instrumentation Calibration

After each installation phase and before any construction work, the piezometers were monitored to develop initial sets of control data. Each piezometer was monitored hourly over an approximately two-day period so that a normal pressure (in pounds per square inch) versus tide elevation (in feet) curve could be established. The difference between the normal pressure at a given tide elevation and the reading during the construction for the same tide level was considered the excess pressure caused by construction. These data were unique for each piezometer.

Results of Phase A

Only minor increases in pore pressure were observed during the dredging operation (October and November 1979). These small increases did not approach the yellow level. Figure 7 shows the pore pressures observed at old bent 40 (Figure 4) during the filling operation. Filling began at the south end of the new embankment while dredging was being completed at the north.

The filling was accomplished by dumping from a bottom-dump barge at a rate of approximately 2000 tons of fill per dump. When a barge dumped close to

Figure 6. Piezometer locations (phase C).

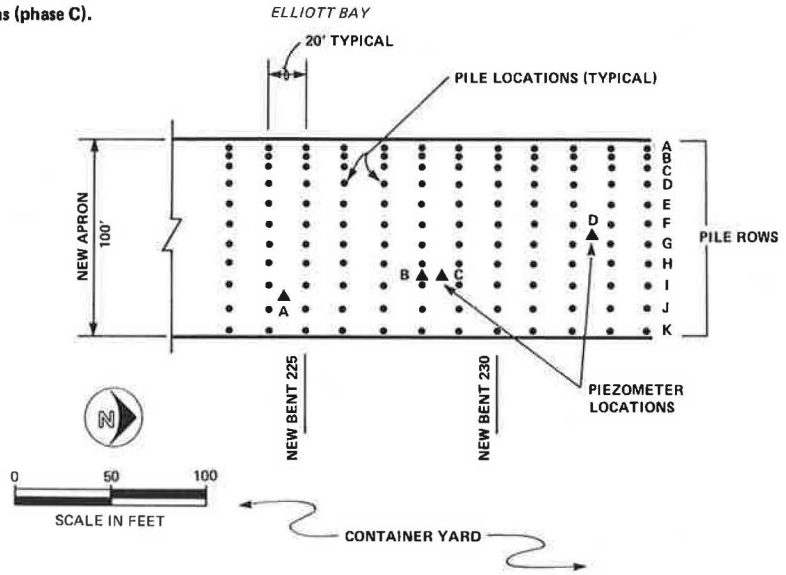

Figure 7. Pore pressure versus time from filling operation (old bent 40).

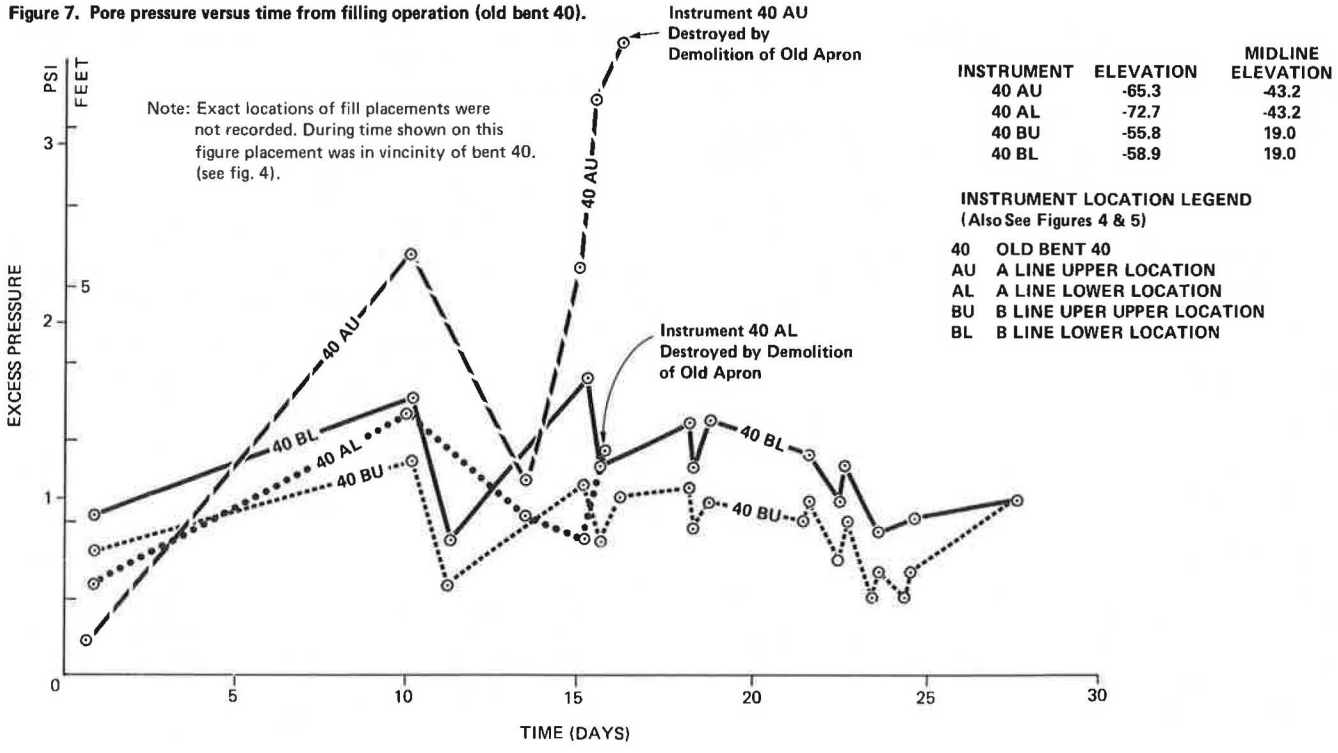

Figure 8. Instrument A pore-pressure increase during pile driving (phase C).

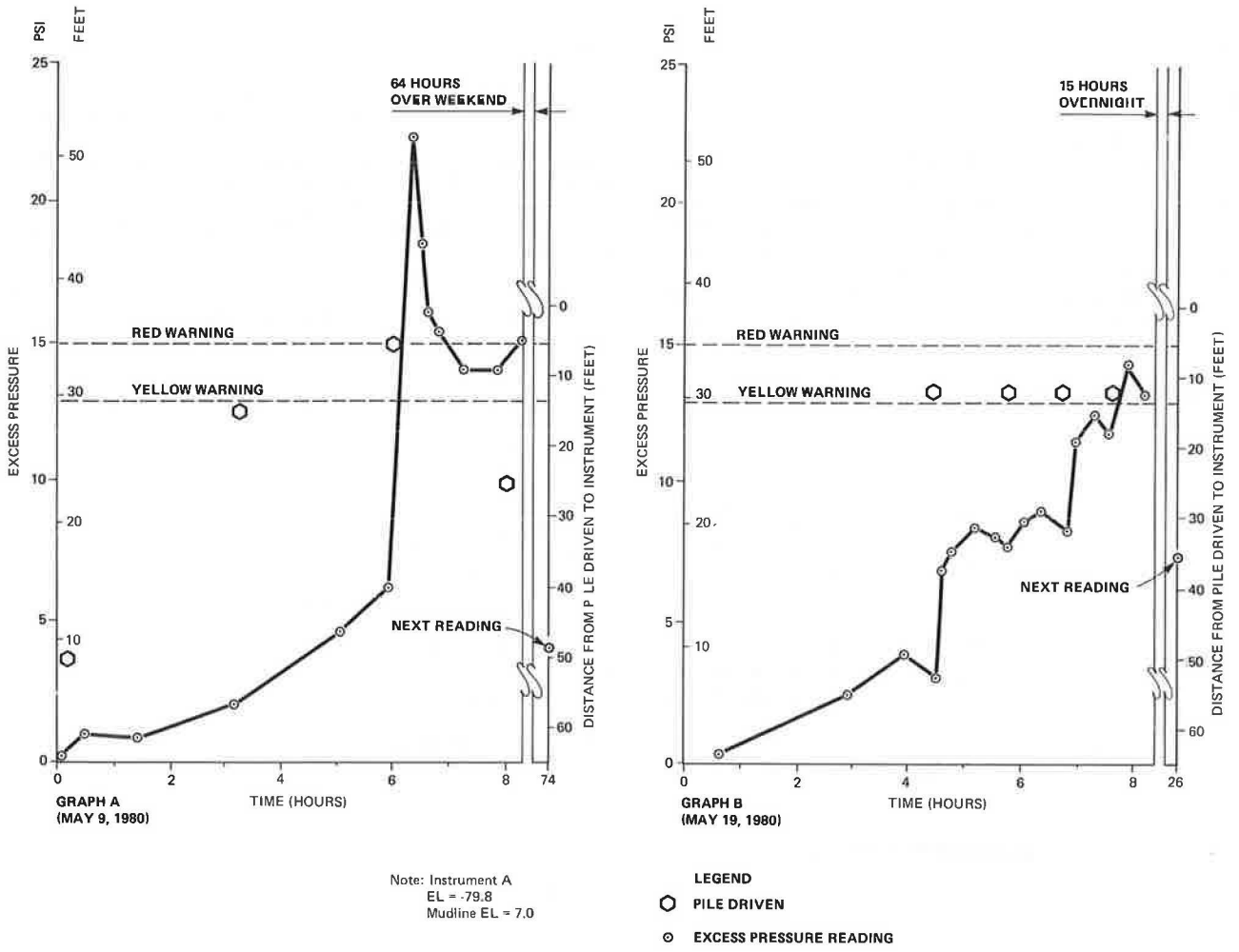

a piezometer, the pressures typically rose and then dissipated during the next 1-2 h if no additional dumps were made in the vicinity. Piezometer 40AU on day 14 (Figure 7) showed the accumulated effect of several successive dumps close to its location. Coincidentally, this piezometer was destroyed shortly after this reading.

All observations indicated that the induced pore pressures were below the yellow warning level. By mid-December, the remaining phase A piezometers were destroyed during demolition of the old apron, thereby preventing additional monitoring of the dredging and filling operations.

Results of Phase B

With few exceptions, pore pressures observed in phase B piezometers were below the yellow warning level. Detailed data from these instruments have not been included in this paper.

Results of Phase C

Figure 8 presents pore-pressure data taken from piezometer A of phase C during the pile-driving operations. Two separate sets of data are shown on each graph to give the relation among increase in excess pressure, distance from driven pile to piezometer location, and time. The first set of data (connected by the line) shows excess pore pressure (left ordinate) as a function of time (abscissa). The second set of data (hexagons) shows the distance from the driven pile (right ordinate) as a function of time.

Graph A of Figure 8 shows the relation between pile-driving distance and pore pressure. Piles driven more than 50 ft away did not significantly affect the pressures. However, as pile driving moved to within 15 ft, pressure increases were noticeable, and a pile driven within 5 ft caused sharp increases. Pore pressures dissipated rapidly after the sharp increase and increased again as the final pile for the day was driven 25 ft away. Dissipation occurred when no piles were driven nearby.

Graph B of Figure 8 shows the results of driving four successive piles within 12 ft of piezometer A. Results were cumulative, in that each pile caused an increase in pressure followed by a slight dissipation before the driving of the next pile. Each additional pile caused the same effect, which resulted in pressures above the yellow level; however, dissipation occurred overnight.

Figure 9 presents data similar to Figure 8 for three piezometers of phase C. At this time, the contractor was driving 7-8 piles/day (one shift per day). The data indicate that piles driven 20-30 ft from the instruments increased the pore pressures to the 10- to 12-psi range. When pile driving came to within 10 ft of a piezometer, the pressures increased significantly and entered the red level.

Figure 9. Pore pressures during pile driving (phase C).

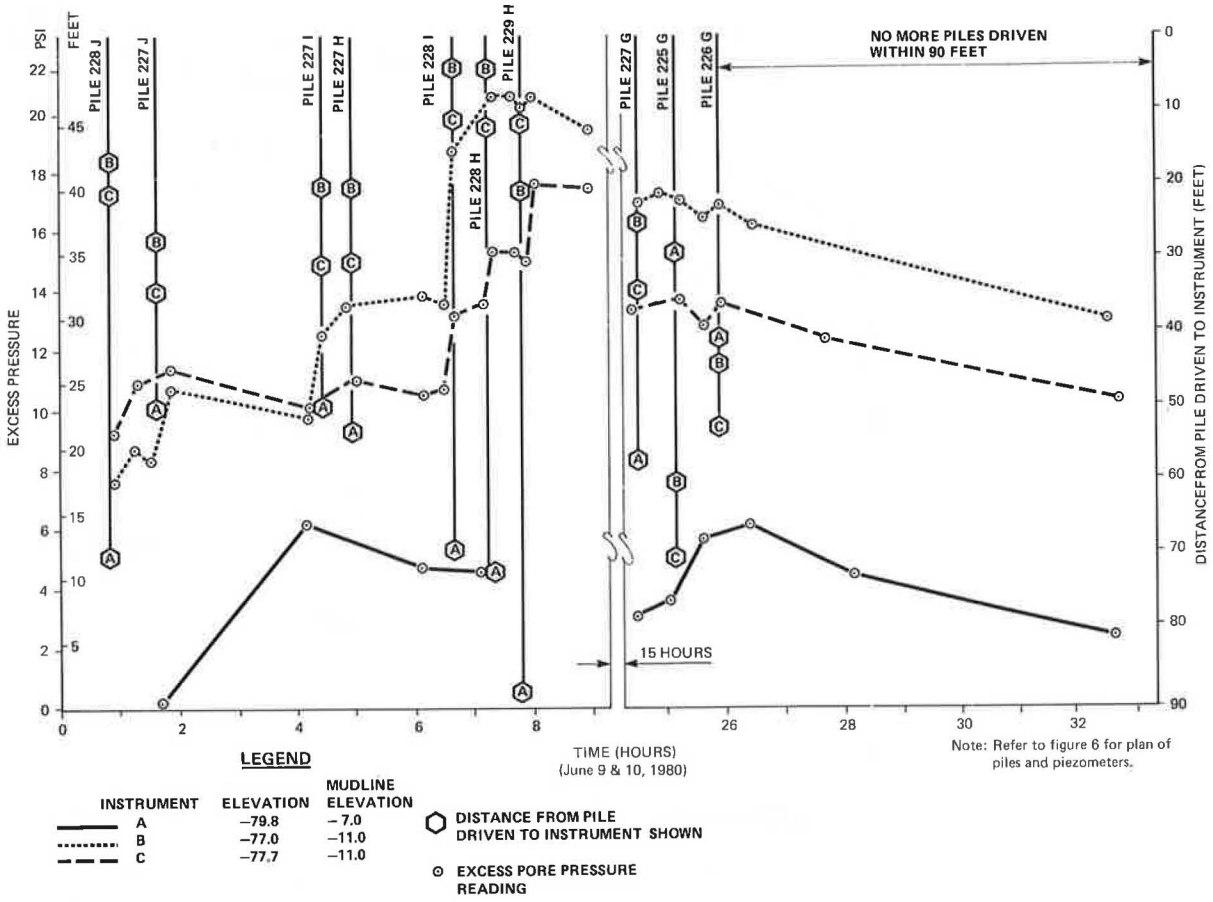

The pressure decreased more slowly than during the initial pile-driving observations (Figure 8).

RESULTS OF SLOPE INCLINOMETER MONITORING

The results of the phase A inclinometer monitoring indicated no significant slope movement during the dredging and filling operations; however, some interesting results were recorded in phase B.

Figure 10 presents data from one typical slope inclinometer from phase B at station 4+25. No deep stability problems were observed in the deep silt layer, as shown by the small size and slow rate of movement. In the upper 20-40 ft of fill, large horizontal movements (about 5 in) and significant acceleration of movements were observed during pile driving within 50-60 ft of the inclinometer casing. After pile driving had moved away from the vicinity of the instrument location, the rate of movement decreased.

DISCUSSION OF RESULTS

The dredging work did not cause any significant increase in pore pressures nor any appreciable soil movements. All of the dredging work, therefore, was performed without changes in the construction techniques.

During filling, the observations indicated no instability except when several dumps were concentrated in one area (Figure 7). As a consequence, the continued dumping of fill was distributed over a larger area to keep the pore-pressure increases low.

During pile driving, phase B piezometers, which were located more than 30 ft from the nearest pile location, registered only occasional pore pressures above the yellow warning level. However, the phase C piezometers, which were located near the pile locations, registered noticeable increases when piles were driven within a distance of 15 ft (11 pile diameters) of the instruments (Figures 8 and 9). When piles were driven within a distance of 12 ft (8.7 pile diameters), the accumulated pore pressures in the silt rose above the yellow warning level. Driving within a 10-ft distance (7.3 pile diameters) caused pore pressures to rise above the red warning level.

The indication in phase B piezometers that the effect of pile driving in the silt was local and did not extend beyond 30 ft (21.8 pile diameters) was confirmed by the phase B inclinometer observations, which showed only small movements in the silt layer (Figure 10).

The horizontal movements in the new fill shown in Figure 10 were considered a result of compaction of the fill from the pile-driving vibrations. The movements, although large, were not considered to indicate instability of the embankment and confirm the densification effect of driving displacement piles into loose granular materials.

Because induced pore pressures were relatively local and dissipated rapidly, and because no slope movements were observed, the pile-driving work suffered only minor disruptions. The results indicated that no more than three piles were to be driven within 30 ft of each other in a 24-h period. This

Figure 10. Slope indicator movement (station 4+25).

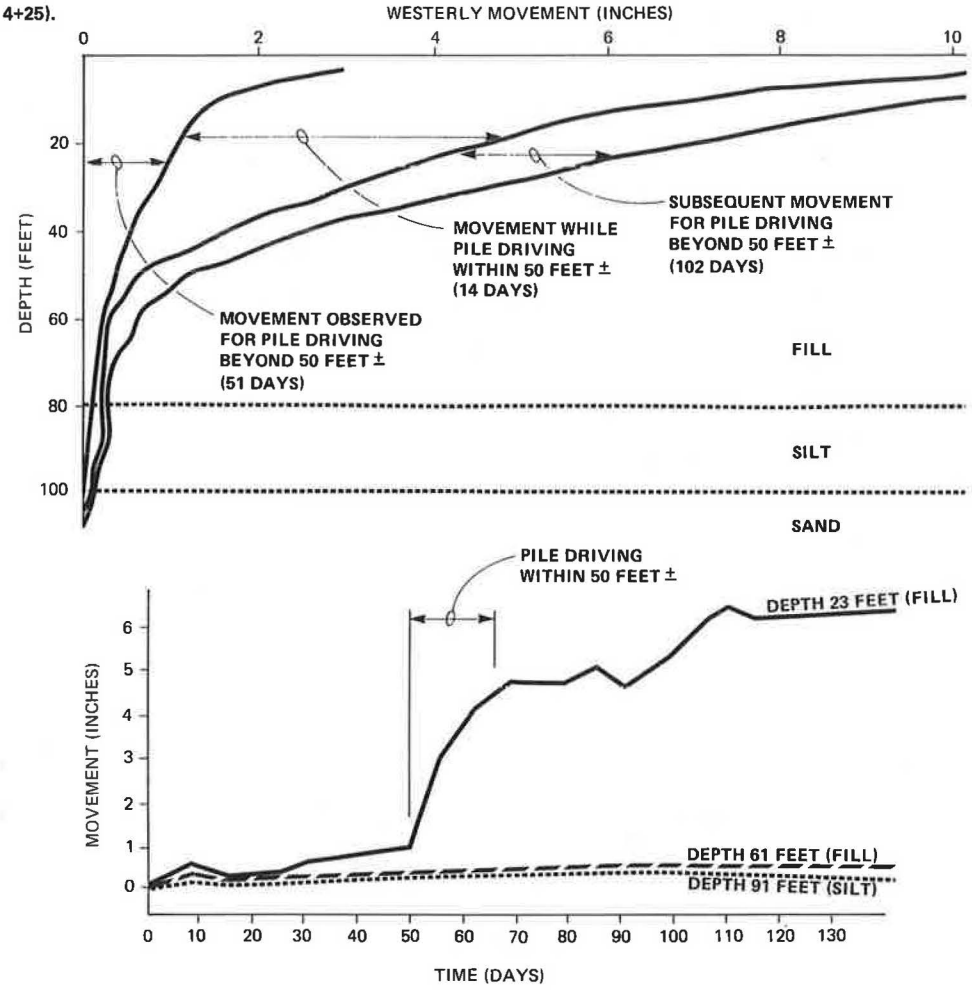

proved to be no hardship on the contractor and caused the pore pressures to remain below the yellow warning level for the remainder of the pile-driving work.

CONCLUSIONS

The construction-control program enabled phase 3 of the port development (new terminal 46) to be designed and built for costs comparable with those for phases 1 and 2. Close monitoring of the silt layer allowed implementation of a design that had factors of safety during construction that would have been unsatisfactory without the use of instrumentation data to control the construction sequence.

ACKNOWLEDGMENT

The project was designed by CH2M Hill and Bengt Fellenius under contract to the Port of Seattle: Vern Ljungren, chief engineer; Eric Soderquist, project manager; and Dean Poole, chief resident inspector. The piling and general contractor was Manson Construction, Seattle, Washington: Gus Lorenz, superintendent.

Discussion

Philip Keene

Fellenius, O'Brien, and Pita are to be congratulated on their clear description of a difficult project. By using modern geotechnical techniques and seasoned judgment, they successfully completed this project, which involved loose inorganic silt, and saved the owner about $1 million. Of special note for the reader is the section on practical problems associated with geotechnical instrumentation; the warnings in this section are a valuable part of the paper.

The most critical feature of the project was the control of pile driving to avoid widespread temporary liquefaction that results in a slide in the silt. Temporary liquefaction of fine-grained soils due to pile driving can be a difficult phenomenon, particularly when the piles are closely spaced (as for a large bridge abutment). As there appear to be rather few case histories of this in the literature, I will describe two cases from my experience when I was head of the geotechnical division of the Connecticut Department of Transportation. The projects were built in 1953 and 1958 and involved cast-in-place piles driven in fine-grained soils. In both cases, temporary liquefaction was generated by pile driving; it took approximately 10-20 days after driving was finished for the liquefaction to be dissipated.

The earlier project, a Farmington River bridge in Simsbury, is briefly described in Keene (1). The soil under the abutments is brown silt, 160 ft thick, and has approximately 0.50-in clay layers every foot. It has a natural water content of 35-40 percent and an N-value of 3 or 4 in the SPT. The design called for 35-ton cast-in-place piles in Monotube shells that were 70 ft long; spacing of piles was 4 ft on centers (front to rear) and 3-6 ft

Figure 11. Simsbury: two pile load tests.

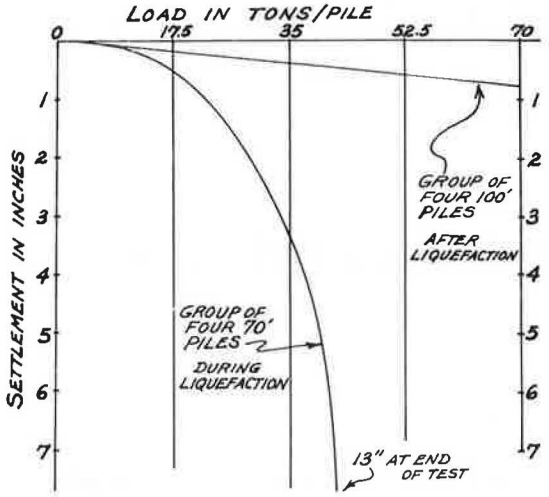

Figure 12. Danbury: load test on test pile.

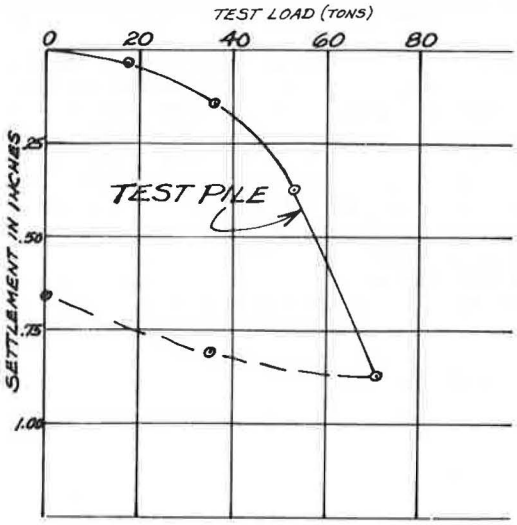

laterally. The plans called for a pile load test on a group of four piles--to be performed after the 25 adjacent piles were driven--to determine their effect on the test. Each load increment (17.5 tons/pile) was to be held for 48 h. The test began 10 days after these 29 piles had been driven; the test piles settled an average of 13 in at 44 tons/pile (Figure 11). Two days after the test was stopped, 30-ft extensions were added to the four test piles at the insistence of the construction engineers. These four piles were then redriven, but the piles had firmed up so much that it required about 130 blows on each of the extended piles to drive the first foot and, after some jetting along the sides of the piles, from 60 to 80 blows/ft to the new penetration of 100 ft. A subsequent load test showed 0.75-in settlement at 280 tons, which was twice the design load (Figure 11). Final pile lengths were made 90 ft. Movements of the abutments were monitored for 18 months and showed settlements of 0.5 in or less. It appears from the above that liquefaction was dissipated at about 17 days after

Figure 13. Danbury: load tests on two separate production piles.

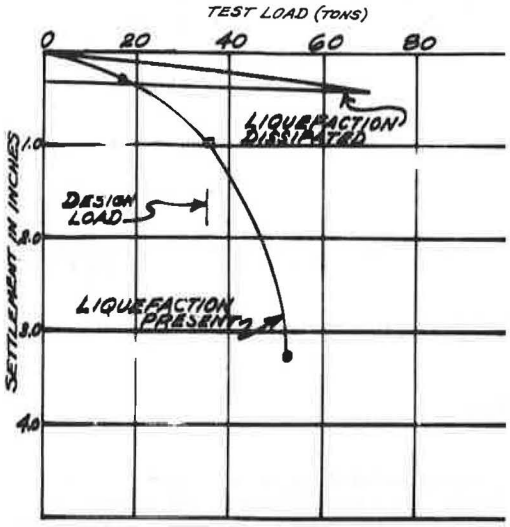

the piles were originally driven, although it may have been hastened around the four test piles by the effect of the first load test.

The other project is in Danbury, Connecticut. A four-lane expressway (later a part of I-84) goes over Tamarack Avenue, a local two-lane street. At the east abutment, four 60-ft test borings that were made under the direction of the consulting (contracting) engineers described the soil as fine sand, trace of silt. The SPT gave N-values of 14 to 20. The 35-ton cast-in-place concrete piles, which were 30 ft long, were designed with spacing similar to those in the project described above. The total for the abutment was 185 piles.

When work began, the contractor chose Raymond standard step-taper piles and drove a 30-ft test pile at each corner of this abutment. The softest pile, driven to 29 blows/ft under a Vulcan 65C hammer (39-ton formula value), was then load tested to 70 tons (Figure 12). It experienced 0.87- and 0.65-in gross and net settlement, respectively. Consequently, 30-ft piles were ordered.

Very soon after production pile driving began, blow counts became very low--about 8-12 blows/ft at the 30-ft depth. Then 40-ft lengths were tried for a few piles; but there was no significant improvement in driving resistance; thus, the rest of the piles were made 30 ft long. Nineteen days after all piles for this abutment were driven, a load test on one of the softest piles (driven five weeks earlier) was performed, with distressing results of more than 3-in settlement at 52 tons (Figure 13). It should be noted that the remaining piles at the far end of the other abutment, which were about 130 ft from the load test, were being driven before and after this load test. At this time, it was discovered that the consulting engineers had made no laboratory tests on the test boring samples. Therefore, grain-size analyses were immediately made of the samples, and it was found that the fine sand, trace of silt had 10-40 percent silt, averaging about 17 percent.

Finally, five days after the distressing load test, all pile driving was completed; six days after that a final load test was made on a different but soft pile. This last test (Figure 13) showed a settlement of only 0.17 in at the 35-ton design load. A review of the dates indicates that liquefaction of the east abutment piles had dissipated about four weeks after all east abutment piles had been driven

or about one week after the last of the west abutment piles, which were 130 ft away, had been driven. Settlement points established when the footing was poured showed final settlement of the east abutment was less than 0.25 in.

REFERENCE

1. P. Keene. Tolerable Movements of Bridge Foundations. TRB, Transportation Research Record 678, 1978, pp. 1-6.

Composite Piles with Precast Enlarged Bases Driven for Fuel Oil Tank Foundations

STANLEY MERJAN

Deep foundations were required for the support of six large fuel oil storage tanks in Queens, New York. A system of 150-ton-capacity composite piles with precast enlarged bases (TPT piles) was selected for the job. An extensive load test program, which included testing of a dogleg pile, was conducted to establish the criteria for pile installation. A variety of installation procedures was required to overcome difficulties in penetrating cumbersome overburden materials to reach the bearing stratum. Hydrostatic loading of the completed tanks showed settlements of less than 0.25 in.

The Power Authority of New York State recently constructed six 6 000 000-gal fuel oil storage tanks for the Astoria Generating Station No. 6 in Queens County, New York City. These tanks each measured 160 ft in diameter by 40 ft high. A fuel oil auxiliary building was also built at this time. All of these structures were designed to be supported on 150-ton-capacity piles. Figure 1 shows the job layout.

CONSIDERATIONS IN SELECTION OF PILE TYPE

The Stone and Webster Engineering Corporation of New York City was the project administrator for the Power Authority and supervised all of the foundation work for the job. They did an extensive subsurface and foundation study to determine the most appropriate support system for this work. Much of the site had been filled in over a number of years. Old drawings were retrieved that showed the location and construction of timber piers and bulkheads that were no longer visibly in evidence. It had been assumed that the remnants of these structures were buried under the fill. This fill contained wood, cinders, and boulders that extended to depths of up to 30-35 ft. Some preliminary excavation at the site in connection with other work revealed the presence of large areas of "subway rock"; i.e., large blocks of mica schist and granite in sizes up to 5 yd^3 that, in all likelihood, were dumped during the construction of the New York City subways.

The soil profile below the fill was not uniform. In general, it consisted of a layer of soft river silt, varved lenses of silt and sand, dense cemented sands and boulders (hardpan), weathered mica schist, and, finally, bedrock that consisted of mica schist and granite that had recoveries of about 40-60 percent in the upper 5 ft. The water table, which was influenced by the tide variations in the adjoining East River, varied between elevation 0 and +5.

The total maximum load on each tank mat was of the order of 30 000 tons distributed over an area of approximately 20 000 ft^2, or 1.5 tons/ft^2. For less onerous soil profiles, the tank slab design would have governed the pile design capacity. Usually this would indicate the use of low-capacity piles spaced closely together, such as 30-ton piles at 4-6 in on center. However, the cost of installing any type of pile through the rough fill material and compressible soils into acceptable bearing soils mandated the selection of a high-capacity pile in order to limit the total number of such units.

A composite pile that had an enlarged base and a capacity of 150 tons was selected to be driven into the dense sand and glacial till below the poorer soils. The enlarged base was needed to develop this high capacity. H-beams or closed-end pipe piles would have to be driven to bedrock to satisfy this design load. The stem of the composite pile was a corrugated shell filled with plain 5000-psi concrete by using type 2 cement for compatibility with the groundwater that had a high salinity because of the adjoining estuary. H-beams would have required an

Figure 1. Test pile location plan.

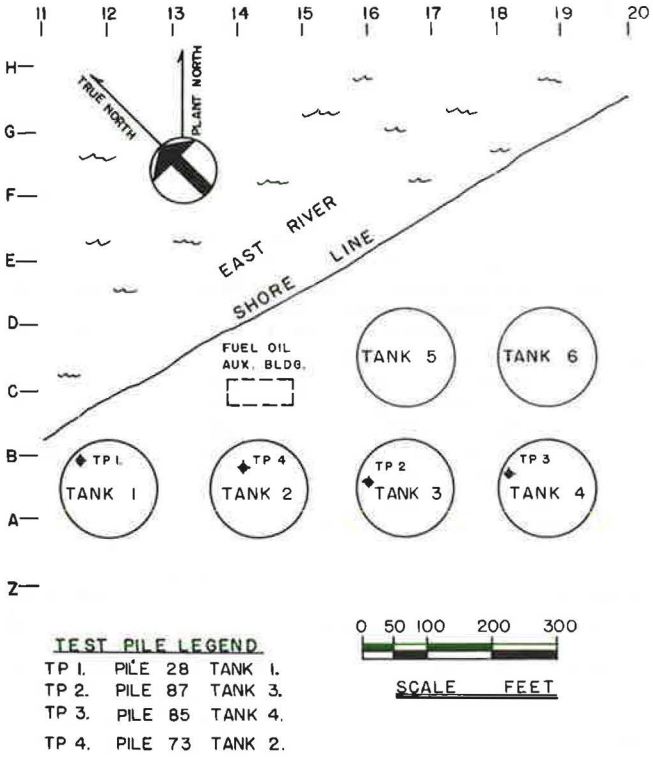

expensive (and vulnerable) bitumastic coating to offset potential corrosion; pipe piles would have needed similar treatment or the discounting of the pipe thickness in determining useful pipe capacity. A total of 213 piles were needed for each tank when spaced on a 10-ft grid pattern.

Figure 2. TPT schematic.

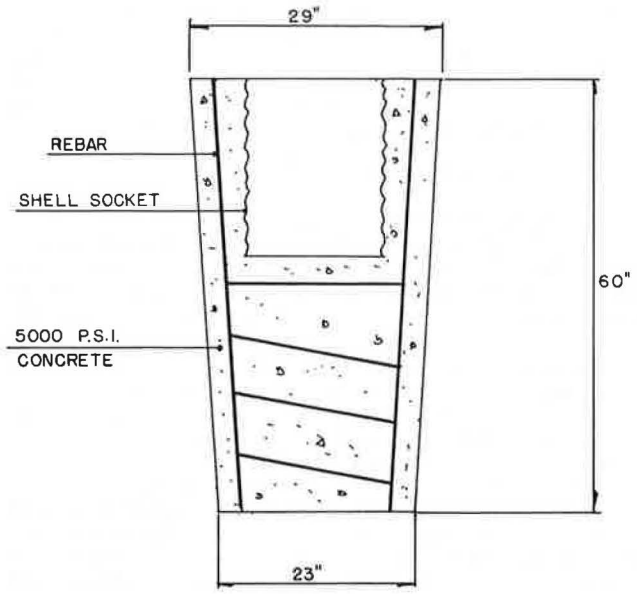

Figure 3. Wave-equation analysis.

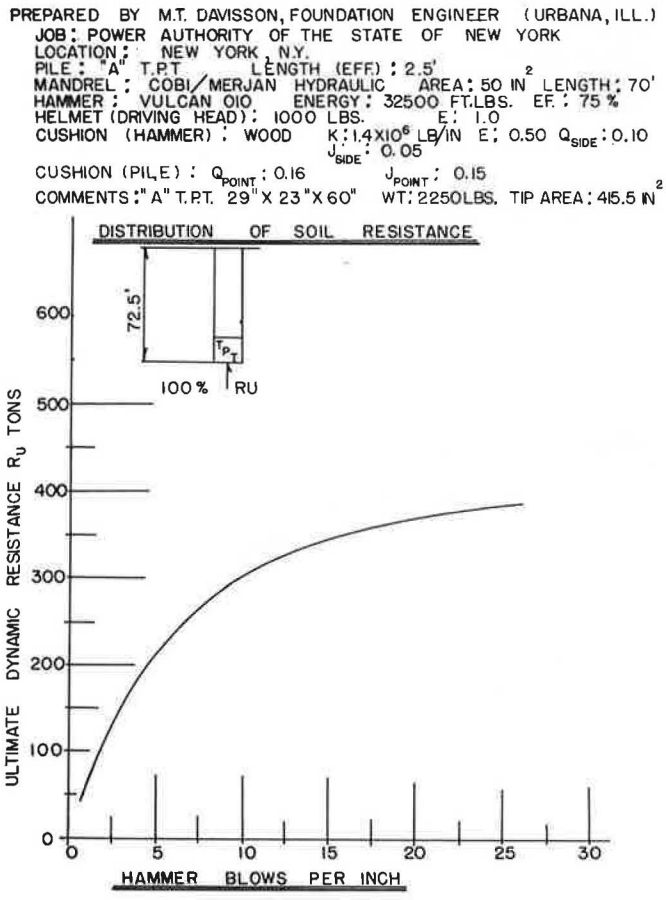

CONTRACT FOR PILING WORK

The bid package was for the foundation piling only. The excavation, concrete, and other work were let separately. Bidding documents called for the use of pressure-injected footings to be installed as end-bearing units into the dense sand, glacial till, weathered rock, or bedrock. However, the Power Authority agreed to consider bids based on the use of other piling types, including H-piles and composite concrete piles with precast bases. The form of the bid was "lump sum"; the pile capacity was to be guaranteed irrespective of pile length. There was no provision for payment of any costs resulting from installation difficulties.

Underpinning & Foundation Constructers, Inc., of Maspeth, Queens, was the low and successful bidder for this work at $1 931 000. This bid was based on the use of composite piles with precast enlarged bases (TPT piles, a patented piling system licensed for use by Underpinning & Foundation Constructors, Inc.). Another bidder proposed the use of the specified pressure-injected footings for $2 490 000. There were several other bids tendered based on the use of H-piles and cast-in-place shell piles. These bids were not responsive, in that the costs due to obstructions were excluded.

The unit price per 150-ton-capacity TPT pile was $1350 each, or $9.00/ton of pile capacity. The pressure-injected footings were bid at approximately $1750 each, or $11.67/ton of capacity. The H-pile and shell pile bids cannot be compared on an equal basis because these bids were not all-inclusive. However, the unit prices for each of these piling types, as bid, were well in excess of $9.00/ton.

DESCRIPTION OF TPT PILES

The composite piles (TPT piles) selected for the job consisted of the following items:

1. Precast concrete base: The top diameter was 29 in, bottom diameter 23 in, and height of the base 60 in. A helically corrugated shell socket that had a nominal diameter of 16.25 in and a steel plate welded to its bottom was cast into the 5000-psi concrete base to a depth of 30 in. Steel reinforcing consisted of vertical bars arranged around the perimeter and U-shaped bars under the socket (see Figure 2).
2. Pile system: A length of 16-in nominal diameter by 16-gauge-thick helically corrugated steel shell was threaded mechanically into the socket. Mastic waterproofing material was applied to the base of the stem to seal the joint. Subsequent to the driving of the pile, the shell stem was filled with plain concrete that had a 28-day strength of 5000 psi.

TEST PILE PROGRAM

Job specifications called for the installation of test piles and the performance of three load tests. A fourth load test was added to establish a maximum sweep limitation for doglegged piles.

The test pile-driving criteria were established with wave-equation analysis (Figure 3). The hammer selected for the job was an air-operated single-acting Vulcan Model 0-10 that had an energy rating of 32 500 ft-lb. An expandable mandrel with a 1-in pipe wall thickness transmitted the hammer blows to the base of the socket in the precast pile tip. The wave-equation analysis indicated that a final driving resistance of 10 blows/in was necessary to produce an ultimate capacity, as required, of 300 tons. The contractor chose to increase this final

resistance to 12 blows/in, adding 2 blows/in to compensate for some of the indeterminate and variable elements of the assumptions required for the theoretical analysis. A fourth load test was added to establish the maximum sweep limitation for doglegged piles.

The load tests were conducted in accordance with ASTM D1143-74. The test arrangement consisted of a group of four 200-ton-capacity hydraulic rams set over the test pile to jack against a steel platform loaded with cast steel weights. The load was monitored by means of three pressure gauges, which had been calibrated in conjunction with the rams, and an electronic load cell. During the tests, there was good correlation between the two measurement systems. Ames dial extensometers, which are accurate to 0.001 in, were used to measure pile movement at the butt and the tip. Measurements of pile tip movement were facilitated by means of a 0.5-in-diameter steel rod dropped into a 1-in-diameter casing cast into the pile stem that extended to the base of the socket in the pile tip. This tip-measuring arrangement was not possible for the dogleg pile test; in that instance, a grooved plastic casing was set in the pile and an inclinometer was inserted into the casing to measure slope changes at each loading increment.

LOAD TEST RESULTS

The results of the first three load tests showed that the driving with the Vulcan 0-10 hammer to 12 blows/in for the 150-ton-capacity piles was satisfactory. Net settlements (after unload) at the pile tip were less than 0.25 in for tests 1 and 2; test 3 sustained a net settlement of about 1.125 in, but this pile was driven to only 9 blows/in (see Figures 4, 5, and 6).

Load test 4 (Figure 7) was conducted on a pile where the sweep was such that the tip was deflected in excess of 19 in over the total pile length of approximately 50 ft; most of this deflection occurred in the lower 35 ft. As was the case for all other piles, no reinforcing was used with the concrete in the pile stem. The net butt settlement after the completion of the test was about 0.75 in; a maximum lateral displacement of about 2 in was measured at the midpoint of the pile under the 300-ton load with continuing creep, which indicated the possibility of eventual pile failure at the 300-ton loading level. The effect of the lateral displacement on vertical settlement was determined to be minimal (less than 0.000 07 in at 2-in horizontal displacement). After unloading, the lateral displacement rebounded to 1 in. The results of this load test were used to establish the geometry of the sweep of this pile, which was to be the limiting condition for acceptance. Of all piles subsequently driven for the job, less than 2 percent were doglegged and none of these was as severe as the pile load tested.

INSTALLATION OF CONTRACT PILES

The driving of the contract piles was done over a five-month period; two pile drivers worked 5-day, 40-h work weeks. Many problems were encountered during the course of the job, and virtually all of these were in connection with difficulties that developed in the attempt to penetrate the upper soils to the bearing strata.

Before pile driving was begun in each of the tanks, the contractor first preexcavated along the pile grid lines to a depth of about 20 ft by using a 2-yd³ hydraulic backhoe. This was an essential operation because of the impenetrable fill in this zone. Old bulkheads had to be ripped apart and rock boulders excavated. Most of this excavation was done below water, as the water table was only 5 ft below grade. Large obstructions were culled from this material and hauled away. Unclassified soil was added to the remainder, and a front-end loader restored each area to subgrade.

Those areas of the job that had obstructions below the effective digging depth of the backhoe (about 20 ft) were spudded. The spud consisted of a 14-in-diameter by 1-in-thick pipe mandrel that was 50 ft long and driven with the Vulcan 0-10 hammer. The spud was driven to a depth of about 40 ft or

Figure 4. Pile load test 1.

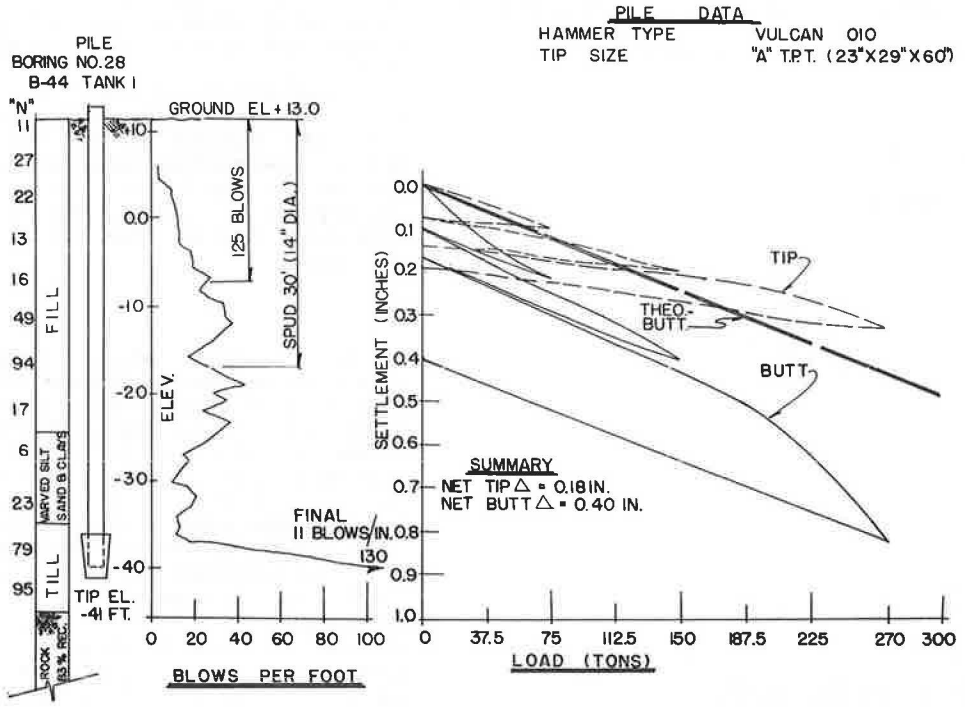

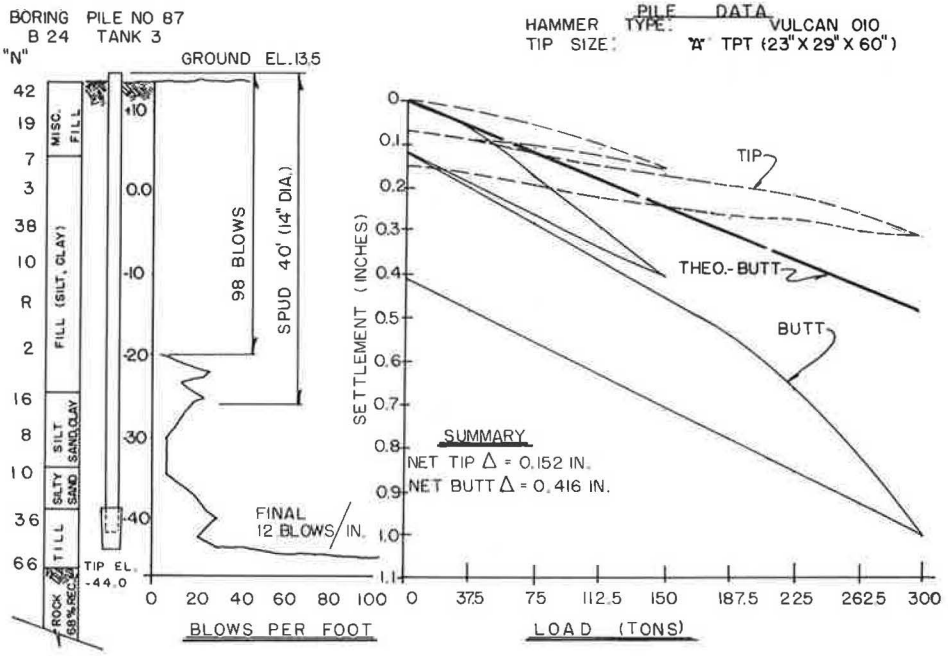

Figure 5. Pile load test 2.

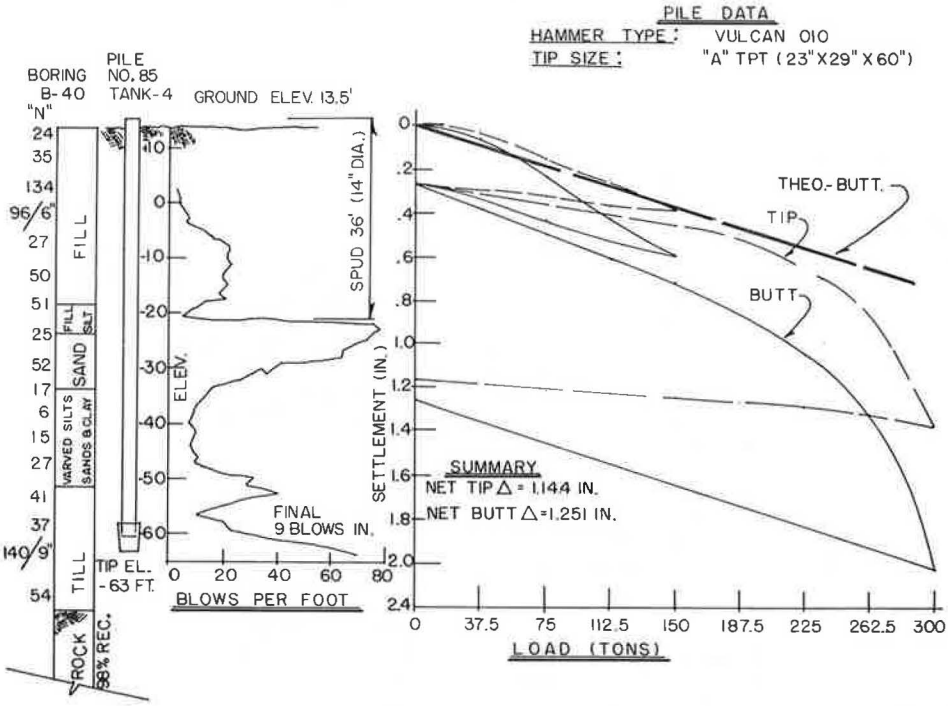

Figure 6. Pile load test 3.

less when the driving resistance indicated that the obstructed zone was penetrated. This was an effective procedure. Old cribbing and timbers were split and medium-sized obstructions were broken up or dislodged, thereby making it possible to penetrate the obstructed zones with the piles. There were some locations that were abandoned, and these piles were relocated to avoid the obstructions. The specifications required piles to be driven within 12 in of plan location; when piles were relocated, the concrete mat was redesigned as required.

Driving difficulties developed in areas of the site that had intermediate zones of dense sand above the varved silts and clays that had to be penetrated. A wet-rotary-drilling system was attempted, but without success, because of the character of the overlying fill. Therefore, it was necessary to hard-drive through the dense soil, and driving resistances of 600-1200 blows/ft were sometimes necessary to penetrate this zone. Once the pile tips were advanced below this layer, driving resistance abated and the piles successfully reached the intended bearing soils.

One localized area existed at the westerly side of tank 6 where the intermediate sand stratum was too dense to be penetrated by the enlarged base piles. In this area, approximately 15- to 100-ton-capacity pipe piles, which were 14 in in diameter by 0.375 in thick, were substituted in accordance with criteria that had been established for a nearby liquefied natural gas tank foundation.

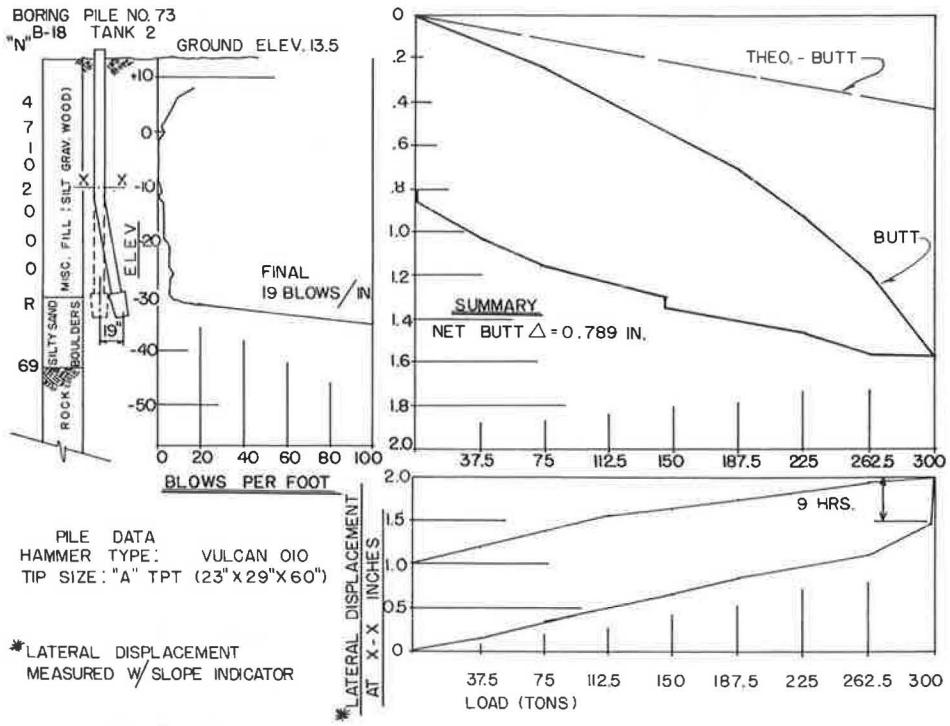

Figure 7. Pile load test 4.

Another type of difficulty was encountered in an area where the soft silts extended to a depth of 50 ft and below. These piles were driven with little difficulty, but the shells collapsed near the bottom of the silt zone almost immediately after the mandrel was withdrawn. This area was defined, and shell stems of 14 gauge thickness were substituted for the 16 gauge thickness to overcome the intense pressure buildup that caused the shell failure.

Where abandoned piles required replacement at locations within 7 ft or less of other driven piles, "keeper pipes" 14 in in diameter by 0.250 in thick were inserted into the stems to prevent collapsing of the shell. In some of the more heavily obstructed areas, 16-in-diameter by 0.250-in-thick pile stems were substituted for the corrugated shell.

The precast enlarged bases of these piles proved to be extremely effective in displacing obstructions beyond the radius of the ensuing shell stems. This is a particular advantage of this pile system. Other advantages demonstrated by this piling type were as follows:

1. Bearing capacity was achieved with relatively shallow penetration into the designated bearing stratum. This was the result of the large displacement area of the pile tip and the densification that increased the strength of the soil below.
2. The piles were driven by using conventional equipment and methods of inspection.
3. Productivity was high, particularly with respect to what could have been anticipated for pressure-injected footings. An average of seven piles were installed during each rig shift. Pile driving was completed within the allocated time frame of six months by using two driving rigs.
4. Relatively few piles (less than 10 percent) were damaged or failed to reach the bearing stratum.

MEASUREMENTS OF SETTLEMENT FOR COMPLETED TANKS

Prior to filling the tanks with fuel oil, each was filled with water. This was done to confirm the soundness of the welded-steel-tank construction as well as the performance of the reinforced concrete mat and pile foundation. The total load of the tanks when filled with water was 150 tons/pile; the weight of the unfilled tank loaded the piles to about 25 tons apiece. The measured settlement of the fully loaded tanks varied from 0.16 to 0.24 in, which was less than the engineer's predicted settlement.

CONCLUSION

The composite piles with precast enlarged bases were a good choice for this high-capacity foundation system. Although many serious difficulties arose during the course of this installation, the various minor modifications in procedures and materials that were chosen to contend with each variety of difficulty produced, in total, a successful and economical job. The testing program was used effectively to prescribe practical driving criteria and procedures to ensure the satisfactory performance of the foundations.

Notice: The Transportation Research Board does not endorse products or manufacturers. Trade and manufacturers' names appear in this paper because they are considered essential to its object.

Pile Foundation: West Seattle Freeway Bridge Replacement

GEORGE YAMANE AND MING-JIUN WU

The planning and methods used in assessing an economically optimal and technically appropriate pile foundation for the construction of the West Seattle Freeway Bridge are described. The site and subsurface conditions also are described. Of special interest is the process of foundation selection and the consequent test procedures and equipment used. A test pile program was initiated at five selected locations along the proposed alignment to determine and evaluate the driveability and vertical load-carrying capacity of the concrete and steel piles. This testing program was accomplished during the initial design stage. The program included hammer selection, test pile driving, pile loading tests, load transfer, and dynamic measurements. The results of these operations are presented. The pile test program provided the information necessary for development of pile installation specifications. Test pile-driving records are believed to have assisted the contractors in preparing their bids. Overall project costs were below the engineer's estimate.

The City of Seattle is constructing a replacement bridge and related roadway system where a ship collision left the north bascule bridge across the west waterway inoperable at the Southwest Spokane Street corridor of the West Seattle Freeway. The corridor is one of the busiest in the State of Washington; a daily traffic count of 80 000 vehicles/day is projected for this corridor by year 2000. The bridge replacement consists of elevated structures and interchanges located at the east and west ends of the project, as shown on Figure 1.

The project is divided into four major parts for design and contract award purposes: (a) main span structure, (b) Harbor Island structure, (c) east interchange structures, and (d) west interchange structures. Construction began on the main span structure in November 1980, and the total project is scheduled to be completed by 1984. Because of thick deposits of alluvial sands and silts along the project alignment, heavy structural loads, and the potential of soil liquefaction during a strong earthquake, deep pile foundations were selected for support.

This paper describes the selection process for the piles and capacities, verification by the pile load test program, and the incorporation of the pile test results into the contract specifications.

SITE DESCRIPTION AND GEOLOGY

The site of the bridge replacement is near the mouth of the Duwamish River where it empties into Puget Sound on the south shore of Elliot Bay. A mile before the Duwamish reaches Elliot Bay, it divides into two channels that flow on either side of Harbor Island. Both waterways are about 350 ft wide. The west waterway is used as a navigation channel for large vessels.

The Duwamish Valley is situated in the central part of the Puget Lowland, which is a structural and topographic trough. It is underlain chiefly by thick deposits of Quaternary sediments that overlie interbedded Tertiary volcanic and sedimentary bedrock. Most of the major topographic features of the lowlands are the results of glacial deposition or erosion.

The original valley floodplain has been raised about 10-15 ft by hydraulic fill. The alluvial deposits are as much as 270 ft thick and consist of loose to dense sand with scattered layers of silt that have some plasticity. A generalized subsurface profile is shown in Figure 1.

FOUNDATION SELECTION AND TESTING

Timber, steel pipe of various diameters and wall thicknesses, and prestressed concrete piles of various diameters were considered during the preliminary design stage in order to select a cost-effective pile foundation for this project. In selecting the pile type and capacity, foundation settlement, lat-

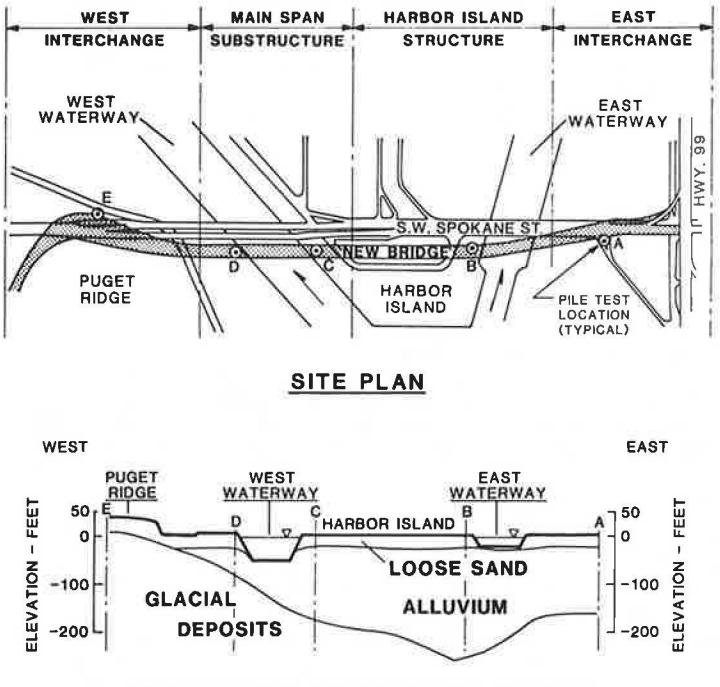

Figure 1. Site plan and generalized subsurface profile.

Table 1. Concrete pile load testing program.

Item	Site A	Site B	Site E
Load test pile diameter (in)	24	24	24
Anchor piles (concrete)	Two at 16.5 in and two at 24 in	Four at 24 in	Four at 16.5 in
Tests performed			
Dynamic measurements	2	5	4
Compression load	1	1	1

Table 2. Steel-pipe pile load testing program.

Item	Site C	Site D
Load test pile (open-ended)	24x1.25 in	24x1.25 in
Anchor piles (steel pipe)	36x0.75 in; open-ended 24x1.25 in; closed-end 24x0.75 in; open-ended	36x0.75 in; open-ended 24x1.25 in; open-ended 24x0.75 in; closed-end
Tests performed		
Dynamic measurements	3	3
Compression load	1	1
Tension load	1	1

eral resistance, and bending of piles (with and without soil liquefaction under the earthquake design) were considered among other structural factors.

The preliminary pile lengths and capacities were estimated by using several static-capacity analysis methods and results of pile load tests performed near the project site. Based on the studies, structural requirements, and economic considerations, the following piles were selected for design:

Structure	Pile Type
Main span	36-in-diameter, 0.75-in-wall steel pipe pile, driven open-ended; 600-ton design capacity
Main line structure	24-in octagonal prestressed concrete piles with 15-in-diameter hole in the center and the bottom end plugged; 200-ton design capacity

The estimated pile lengths were about 140-220 ft for the steel pipe piles and about 70-120 ft for the concrete piles.

Field explorations consisted of test borings, Dutch cone probes, and in situ pressuremeter tests. Laboratory shear tests were performed to evaluate the frictional resistance between concrete or steel and soil. Triaxial compression and consolidation tests were also performed.

TEST PILE PROGRAM

During the initial design stage, a pile-driving and pile-loading test program was initiated at five selected locations (as shown in Figure 1) along the proposed alignment to determine and evaluate the drivability and vertical load-carrying capacities of the concrete and steel piles. Driving test piles consisted of 16.5- and 24-in octagonal prestressed concrete piles and 24- and 36-in-diameter steel pipe piles. The wall thickness of steel piles varied from 0.75 to 1.25 in and were driven either closed-ended [fitted with an Associated Pile and Fitting Corp. (AP&F) conical tip] or open-ended (tip reinforced). Dynamic measurements were made by Goble & Associates on selected piles during test pile driving. The load test piles were instrumented to determine the load distribution along the pile.

Pile load tests were made on 24-in prestressed hollow concrete piles at three locations that were designated sites A, B, and E. Pile load tests on 24-in-diameter by 1.25-in-wall steel pipe piles were made at each of the two main pier locations designated as sites C and D. The locations of these five load tests are indicated in Figure 1. A brief summary of the pile load testing program in given in Tables 1 and 2.

CONCRETE PILES: SITES A, B, AND E

Pile load test results and interpretations at sites A and B are presented separately from site E because of differences in subsurface conditions. The soil conditions encountered at sites A, B, and E are shown in Figures 2, 3, and 4, respectively.

Hammer

Air, steam, or diesel-operated hammers that had rated energies ranging from 60 000 to 90 000 ft-lbf/blow were specified for the test program. Preliminary wave-equation analysis indicated that diesel hammers may be more effective in obtaining the desired pile penetration due to the higher hammer stroke for the long piles. The contractor selected a single-acting Kobe K45 diesel hammer because of lighter weight. The stroke of the hammer was determined by several identifiable features on the ram along with a saximeter developed by Pile Dynamics, Inc. The observed hammer energy for the last 5 ft of driving ranged from 71 420 to 79 400 ft-lbf/blow, and averaged around 74 400 ft-lbf.

Pile-Driving Resistances

Generally, the pile-driving resistance of the 24-in concrete piles within the alluvium was about equal to the N-values, as shown in Figures 2 and 3. Hard driving conditions were encountered when the pile was driven through very dense sand that had N-values greater than 50 blows/ft. At site E, the driving resistance of the 24-in concrete piles was somewhat less than the N-values until the pile tips penetrated into glacial clay, after which the driving resistance increased with pile penetration, as shown in Figure 4. Dynamic measurements were taken at the end of continuous driving and at redrive after 12 h or more.

Pile Load Tests

One compression load test each was performed at sites A, B, and E. The piles were tested to plunging failure or to the proposed maximum test load of 600 tons. Load versus pile settlement re-

sults are presented in Figures 2, 3, and 4 for sites A, B, and E, respectively.

Two independent measuring systems were used to measure the strain at various points along the load test piles to estimate the load distribution. These were (a) the Slope Indicator Company (SINCO) vibrating-wire strain gauges and (b) stainless-steel telltale rods that were 0.25 in in diameter. The strain gauges and the base mounts for the telltale rods were welded to a 2.5-in square steel casing that had a 0.125-in wall thickness. The instruments were installed in the central hole of the pile after pile driving. Following installation of the instruments, the pile was backfilled with high-early-strength sand-cement grout.

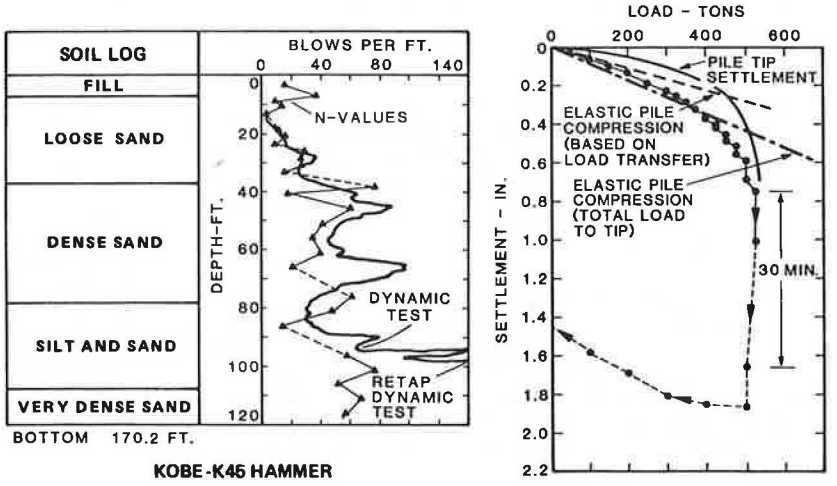

Figure 2. Site A 24-in concrete load test pile (A-LTP): driving resistances and load versus settlement.

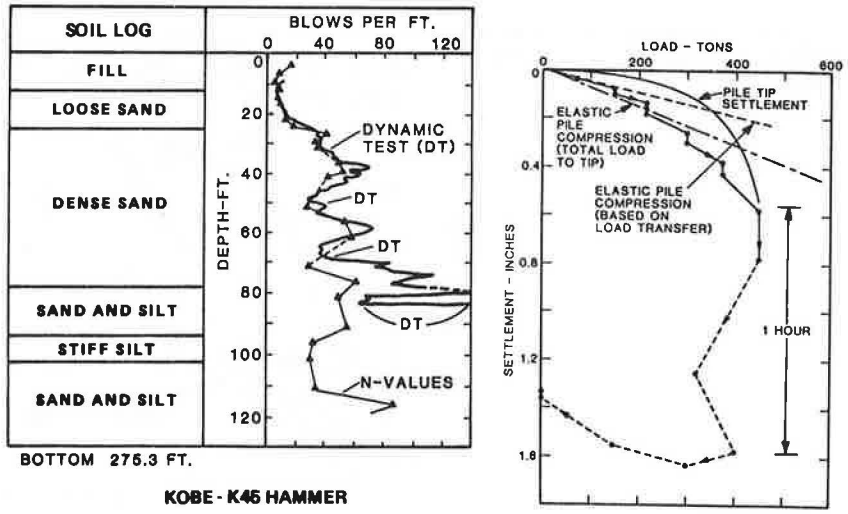

Figure 3. Site B 24-in concrete load test pile (B-LTP): driving resistances and load versus settlement.

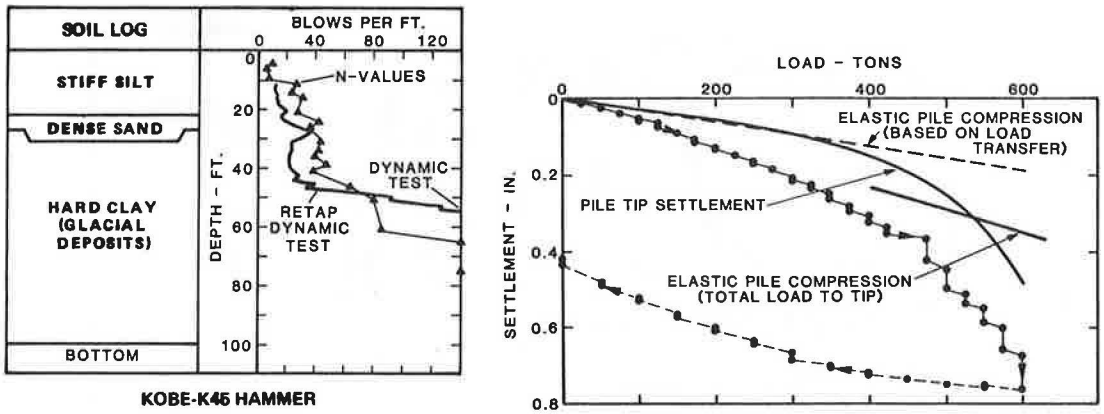

Figure 4. Site E 24-in concrete load test pile (E-LTP): driving resistances and load versus settlement.

Load Transfer Measurements

Loads at the strain gauge level were computed by using the following formula:

$$P = E_c * A_p * q_e \quad (1)$$

where

P = applied load,
E_c = composite elastic modulus,
A_p = cross-sectional area of pile, and
q_e = change in strain of pile between zero load and applied load.

The deflection between the top of the telltale rod and the top of the pile was measured with a linear potentiometer. The average load between two telltale tips was determined by the following equation:

$$P = E_c * A_p * \Delta L/L \quad (2)$$

where L is the distance between the two telltale tips and ΔL is the measured deflection difference of the two telltales. The possible residual strain of the backfilled grout was not measured. The composite elastic modulus of concrete was computed by assuming that the load at the top-level instruments was equal to the applied load on top of the pile by using the above equations.

The load distributions along the load test piles are shown in Figures 5, 6, and 7 for sites A, B, and E, respectively. Loads computed from strain gauges are shown at the instrumentation level. The tip of the telltale rods were located at the strain gauge level. Therefore, the average load from the telltale-rod data are plotted midway between strain gauge levels.

Ultimate Pile Capacities

The ultimate pile capacities, as obtained from static pile tests and dynamic measurements at sites A, B, and E, are summarized in Table 3. The results in Table 3 indicate that the ultimate capacities, as determined by dynamic measurements during restrike of piles A-LTP and B-LTP, corresponded closely to the static test loads at failure. Restrike dynamic measurements were not made on the 24-in concrete pile at site E due to scheduling. Pile freeze capacity (or setup) ranged from 70 to 200 tons for the 24-in concrete piles, depending on soil conditions, pile penetration, and setup time allowed.

Piles A-LTP and E-16.5 (corrected to simulate the E-LTP 24-in pile) were analyzed by using the CAPWAP method to provide an estimate of ultimate frictional resistance along the pile during a selected hammer blow. These results are shown in Figures 5 and 7. The plots indicate a shape similar to that of the measured static load transfer data, but the magnitude in loads is slightly greater.

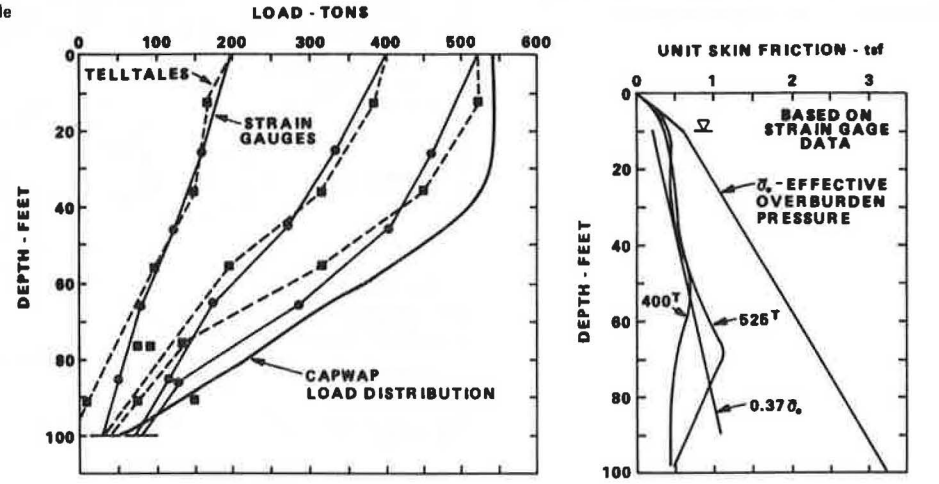

Figure 5. Site A 24-in concrete load test pile (A-LTP): load distribution and unit skin friction.

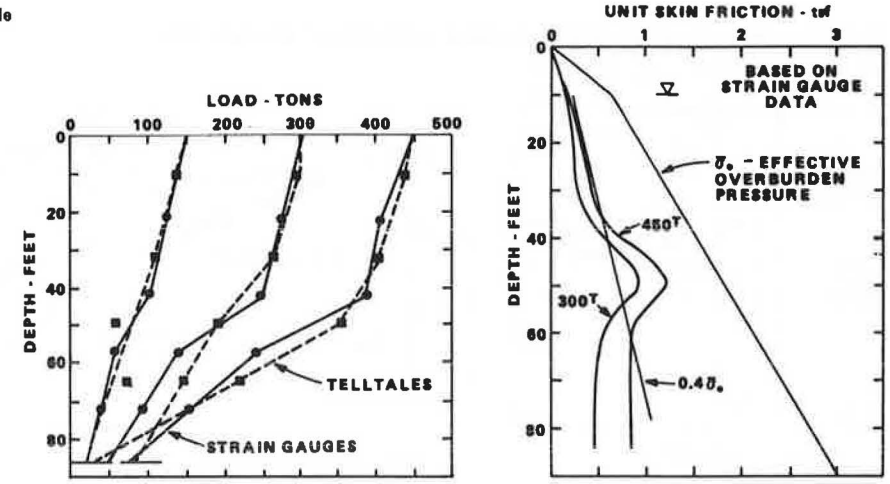

Figure 6. Site B 24-in concrete load test pile (B-LTP): load distribution and unit skin friction.

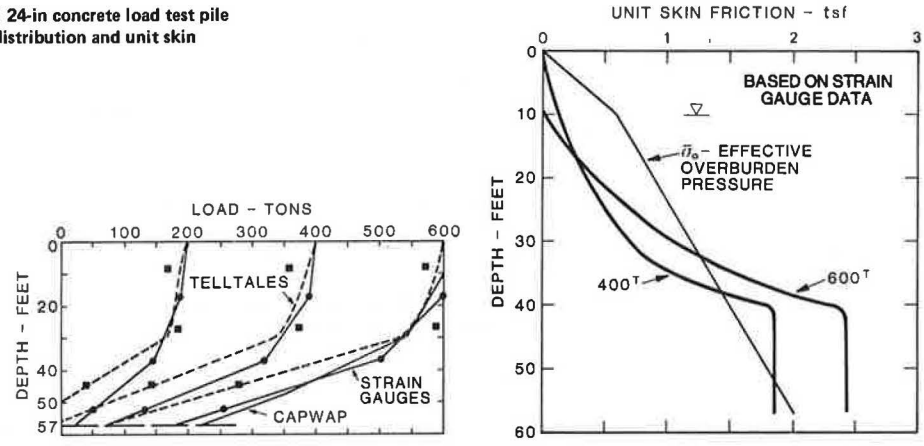

Figure 7. Site E 24-in concrete load test pile (E-LTP): load distribution and unit skin friction.

Note: CAPWAP load distribution was extrapolated from E-16.5 dynamic measurements.

Table 3. Summary of pile capacities (concrete).

Site	Pile	Penetration (ft)	Ultimate Capacity (tons)	Method	Failure Load (tons)
A	A-LTP	98.5	542(R)[a]	CAPWAP	525
	A-16.5	96	321(R)[b]	CAPWAP	
B	B-LTP	83.5	352(EOD)	CAPWAP	425
			422[c]		
	B-NE	72	423(R)	CM J = 0.15	
		77	357(EOD)	CM J = 0.15	
			427[c]		
E	E-LTP	45	235(R)	CM J = 0.5	
		57	NA		>600
	E-S(24)[d]	50	376(R)	CAPWAP	
	E-16.5	63	448(R)	CAPWAP	

Note: R = restrike, CAPWAP = Case pile wave analysis program, EOD = end of continuous driving, CM = Case method, J = Case damping value, NA = not available, and Setup (pile freeze) determined from EOD and R data.
[a]Setup = 200t.
[b]Setup = 65t.
[c]Assumes Setup of 70 tons.
[d]Driving test pile.

Load Test Results and Interpretation

The elastic pile deflections, which were based on the measured load transfer data, were calculated by using the formula developed by Vesić (1) and are shown on the load settlement plots (Figures 2, 3, and 4). The elastic pile compression, assuming that the total applied load was transmitted to the tip, is also shown.

Sites A and B: Alluvial Deposits

Apparent Skin Friction

The magnitude and distribution of apparent skin friction (Q_s) were developed by using the measured load transfer data and the following equation:

$$Q_s = p^* f_s \quad (3)$$

where

p = surface area of pile,
f_s = unit skin friction (alluvial deposits) = $\bar{\sigma}_o$ Ktanδ,
$\bar{\sigma}_o$ = average effective overburden pressure along pile shaft,
K = lateral earth pressure coefficient, and
tanδ = coefficient of friction between pile and soil.

Estimated average Ktanδ values were about 0.37 at site A and 0.40 at site B. The ultimate apparent unit skin friction was about 1 ton/ft², which corresponds well with values recommended by Meyerhof (2) and Reese and Wright (3) for N = 40-50 blows/ft cohesionless soils.

The frictional angle (δ) between sand and a concrete block was about 31° when measured by using direct shear equipment. Thus, tanδ = 0.6. By using this value, the K values at sites A and B would be about 0.62 and 0.67, respectively.

Apparent End Bearing

The measured point loads at failure were about 84 and 77 tons at sites A and B, respectively. The apparent end-bearing pressures would then be 25.7 and 23.6 tons/ft². These apparent end-bearing pressures are less than those calculated from the ultimate end-bearing capacity formula for deep foundations.

Test data obtained by Bozozuk and others (4) indicate that ultimate skin friction is fully mobilized when the pile tip settlement is about 0.16-0.2 in. Once the ultimate skin friction is fully mobilized, the frictional resistance may remain constant or may decrease but would not increase under additional applied load. Thus, the additional load will be transmitted to the pile tip. The amount of strain or deflection of the pile tip to develop end bearing is believed to be greater than that required to develop the ultimate skin friction. In addition, Vesić (1) and Hunter and Davisson (5) found that, after pile driving, residual stresses may remain in the soil around the pile and below the pile tip. We believe that the end-bearing capacity would be

greater than that measured if residual stresses are considered.

Site E: Glacial Deposits

A plot of measured pile top and tip settlement versus applied load for a 24-in concrete pile driven into glacially overridden clay at site E is presented in Figure 4. Under the maximum test load of 600 tons, the net settlement (after rebound) was 0.44 in. The ultimate load is estimated to be about 650 tons.

Apparent Skin Friction

The apparent skin friction between a pile and clay was determined by the following equation:

$$Q_s = p*f_s \quad (4)$$

where

Q_s = shaft friction load,
p = surface area of pile,
f_s = unit skin friction (clay) = $c*\alpha$,
c = undrained shear strength, and
α = reduction factor.

The apparent unit skin friction was about 2.43 tons/ft² at an applied load of 600 tons below a depth of 40 ft, as shown in Figure 7. The apparent skin friction appears to be relatively uniform. The N-values were generally greater than 50 blows/ft in this zone.

The undrained shear strength of the glacially consolidated clays was determined in triaxial compression by first consolidating undisturbed specimens under an effective confining pressure of 400 psi, which is the estimated preconsolidation pressure. The confining pressures were then reduced to three selected pressures and each specimen allowed to swell. The specimens were then sheared in an undrained condition. These tests resulted in an undrained shear strength of 6.5 tons/ft² at an overburden pressure of 3 tons/ft².

The apparent unit skin friction (f_s) under the maximum test load of 600 tons is about 2.43 tons/ft². Assuming c = 6.5 tons/ft², the reduction factor (α) is 0.38. Considering that the skin friction was almost fully mobilized under a test load of 650 tons, the reduction factor (α) would be 0.4.

Apparent End Bearing

As shown on the load transfer plot (Figure 7), the point bearing load (Q_p) increased from 22 to 73 to 178 tons at applied loads of 200, 400, and 600 tons, respectively. These correspond to end-bearing pressures of 6.6, 22, and 54 tons/ft², respectively. The pile tip settlements were about 0.06, 0.15, and 0.49 in, respectively, which indicate that the rate of pile tip settlement increased after the 400-ton load.

The ultimate end bearing of driven piles in clay may be determined from the following equation:

$$Q_p = 9*c*A \quad (5)$$

where

Q_p = end bearing,
9 = bearing capacity factor for deep foundations in clay,
c = undrained shear strength, and
A = area of pile tip.

At an estimated load of 650 tons, the end-bearing pressure from the load transfer plot is about 60 tons/ft². By using the above equation, the calculated c would be about 6.7 tons/ft², which is near the ultimate c-value of 6.5 tons/ft² that was obtained from the high-pressure triaxial compression test.

STEEL PIPE PILES: SITES C AND D

The main span substructure piers are to be supported by 36-in-diameter by 0.75-in-wall steel pipe piles, which are to be driven open-ended. These piles are designed for a 600-ton static dead plus live load, plus an additional 600-ton seismic load. It was not considered feasible to conduct a pile load test on a 36-in-diameter pipe pile. Therefore, a 24-in-diameter by 1.25-in-wall steel pipe pile driven open-ended was tested and the results used to analyze the 36-in pile. The ultimate capacity of the 36-in steel pipe pile was also estimated by dynamic measurements.

As shown in Figures 8 and 9, sites C and D are underlain by fill and alluvial deposits consisting of sand, silt, and clay and then by the glacially overridden deposits of interbedded hard clay and very dense sand and silt.

Hammer

Several hammers, including a steam-powered Vulcan 060 (rated energy = 180 000 ft-lb/blow), a Conmaco 300/5 (rated energy = 150 000 ft-lb/blow), and a Delmag D62-12 diesel hammer were initially considered for driving the steel pipe piles. Wave-equation analyses that used a revised wave-equation analysis for pile driving (WEAP) program for the three hammers along with pile and subsoil combinations were performed by Goble & Associates. The results revealed that, under the same rated energy, the hammer with a longer stroke would drive the long steel piles (>150 ft) more efficiently. Thus, a single-acting Delmag D62-12 diesel hammer was selected. Based on the hammer strokes measured from a saximeter, the range of average hammer energy for the last 5 ft of penetration was 112 000 to 156 300 ft-lb/blow.

Driving Penetrations and Resistances

All steel pipe piles were driven into the glacially overridden deposits. At site C, the piles penetrated 30-34 ft into the glacial bearing layer, while at site D the piles penetrated 52-63 ft (excluding closed-end piles) into the glacial bearing layer. The 24-in closed-end pile at site D penetrated only 31 ft into the glacial bearing layer.

The driving resistances above the glacial deposits were on the order of 10-40 blows/ft at site C (Figure 8) and about 10 blows/ft at site D (Figure 9). These resistances increased with depth to more than 120 blows/ft when the piles were penetrating into the glacially overridden deposits. At sites C and D, the driving resistances of the 24-in open-ended and closed-end piles were about the same magnitude above the glacially overridden deposits, but the closed-end piles drove harder in the glacially overridden deposits.

Pile Load Tests

Pile load tests were performed on 24-in-diameter open-ended steel pipe piles to form the design criteria for the open-ended 36-in steel pipe piles. The instrumentation system for steel pipe piles was the same as for the concrete piles. The instruments

were installed after removing the soils inside the pile with a churn drill.

At site C, the compression test was terminated at an applied load of 750 tons when a shop weld on the 36-in-diameter anchor pile (pile C-N) failed. The pile was then tested in tension to the proposed maximum test load of 800 tons.

At site D, the pile was loaded in 100-ton increments to 940 tons, which was held for 12 h. After unloading, the pile was reloaded to 1050 tons.

The results of the vertical pile load tests are presented in Figure 9 for site D. The measured pile deflections were less than the elastic pile compression, assuming that the total load is transmitted to the pile tip. Therefore, applied loads are probably resisted in skin friction, and end bearing has probably not been mobilized under the maximum applied loads of 750 and 1050 tons at sites C and D, respectively.

Ultimate Pile Capacities

The ultimate pile capacities, as predicted from dy-

Figure 8. Site C pile-driving resistances.

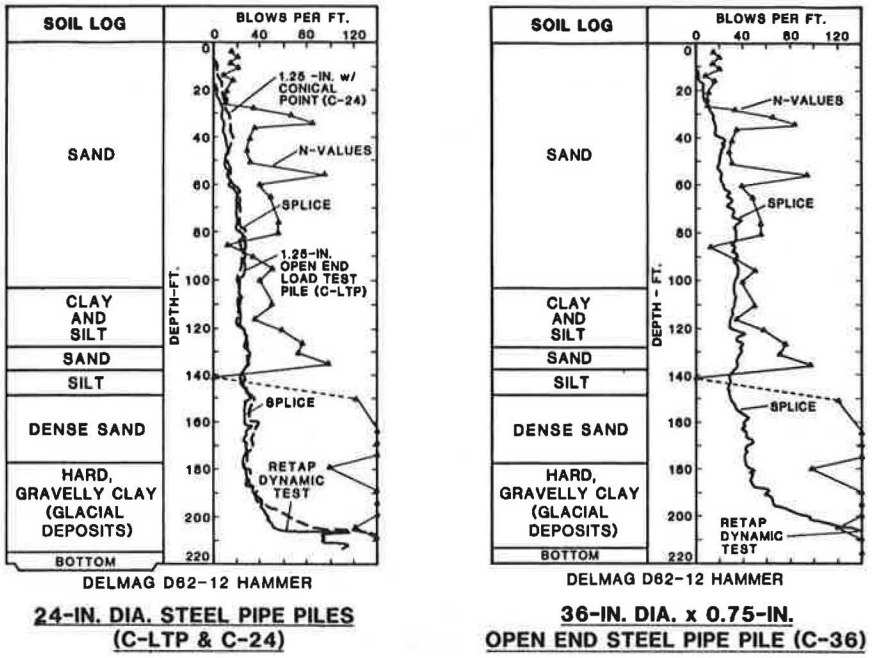

Figure 9. Site D pile-driving resistances and load versus settlement.

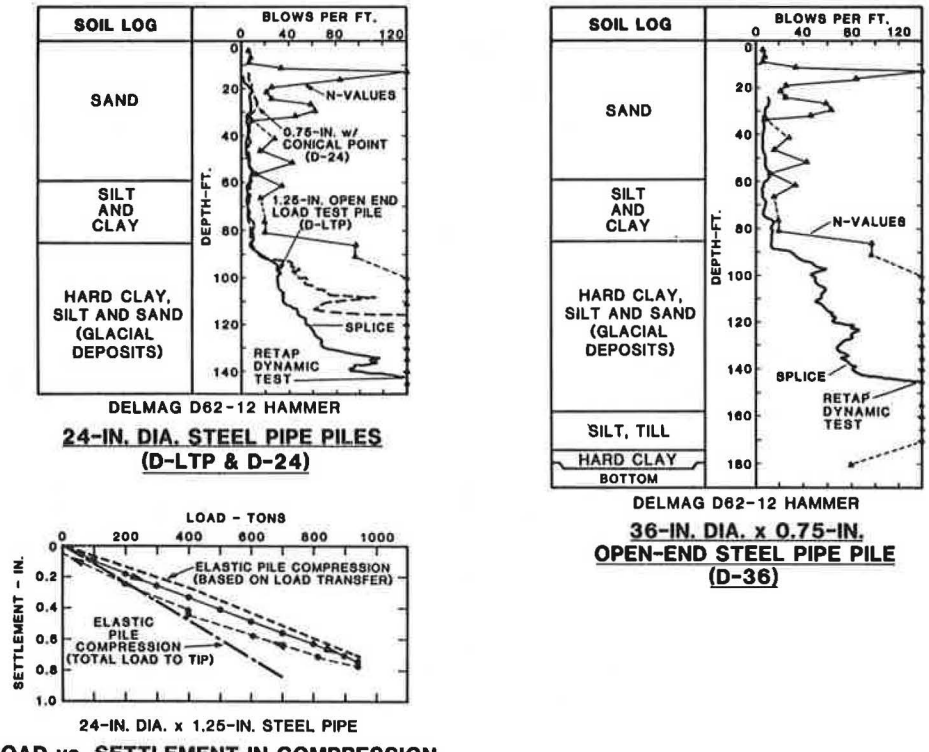

namic measurements and as determined from pile load tests, are given in Table 4.

The piles at sites C and D did not fail under the maximum test loads. Pile D-LTP was loaded to 1050 tons in compression, and the predicted ultimate capacity, which was based on the dynamic measurements, was 1125 tons, which we believe is reasonable. For pile C-LTP, the predicted ultimate capacity of 826 tons may be low. Because the 24-in load test pile and the 36-in pile were driven to about the same depth, and because the surface area of a 36-in-diameter pile is 1.5 times that of a 24-in-diameter pile, the capacity of a 36-in-diameter pile should also be about 1.5 times that of a 24-in-diameter pile. On this basis, the ultimate capacities of the driven 36-in-diameter test piles at sites C and D would be about 1200 and 1700 tons, respectively.

Table 4. Summary of pile capacities (steel pipe).

Site	Pile	Predicted Capacity Dynamic Measurements (tons)	Method	Applied Maximum Test Load (tons)	
				Compression	Tension
C	C-LTP[a]	826	CAPWAP	750	800
	C-N[b]	1150	CM	–	–
D	D-LTP[a]	1125	CAPWAP	1050	1000
	D-E[b]	1200	CAPWAP	–	–

[a]24-in diameter.
[b]36-in diameter.

Load Test Results and Interpretation

At site C, the average Ktanδ value for the alluvium was about 0.18 during compression and 0.15 during tension. At site D, the average Ktanδ value was about 0.16 during compression and about 0.10 under tension. Because these piles were not load tested to failure, the calculated Ktanδ values may not be the ultimate values. The results of the load transfer data indicate that the majority of the applied loads were apparently taken up in skin friction only.

Distribution of unit skin friction for various applied loads is presented in Figures 10 and 11 fof sites C and D, respectively, based on our interpretation of the load transfer data.

A CAPWAP analysis was made on the load test pile at site D by Goble & Associates. The results indicate the ultimate compression capacity to be 1125 tons with an estimated end bearing of 155 tons, which indicates that almost all of the load was carried by skin friction.

PILE INSTALLATION CRITERIA

Specifications for pile installations were developed

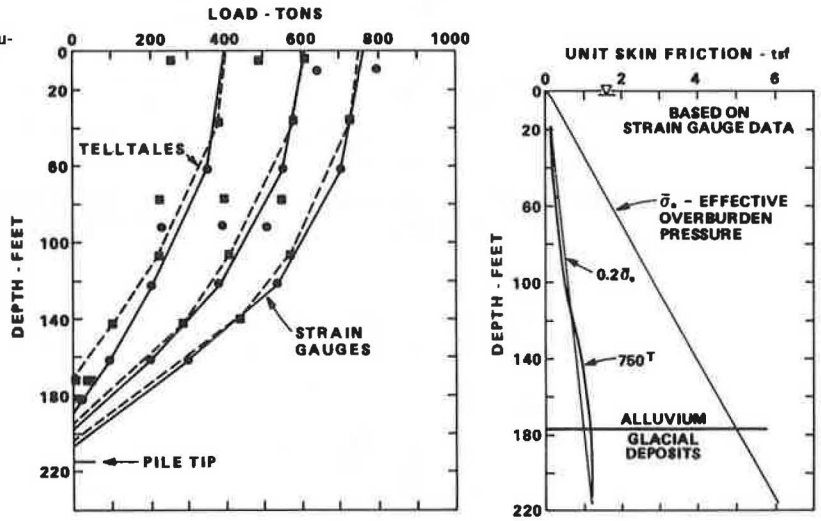

Figure 10. Site C 24x1.25-in steel load test pile (C-LTP): load distribution and unit skin friction in compression.

Note: Unit skin friction may have been mobilized within the alluvium, but may not be the ultimate within the glacial deposits since pile did not fail.

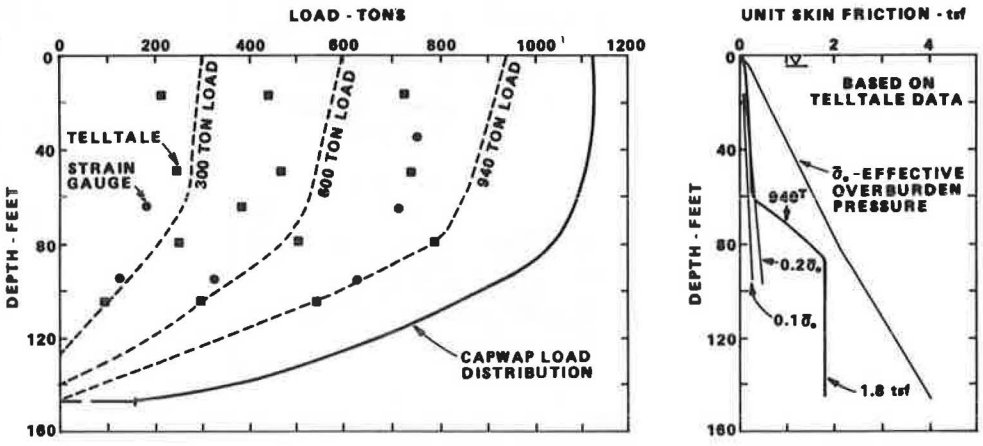

Figure 11. Site D 24x1.25-in steel load test pile (D-LTP): load distribution and unit skin friction in compression.

based on the results of the pile test program and subsurface data. In general, there were two main considerations. One was to estimate the necessary penetration to develop the design ultimate capacity and the other was to develop a driving resistance to satisfy the dynamic pile-driving formula that, in this case, was the WEAP program.

The pile penetration was based on the exploration data and the pile load test results. The estimated pile tip elevations were selected to have the tips in sand with a minimum of about 15 ft of sand below the pile tip to reduce the pile group settlement.

The driving criteria were based on the continuous driving resistance, considering the freeze factor. Tests and previous experience in the area indicated that the freeze factor for concrete piles was about 2 to more than 5.

For the steel pipe piles, the specified pile penetrations were about 30 and 50 ft into the glacial deposits for the east channel (site C) and west channel (site D) piers, respectively.

Hammers other than those used in the pile test program were permitted. However, it was required that those hammers be calibrated by using the dynamic pile analyzer.

CONSTRUCTION PILE INSTALLATION

The test pile program was accomplished after the conceptual design of the West Seattle Freeway Bridge replacement project was developed but prior to the final design. Based on the results obtained from the test pile program, the final pile penetrations for the concrete and steel piles were reduced by about 10-25 percent from the preliminary estimated lengths prior to the load test program. This resulted in a reduced cost for the project. During the bidding process, the geotechnical report, which included the pile test data and results, was made available to all prospective contractors. The pile test data eliminated many questions concerning pile hammer selections and pile drivability. This may have contributed, in part, to the fact that the bid prices were less than the engineer's estimated costs for every project contract.

CONCLUSIONS

A comprehensive pile load test program was accomplished during the initial design stage of this very large project. The information thus gained was very beneficial in the final design and the preparation of contract specifications. It is also believed to have had an impact on the four contract bid prices, which were all below the engineer's estimate.

Static empirical methods supplemented with local pile experience proved satisfactory for estimating pile penetrations and pile capacities. However, instrumentation data indicate that the apparent frictional resistances and end-bearing capacities are different from those calculated from empirical formulas.

The WEAP program was very useful in selecting pile-driving hammers that successfully drove the 24-in concrete and 24- and 36-in steel piles to the required penetration and desired capacities with the driving stresses below the ultimate stress of the pile material. The pile analyzer was used extensively and was useful in the overall understanding of pile driving. It was used to evaluate hammer performance and energy delivered to the pile as well as to estimate capacity and provide soil constants for wave-equation analysis for that particular pile and hammer. The pile analyzer was particularly well suited to evaluate the performance of diesel hammers.

ACKNOWLEDGMENT

We would like to acknowledge B. Wasell of the Seattle Engineering Department and T. Mahoney and B. Currie of Anderson, Bjornstad, Kane, and Jacobson for their assistance and cooperation during this project. We also wish to thank R. Cheney and R. Chassie of the Federal Highway Administration for providing helpful suggestions and comments on the test pile specifications. The assistance of many members of the staff of Shannon & Wilson, Inc., is gratefully acknowledged.

REFERENCES

1. A.S. Vesić. Design of Pile Foundations. NCHRP, Synthesis of Highway Practice 42, 1977.
2. G.G. Meyerhof. Bearing Capacity and Settlement of Pile Foundations. Journal of the Geotechnical Engineering Division, ASCE, Vol. 102, No. GT3, March 1976, pp. 195-228.
3. L.C. Reese and S.J. Wright. Drilled Shaft Design and Construction Guidelines Manual. FHWA, Implementation Package 77-21, Vol. 1, 1977, p. 39.
4. M. Bozozuk, G.H. Keenan, and P.H. Pheeney. Analysis of Load Tests on Instrumented Steel Test Piles in Compressible Silty Soil. ASTM, Special Tech. Publ. 670, 1979, pp. 153-180.
5. A.H. Hunter and M.T. Davisson. Measurement of Pile Load Transfer. ASTM, Special Tech. Publ. 444, 1969, pp. 106-117.

Notice: The Transportation Research Board does not endorse products or manufacturers. Trade and manufacturers' names appear in this paper because they are considered essential to its object.

Foundation Design and Evaluation for Winnemuca Viaduct

G. G. GOBLE, DAVID COCHRAN, AND FLOYD MARCUCCI

In preparation for the construction of Interstate 80 through Winnemucca, Nevada, a pile load test program was performed on candidate pile types to assist in the selection of a foundation design. Six pile types were statically tested at each site. Dynamic tests were also conducted, both at the end of driving and on restrike, and Case method static-capacity predictions were made. The results of this program are reported. Treated-timber piles were selected in the design; they had allowable stresses of 1200 psi. The actual stresses in the foundation piles are reviewed and reported. Also, driving records for one foundation group are presented to illustrate the effect of group behavior on driving resistance.

The initial planning for the section of Interstate 80 through Winnemucca, Nevada, called for twin

viaduct structures more than 4000 ft long. The structures were to span three crossings of the Humbolt River and two city streets. Preliminary foundation recommendations called for 55-ton design load steel H-piles. Because of the large amount of piling required to support the structure, a preliminary full-scale pile load test program was conducted to examine combinations of pile length and type in the hope that improved economy would result. Six different types of piles were driven and load tested at three different locations along the proposed route for the structure. As part of the same test program contract, two locations were tested in Lovelock, Nevada, in preparation for future bridge construction. The results of the Lovelock tests will not be discussed here, since bridge construction there has not yet started.

By rechanneling parts of the Humbolt River to avoid intersection with the I-80 alignment, the design length of the Winnemucca structure was reduced to about 900 ft after the load test program was completed. The layout of the structure and surrounding area is shown in Figure 1. With the reduced length of structure, only two of the load test sites were relevant to the design of the foundation piles. The locations of these load test sites are shown in Figure 1.

Based on the results of the preliminary test program, Douglas fir timber piles, which were approximately 50 ft long, were selected with a design load of 70 tons. Alternatively, the contractor was permitted to use 12-in² precast, prestressed concrete; 14-in monotube; or Raymond step taper. The winning contractor chose to use timber piles in the structure. Because of the higher-than-usual design loads, a review of the preliminary test program, the structural design, and the driving experience will be of interest.

SOIL CONDITIONS

The site is located in a large east-west trending intermontane basin that was occupied during the glacial period by an arm of old Lake Lahonton. From the original ground surface to depths that vary from about 5 to 20 ft, the soil along the viaduct alignment consists primarily of clayey silts and silty clays. This material is relatively firm above the water table and soft to very soft below it. The groundwater surface fluctuates seasonally with the surface of the adjacent Humbolt River. Below these layers of silts and clays, to a depth of about 60 to 70 ft, the soil consists chiefly of slightly compact, medium to very coarse sand and gravel.

Five borings are available from near the structure and preliminary pile load test sites. The boring locations are shown in Figure 1. The borings were made by both 2.875-in wet-rotary and 8-in hollow-stem auger methods. Split-spoon samples were obtained at regular intervals in each of the borings by using the standard penetration test (SPT), according to ASTM 1586. Two of the boring logs obtained at the pile test sites that are representative of the area are given in Figures 2 and 3.

PRELIMINARY PILE TEST PROGRAM

At the test sites presented here, six pile types were tested. They were steel H-sections, treated timber, 12-in² prestressed concrete, monotube, Raymond step taper, and 12-in-diameter closed-end steel pipe. The details of the piles are given in Table 1, and they are shown in place relative to the soil profile in Figures 2 and 3. Anchor piles were of untreated timber, and the general arrangement of the load test setup is shown in Figure 4. This arrangement was attractive in that it was possible to perform three static load tests at the same time. At each site, the timber anchor piles were driven first and then followed by the static test piles. All of the test piles were driven by a DELMAG D-30 hammer, which is rated by the manufacturer at 54 140 ft-lbf. The driving records for the test piles are shown in Figures 5, 6, and 7. All of the test piles drove quite easily; the maximum blow count for all of the test piles was about 80 blows/ft for the monotube at site 4.

Two static-load tests were performed on each test pile. The first test was the 48-h American Association of State Highway and Transportation Officials (AASHTO) test. In this test, the pile was loaded in 10-ton increments at a rate of one increment every

Figure 1. Site plan.

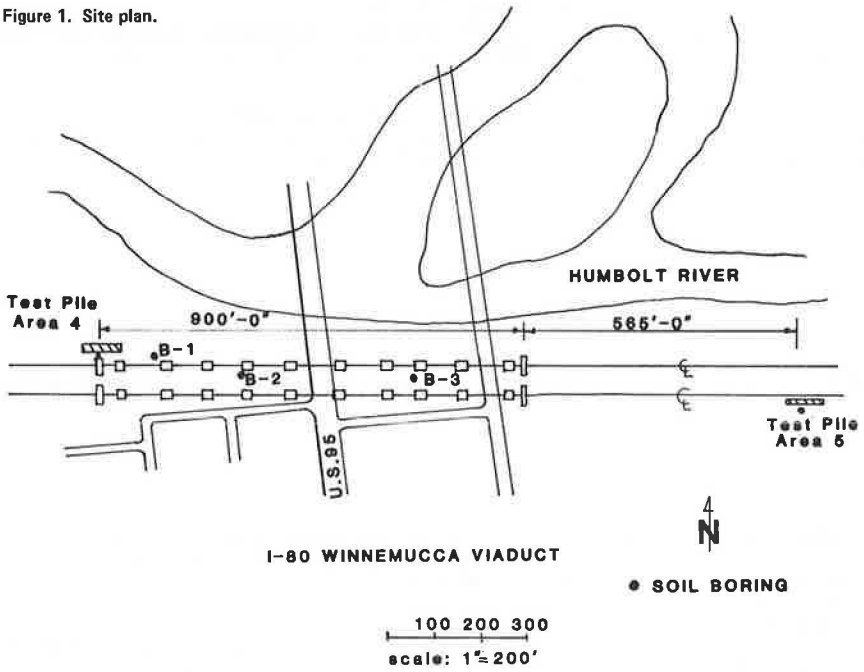

10 min until a load of twice the anticipated design load was reached. The settlement was read before and after the application of each load increment. The load was then maintained for 48 h and the settlement read once each hour. Unloading proceeded in the reverse of the loading procedure. The second load test was the modified Texas quick test. In this test, the load was applied in increments of 5 tons every 2.5 min. Pile top settlements were read before and after each application of each load increment. Loading was continued until plunging failure or 200 tons, which is the capacity of the testing system.

The test results were evaluated by using two

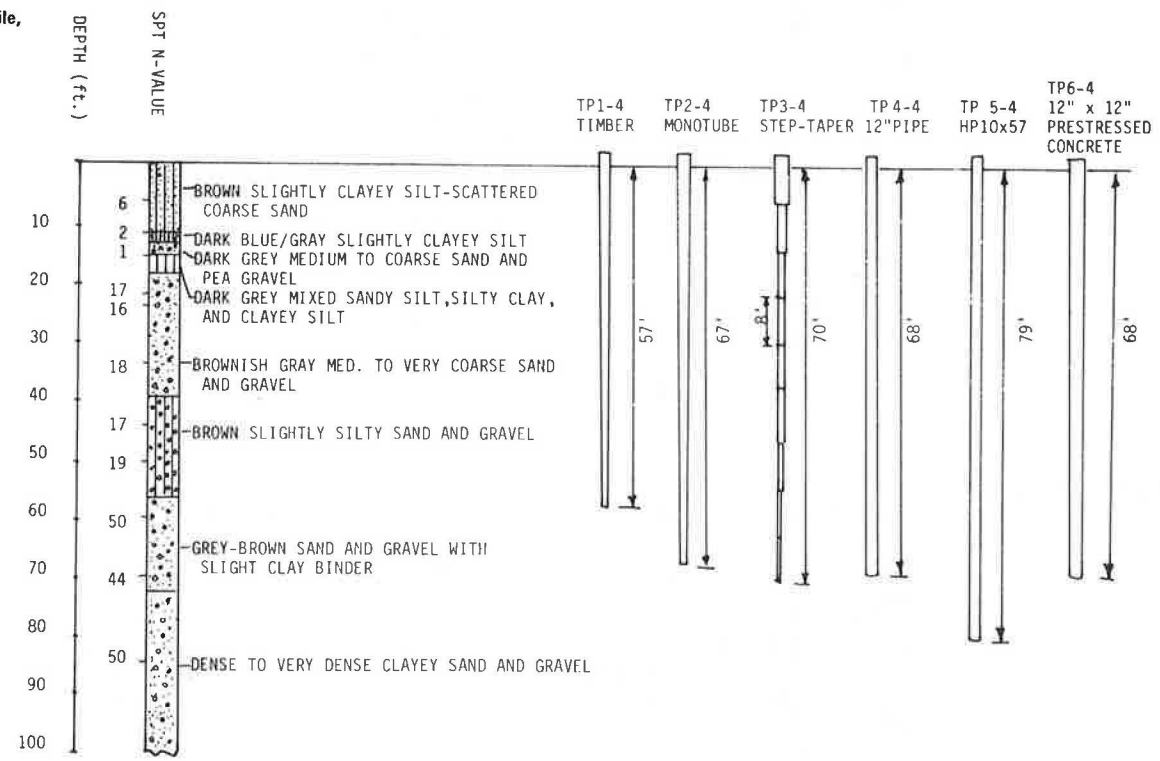

Figure 2. Soil profile, test pile at site 4.

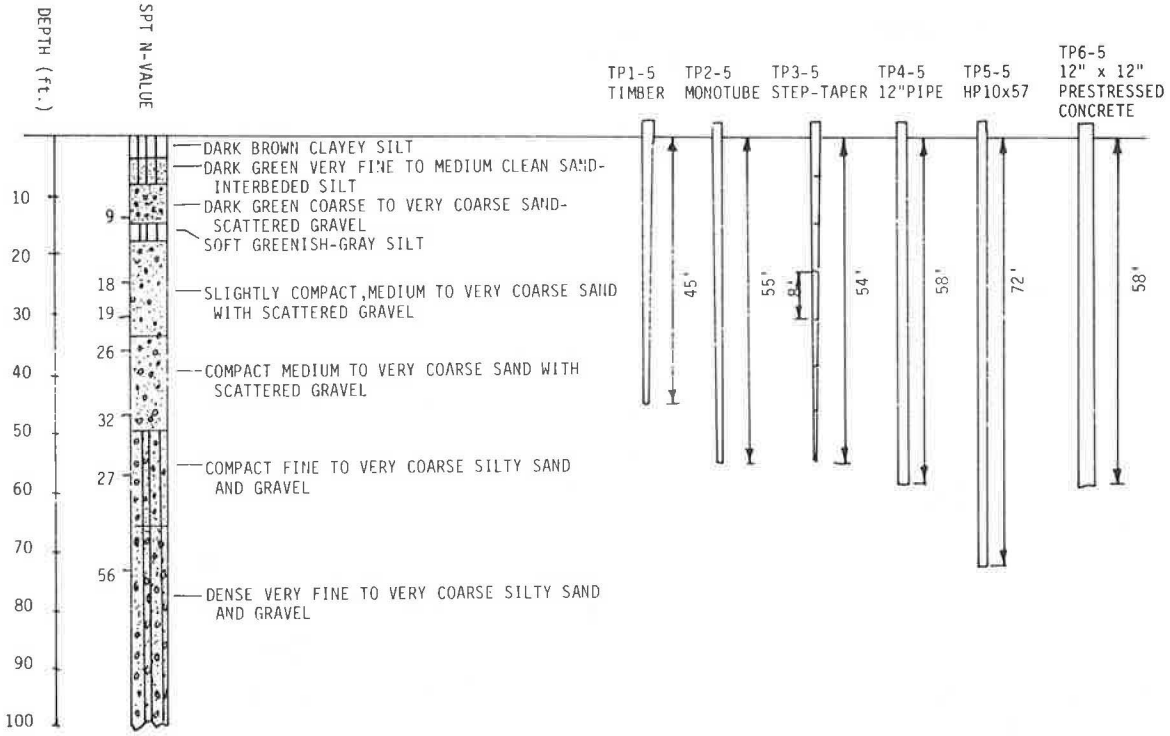

Figure 3. Soil profile, test pile at site 5.

different procedures to define the ultimate capacity. The procedure used by the Nevada State Highway Department is the double tangent method. In this procedure, the ultimate capacity is defined as the load at the intersection of tangents drawn to the load test curve at its beginning and end. The other procedure, which is the Davisson method (1), has been used in evaluating data obtained in the Case piling research project. Static load test curves from site 5 are shown in Figures 8-13. All six piles at site 4 carried the full 200-ton capacity of the static testing system, so the results

Table 1. Test pile details.

Pile No.	Pile Type	Driven Length (ft)	Cross-Section Description
TP1-4	Timber	57	14.7-in-diameter butt 7.3-in-diameter tip
TP1-5	Timber	45	14-in-diameter butt 10-in-diameter tip
TP2-4	Monotube	27	18-in ND-type N7 gage top
		40	18-in butt-type J7 gage
TP2-5	Monotube	15	18-in ND-type N5 gage top
		40	18-in butt-type J7 gage
TP3-4	Step taper	70	9-in tip, 1-in steps each 8 ft
TP3-5	Step taper	54	11-in tip, 1-in steps each 8 ft
TP4-4	Pipe	11	12.75-in outside diameter, 0.5-in wall top
		57	12.75-in outside diameter, 0.4375-in wall
TP4-5	Pipe	45.5	12.75-in outside diameter, 0.5-in wall top
		12.5	12.75-in outside diameter, 0.4375-in wall
TP5-4	HP 10x57	73	
TP5-5	HP 10x57	72	
TP6-4	Prestressed concrete	68	12x12 in
TP6-5	Prestressed concrete	58	12x12 in

Figure 4. Load test setup.

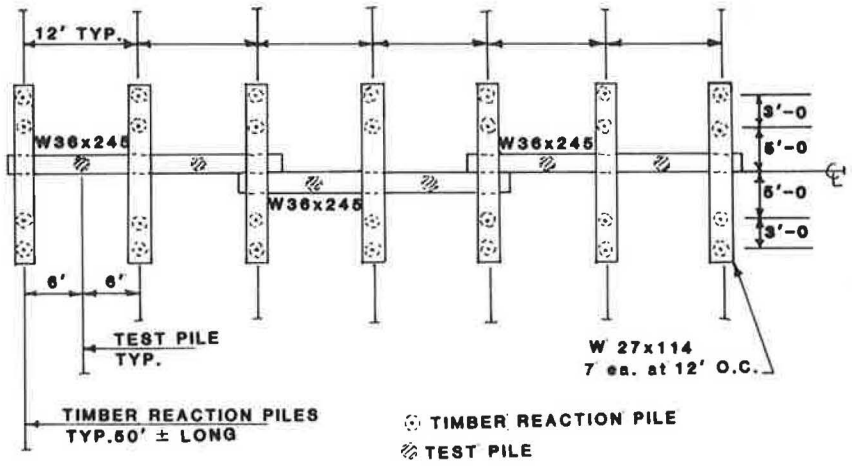

Figure 5. Driving records for timber and monotube piles.

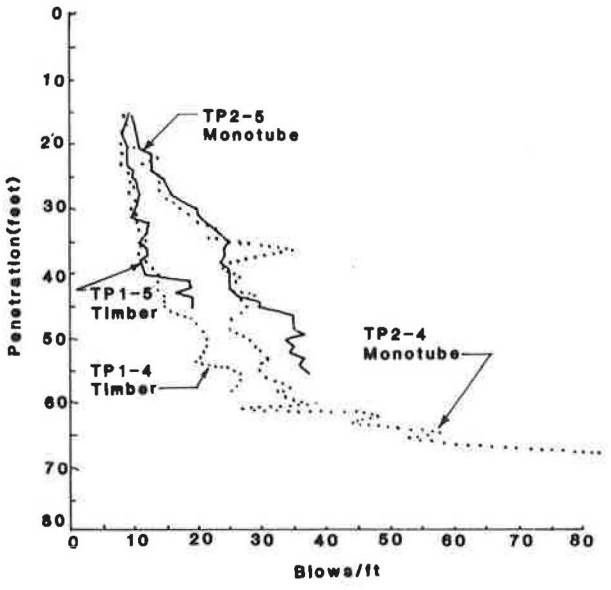

Figure 6. Driving records for pipe and step-taper piles.

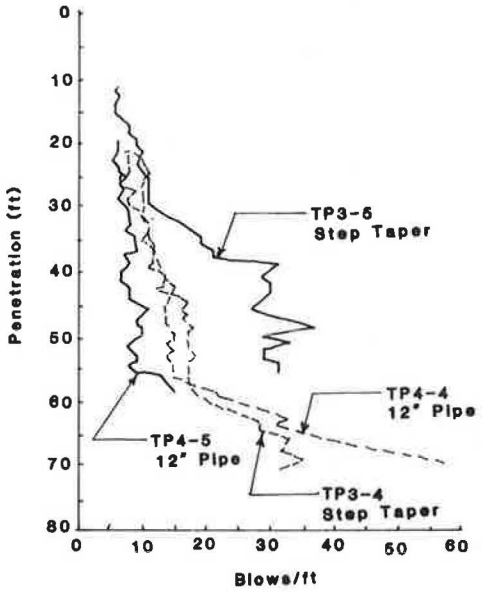

Figure 7. Driving records for prestressed and H-piles.

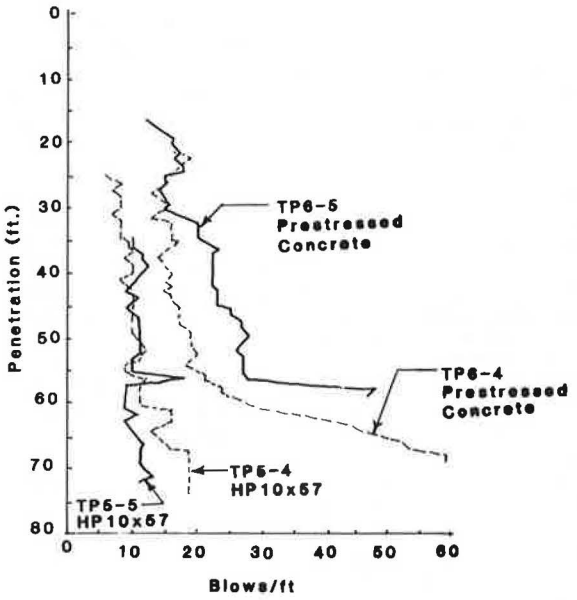

Figure 8. Timber pile static load test.

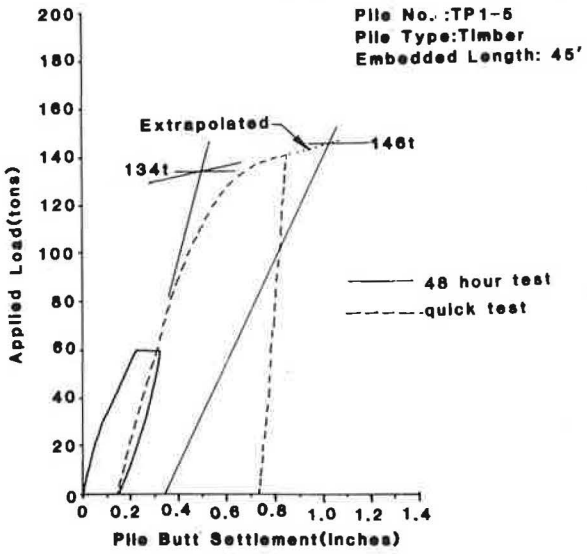

Figure 9. Monotube pile static load test.

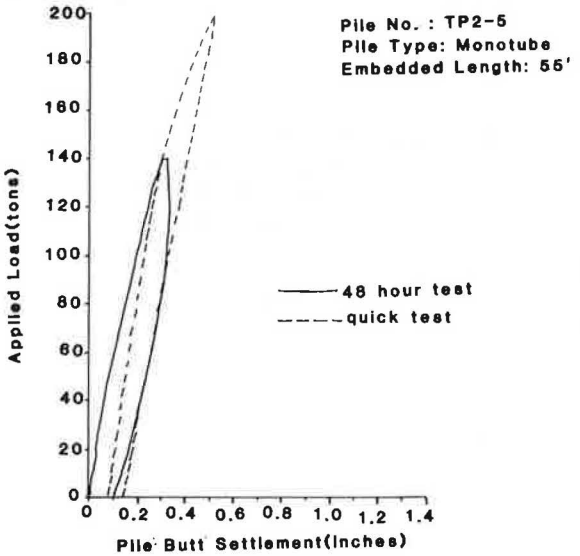

Figure 10. Step-taper pile static load test.

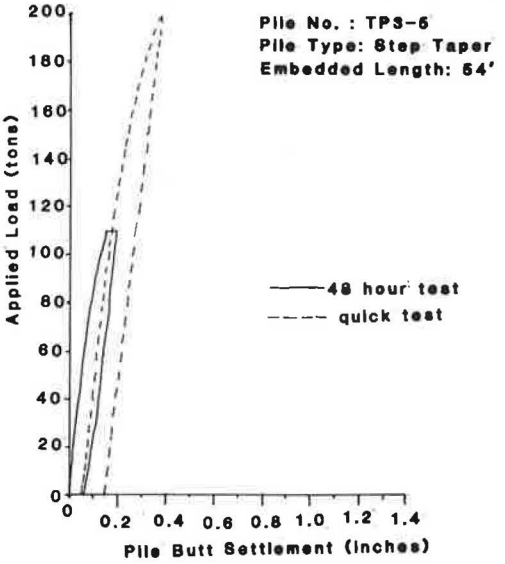

are not tabulated and the load test curves are not presented. The results of the evaluation of the tests at site 5 are given in Table 2.

An extensive dynamic test program was also performed at site 5. Measurements of force and acceleration at the pile top were made during the driving of the test piles. After completion of the static load tests, several of the piles were restruck with several different hammers, and again pile top force and acceleration were measured.

A procedure for determining static pile capacity during impact driving was developed at the Case Institute of Technology beginning in 1964 (2). This procedure, known as the Case method, requires the measurement of force and acceleration at the pile top during the hammer blow. These measurements have become quite routine. The capability to measure impact stresses and hammer energy transferred to the pile have been useful secondary developments. A pile-driving analyzer can perform these computations in the field. One such device was used during the driving of the test piles at Winnemucca site 5. More compact, versatile, and reliable pile analyzers have been constructed since the time of the Nevada tests.

During dynamic testing, the records of force and acceleration were also recorded on analog magnetic tape. This record could then be reanalyzed in the laboratory, and Case method capacity and energy delivered to the pile top could be recalculated. Energy delivered to the pile top is calculated from the following relation:

$$E(t') = \int_0^{t'} F(t)v(t)dt \quad (1)$$

where F is the measured force at the pile top and v is the associated velocity, both given as a function of time (t). The maximum value of delivered energy

(ENTHRU) is a common measure of the performance of the hammer and driving system.

A second method of capacity determination was developed during the Case project. This method, known as the Case pile wave analysis program (CAPWAP), treats the pile as elastic by using the Smith model (3). Soil resistance parameters are calculated from the measured force and acceleration input. An elastic dynamic analysis is required, so a substantial computational capability must be used. CAPWAP cannot be done easily in the field and real-time results cannot be obtained.

The results of the tests are summarized in Table 2. Piles 2-5 and 3-5 were not tested dynamically either during driving or restriking. Pile 2, the monotube, was driven at a later date, and measurements could not be made. Dynamic measurements were made at the top of the Raymond step-taper mandrel. However, they were very noisy due to the reflections from the mandrel joints and they could not be satisfactorily processed. Both of these piles were filled with concrete prior to static load testing. Restrike testing was not successful due to difficulties in determination of the composite elastic modulus.

It can be seen from Table 2 that the agreement between the Case method capacity and the static load test results was good. It should be evaluated by comparing it with the Davisson capacity for which it was developed. Restrike capacities should be used to compare it with the static load test results, since there was a strength gain with time. The Case method results for the timber pile were 16 percent higher than the Davisson capacity. The other results were in error by smaller amounts. In fact, it

Figure 11. Pile static load test, 12.75-in pipe.

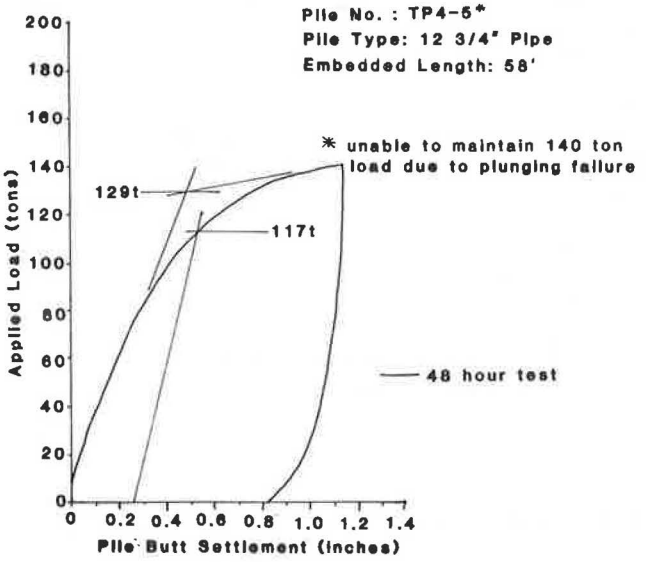

Figure 12. H-pile static load test.

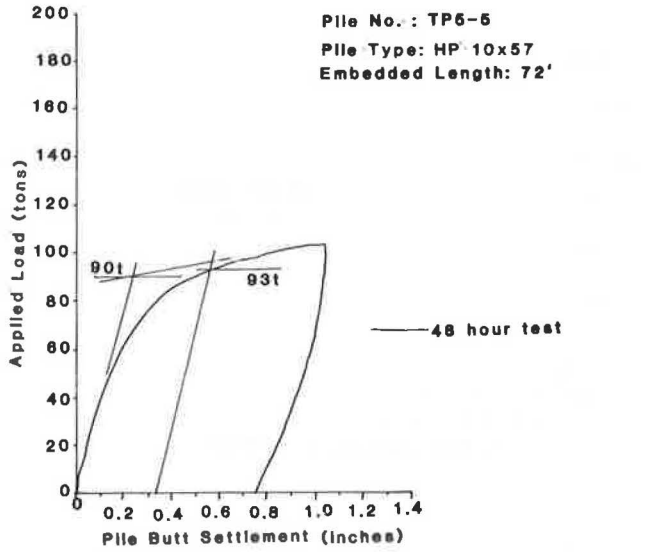

Figure 13. Prestressed concrete pile static load test.

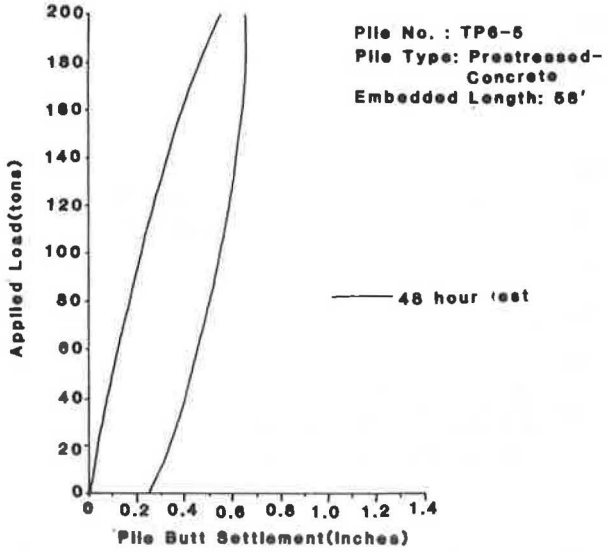

Table 2. Capacity test results for site 5.

Pile	Pile Type	Test Results, Static Capacity (tons)		Time of Dynamic Test	Blow Count (blows/ft)	Dynamic Capacity (tons)		
		Double Tangent	Davisson			Case Method	CAPWAP	WEAP
1-5	Timber			End of driving	19	144	149	160
1-5	Timber	134[a]	146[a]	Restrike	44	170	NA	220
2-5	Monotube			End of driving	38	NA	NA	212
3-5	Step taper			End of driving	32	NA	NA	220
4-5	Pipe			End of driving	20	104	100	190
4-5	Pipe	129[b]	117[b]	Restrike	27	130	151	220
5-5	H			End of driving	12	88	115	110
5-5	H	90[b]	93[b]	Restrike	17	93	96	160
6-5	Prestressed			End of driving	41	139	NA	260
6-5	Prestressed	200+[a]	200+[a]	Restrike	120	301	NA	460

Note: CAPWAP = Case pile wave analysis program.
[a]Texas quick test.
[b]AASHTO test.

Table 3. Restrike test results.

Pile	Pile Type	Hammer	Case Method Capacity (tons)	Blow Count (blows/ft)	ENTHRU (kip-ft) Measured	ENTHRU (kip-ft) WEAP	Apparent Efficiency (%)
4-5	Pipe	DELMAG D-30-10[a]	130	27	22.2	28.7	77
		DELMAG D-30-8	171	46	18.7		
		DELMAG D-30-6	160	51	15.8		
		Kobe K-22	140	70	15.0		
5-5	H	DELMAG D-30-10	143	17	14.1	27.6	51
		Kobe K-22	126	21	13.2	13.2	100
		Link-Belt LB-520	68	23	9.6	12.6	76
		Vulcan No. 1	70	45	6.1	9.4	65
		Raymond R-80CH	83	22	10.6	16.2[b]	65
6-5	Prestressed concrete	DELMAG D-30-10	301→198[c]	120→63[c]	14.1	19.9	71
		DELMAG D-30-8	192	69	15.8		
		DELMAG D-30-6	182	57	14.3		
		Kobe K-22	160	105	9.5		
		Link-Belt LB-520	144	118	7.4		

[a]This notation indicates that the D-30 hammer was operating with the throttle at setting 10, or fully open.
[b]Data on this hammer were not available when the WEAP run was made, so the Vulcan 80C was used as a replacement.
[c]Parameter indicated changed in the range given during the test.

is interesting to note that the difference between the two static test evaluation procedures was of about the same magnitude as the difference between the Davisson method and the Case method capacity.

The prestressed concrete pile could not be tested to failure with the 200-ton capacity test. Of particular interest here is the very large strength gain measured by the dynamic method between driving and restrike. This result is supported by the blow count, which almost tripled. No explanation is offered for the fact that the concrete pile showed so much more strength gain than the other pile types. Analyses by the CAPWAP method (3) produced results similar to the Case method except for the timber pile, where a difference of about 30 percent occurred.

Wave-equation analyses were also made by using the WEAP program. The input data used were considered to be typical for the conditions being analyzed. Most of the results obtained were considerably higher than either the static load test results or the dynamic predictions made by both the Case method and CAPWAP. The most likely reason for this difference is probably hammer performance. If the hammer was not performing properly (as assumed in the wave-equation analysis), then the blow count would be increased. Thus, the capacity predicted would be too high. One other factor is of considerable practical importance. Most of the blow counts recorded were quite low. In this region of the bearing graph, the curve is very steep. Thus, a small change in the blow count indicates a large change in capacity.

During restrike testing, several different hammers were tested, ENTHRU was measured, and a careful measure of the blow count was made. ENTHRU is defined as the maximum value of the energy passing through the pile top, as calculated from Equation 1. The blow count was measured by attaching a piece of paper to the pile and then drawing a pen along a reference attached to the ground so that a record of pile motion is recorded. Thus, the penetration from each hammer blow could be recorded. The results are presented in Table 3.

For TP4-5, the effect of the throttle on the D-30 performance was tested. This hammer had 10 positions on the throttle. At settings below about position 4, the hammer would not run. It is seen that positions 6 and 8 give a measurable reduction in energy output. This is a very useful tool in controlling tension stresses with concrete piles in easy driving.

Extensive testing was done on TP5-5, the steel H-pile. It should be emphasized that in order to obtain the data from all of the various hammers, the pile was driven several feet. Five different hammers were tested: DELMAG D-30, Kobe K-22, Link-Belt 520, Vulcan No. 1, and Raymond 80CH. In the dynamic test, Case method capacity was determined, and it is seen that, as the pile was driven, the capacity broke down from 143 tons to about 70 tons. ENTHRU was also calculated at the pile top and values are recorded for each hammer.

Wave-equation analyses were also made and ENTHRU calculated with WEAP by using the dynamically determined capacity. This ENTHRU calculation assumed the usual hammer and driving-system parameters. The values tabulated in Table 3 represent expected hammer performance. The apparent efficiency is simply the ratio of the measured ENTHRU to the value calculated by WEAP.

The results presented support the conclusion that the D-30 tested was not performing up to its expected operation. However, the K-22 was operating very well. The Link-Belt 520, Vulcan No. 1, and Raymond 80CH did not perform at expected levels. More data of this type would be desirable so that improved recommendations on hammer efficiency values for use in wave-equation analyses could be made.

The above comments only apply to the particular hammers tested on this job. Other hammers of the types tested here are known to have performed better at other sites.

FOUNDATION DESIGN

The pile design load was selected to be 70 tons by using a factor of safety of two against soil failure for the lowest load carried by any of the timber test piles. The design was based on timber piles, but other types were permitted as alternates. The design timber pile was assumed to have an 8-in-diameter tip and a 15-in-diameter top 3 ft below the butt and a length of 50 ft at the 15-in diameter. Due to the pile taper, the critical stress location will depend on the load transfer characteristics of the soil. All of the load was assumed to be carried in granular material on the lower 31 ft of the pile. The force distribution used for design purposes is given in Figure 14. With this force distribution, the stress distribution is also given in Figure 14. The maximum stress in this analysis is 1158 psi with a 70-ton design load. If the same stress-transfer assumptions are made for test pile TP1-4 for the 200-ton applied load and the dimensions given in Table 1, then the critical stress during the static load test was 3300 psi.

The Nevada State Highway Department uses the load factor procedure as defined by AASHTO in bridge structural element design. Thus, the various load

Figure 14. Force and stress distribution in design pile.

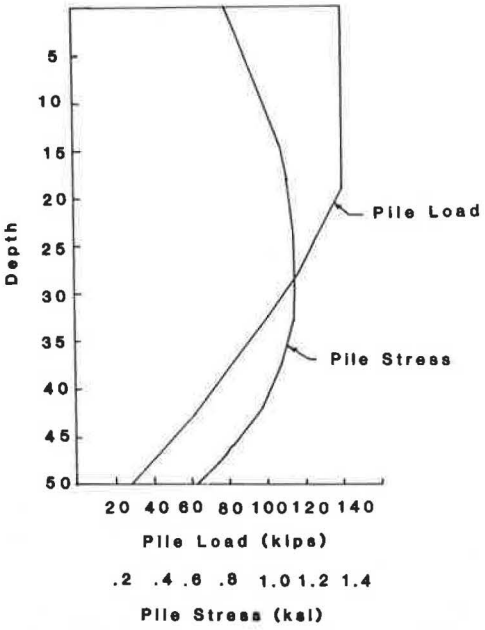

Figure 15. Driving resistances for pier 10W.

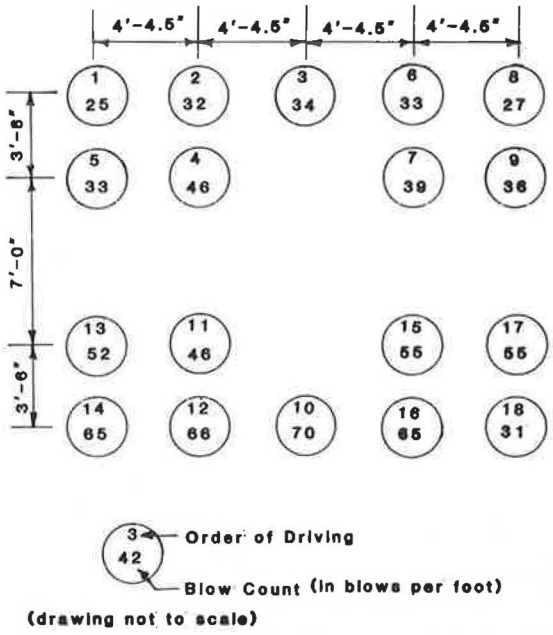

contributions for each load condition are carried down the structure and combined according to accepted procedures for the strength design of each element. In foundation design, pile reactions are calculated for the factored loads in order to design the pile cap. However, since piles are designed by using working stresses, working loads must also be carried to the piles. They are also combined according to the AASHTO working stress procedures, and critical conditions are calculated. Because pile design is based on ultimate strength concepts that have a rather arbitrarily selected factor of safety, a great deal of rationality would be added to the procedure if load factor methods were extended to include pile design.

The structure consisted of precast, prestressed box sections erected in a simply supported configuration in spans up to 100 ft. After erection of the precast sections, they were made continuous in three span units by placement of a cast-in-place deck with negative-moment reinforcement over the piers. The structure was analyzed as continuous for live loads. The piers had a wide single column configuration with a single footing under each pier. Thus, eccentric live loads arising from traffic in a single lane induce substantial moments to the footing, and live load effects can be substantial.

Individual pile groups under the piers ranged in size from 18 to 26 piles. All of the pile groups had some piles loaded to very near the design load under some load conditions. Controlling conditions were either the dead plus live load combination (AASHTO group I) or the dead plus live plus temperature combination (AASHTO group IV). The highest dead loads were about 45 tons on one pile group. Because dead load was concentrically applied, all of the piles in the group were equally loaded. This gives a critical pile stress of 740 psi (assuming the same load transfer ratios as given in Figure 14).

CONSTRUCTION

The production piles were driven with a Kobe K-22 open-end diesel hammer, which is rated at 41 300 ft-lbf. Three static test piles were driven and tested. Two were driven to 25 blows/ft and the third to 87 blows/ft. All piles were loaded to 200 tons by using the Texas quick test defined earlier. One of the piles failed by soil failure at a defined failure load of 164 tons, while the other two carried 200 tons without failure. The driving criterion was defined to be 25 blows/ft with a prescribed minimum tip elevation. In the driving of the production piles, blow counts much higher than the specified minimum occurred prior to reaching minimum penetration. The difficulty was probably due to the densification of the granular material due to driving of the pile group. Some preboring was permitted to achieve the specified tip elevation.

It is interesting to examine the driving record for a foundation where no preboring was done. In Figure 15, the final blow count is shown together with the order of driving for one pier. All piles were driven to the same tip elevation. Except for pile 10, where the blow count is somewhat higher than would be expected, the driving resistance is reasonably consistent with what would be anticipated.

About 500 timber piles were driven for the structure. A total of six piles were damaged during driving and had to be replaced. Damage was either visually detected or was noted by a sharp decrease in blow count. The structure (as of August 1981) has been complete for about two years. It is not yet open to traffic, but it has been used by the contractor for trucks hauling base material for the completion of the roadway. These loads are probably equal to the operating loads that the structure will carry. The structure is performing well, based on a visual inspection.

CONCLUSIONS

Based on the data obtained in the preliminary test program and the results of the production driving, the following conclusions are justified:

1. The use of design stresses of 1200 psi in treated Douglas fir has proved to be successful and should be continued. With these design stresses, good quality construction-control procedures must be followed.
2. Timber piles can be successfully driven with

large open-end diesel hammers. Difficulties during production driving were practically nonexistent.

3. Dynamic-capacity predictions agreed well with the static load test results.

4. Measured hammer performance was poorer than predicted in most cases. Thus, construction control by using dynamic measurements or static load tests is necessary as design loads are increased.

5. A preliminary test program of the type conducted here can be expected to save large amounts of money.

REFERENCES

1. M.T. Davisson. High Capacity Piles. In Proc., Soil Mechanics Lecture Series--Innovation in Foundation Construction, Soil and Mechanics Division, ASCE (Illinois Section), 1973.
2. G.G. Goble, G. Likins, and F. Rausche. Bearing Capacity of Piles from Dynamic Measurements, Final Report. Ohio Department of Transportation, Columbus, and Department of Solid Mechanics, Case Western Reserve Univ., Cleveland, Rept. OHIO-DOT-05-75, March 1975.
3. F. Rausche, F. Moses, and G.G. Goble. Soil Resistance Predictions from Pile Dynamics. Journal of the Soil Mechanics and Foundations Division, ASCE, Vol. 98, No. SM9, Proc. Paper 9220, Sept. 1972.

Notice: The Transportation Research Board does not endorse products or manufacturers. Trade and manufacturers' names appear in this paper because they are considered essential to its object.

Pile Selection and Design: Lock and Dam No. 26 (Replacement)

BRUCE H. MOORE

Lock and Dam No. 26 is a major navigation structure on the Mississippi River some 25 miles north of St. Louis, Missouri. At the site there is a large, unbalanced horizontal water load of 24 ft. The soils at the site are sands, gravels, cobbles, boulders, and clay tills that are 80 ft thick. The history of, and logic for, the selection of piling on this project is presented. The soil and foundation information available at each stage of design is outlined. The interrelation of capacity determination by testing or by computational methods is discussed. The design process is analyzed and a critique is furnished. An evaluation of pile test extent and timing by using decision-analysis techniques is recommended.

Large projects generally have long histories. The size and related logistics are principal contributors to this lengthy process. Response to conflicting interests, reviewing agencies, and differing engineering advice also provides interruptions. The intent of this paper is to follow the selection of pile type and design capacity through the intermittent stages of a large project with a view toward improving this selection process.

GENERAL

Existing Locks and Dam No. 26 is located on the Mississippi River at Alton, Illinois (Figure 1). The existing structure consists of semigravity locks 110 ft wide by 600 and 360 ft long; the walls are supported principally on vertical 35-ft-long timber piling. The dam portion includes 32 tainter gate bays that are 40 ft wide and are also supported on short vertical wood piling. The soils at the site consist of alluvial sands and gravels grading coarser with depth to limestone bedrock at 65 ft below the base of the structure. The zone of pile embedment is composed of fine to medium sands with variable density. The riverward lock wall has displaced horizontally more than 10 in, and other lock walls have displaced varying distances up to 6 in. Early construction problems, notably the failure of the third-stage cofferdam, are related by White and Prentis (1). Extensive scouring of the river bottom attended this failure. The construction of the riverward auxiliary lock was done in sands placed in this area by dredging shortly before pile installation. The piles were jetted and then seated by driving an additional 5 ft or to refusal. There has been no observed failure of the piles themselves. Drill cores and diver examination of the piling show strong, firm timbers. The problem appears to be inadequate lateral support from the soil and pile system when subjected to a large number of load repetitions. This deficiency is present even though when this structure was designed in the early 1930s a full-scale pile testing program was instituted. The effects of cyclic loads were evaluated through numerous repetitions of a horizontal load on single- and multiple-pile monoliths. The tests were performed within the main lock area, not the auxiliary lock. The tests were reported by the principal engineer, S.B. Feagin (2).

The replacement lock and dam are located about two miles downstream from the present structure (Figure 1). Foundation support and lock chamber shape and size are the principal features altered for the new structure. The present concept for the replacement structure consists of a single 110x1200-ft U-frame lock and nine 110-ft-wide tainter gate bays for the dam. These configurations are shown in Figure 2 (section) and Figure 3 (plan).

Several stages of design can be recognized in the development of these configurations. The U.S. Army Corps of Engineers labels these as survey, general, and detailed stages. Most engineers use similar labels for steps within their practice. Survey involves the evaluation of several major alternative structures and sites by using limited available information and experience. General and detailed, as the names imply, involve increasing amounts of basic information and refinement of design features.

The following discussions relate the amount of information available and the procedures used to establish pile type and predict capacity at each

Figure 1. Site map.

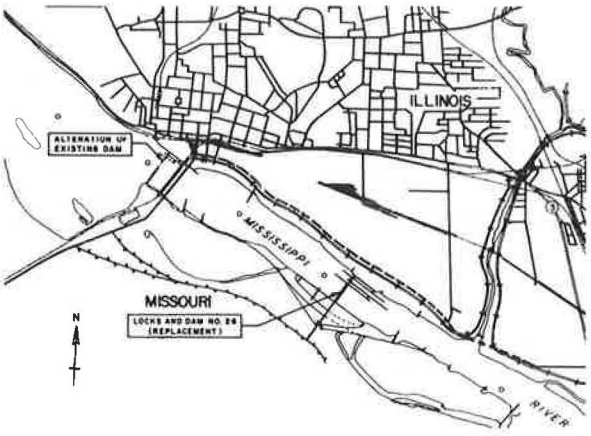

stage. It is not the intent here to enumerate and compare the values assigned as pile capacities but to compare the general procedures used to develop the capacities. These procedures can be reduced to four basic approaches:

1. The chosen pile can by physically placed on site and tested,
2. The results of tests at a similar yet remote site can be used,
3. Soil parameters can be determined and capacities estimated indirectly through the use of many varied formulations based on either soil shear theory or past testing and performance, and
4. An individual long experienced in an area can simply assign a capacity.

This last method is the least scientific and is normally applied with considerable conservatism. Conservatism also attends the use of formulas and soil parameters. The factor of safety assigned is one measure of conservatism in the formula approach. Extensive exploration and careful testing in parameter selection are other avenues to conservatism. These conservative approaches cost dollars in the selection of numbers and type of pile. Conversely, full-scale testing is also costly. A cost-balancing approach is outlined and recommended.

SURVEY REPORT STAGE

A survey report was accomplished during the period 1964-1968. The purpose of this report was to clearly define the major alternatives available to counter the deterioration and capacity limitations of the existing locks and dam. Rehabilitation of portions of the existing dam and replacement of the lock was one alternative. Relocation of the structure at various locations upstream and downstream was also considered. The chosen alternative was construction of the new lock and dam at the downstream site noted in Figure 1.

Six borings were taken at the new downstream location to establish the foundation conditions. Figure 3 presents the plan location of these borings. Pile type and capacity determinations made at that time were based solely on this limited foundation information and the designers' and reviewers' combined experience and preferences. The poor performance of the existing structure strongly influenced the determinations. Battered H-piles to rock was the clear-cut directive. The reviewers clearly stated their experience-based preference for H-piles to rock. Alternative pile types and lengths

Figure 2. Typical dam and lock sections.

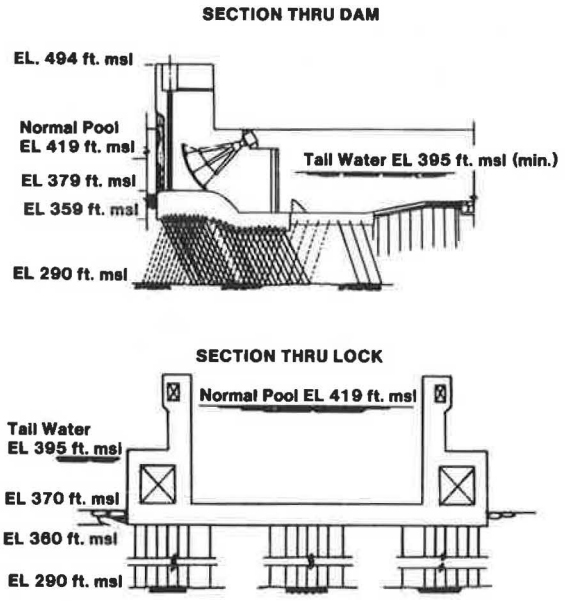

Figure 3. Overwater boring locations: survey report.

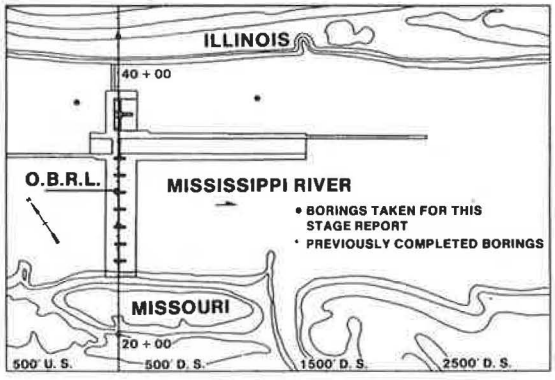

could be, and would be, considered in future studies, but a predilection to this type of foundation was clearly established.

Pile capacities for tension, compression, and horizontal loadings were estimated from experience and the results of remote testing. In this case, the remote tests were performed on the Arkansas River Project (3,4). A large pile load test program was envisioned. It was scheduled for accomplishment during the initial construction phases.

GENERAL DESIGN STAGE

The general design memorandum studied during the period June 1968 through July 1977 was intended to establish all major features of the project. Pile type, capacity, and configuration were included in these studies.

In preparation for the general design memorandum studies, approximately 60 additional borings were taken. Figure 4 shows the extent of this exploration program. Figure 5 presents a typical boring profile. Available to the engineer were N-values for 2- and 3-in outside diameter spoons, drillers' evaluations regarding the presence of cobbles and boulders, D_{10} and grain-size information results, some undisturbed densities, and drained direct shear

Figure 4. Overwater boring locations: general design memorandum.

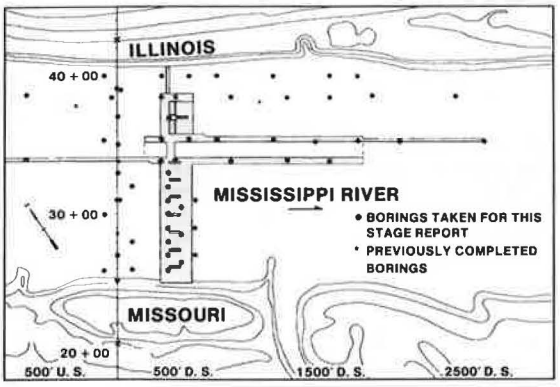

Figure 5. Typical boring profile.

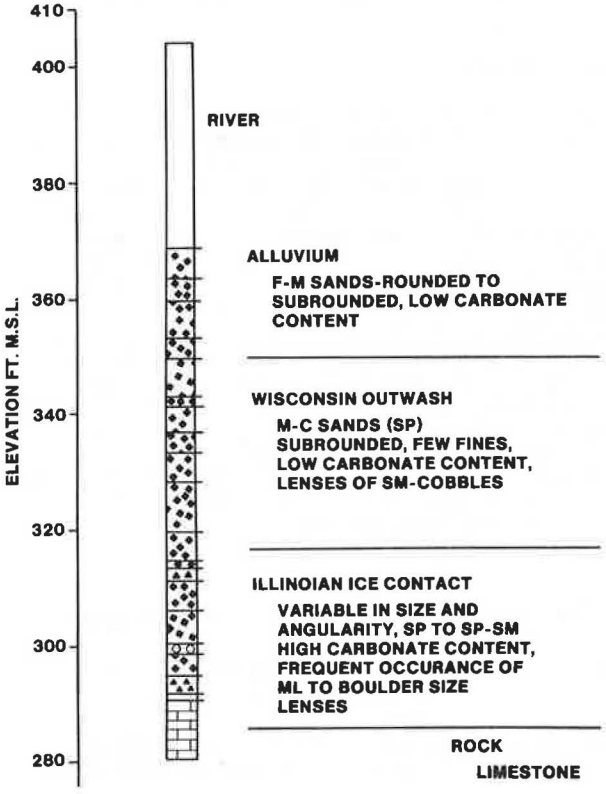

data from testing on reconstituted sand samples. Boulders and cobbles were found scattered across the site. The thickness of these zones varied greatly. Cobble and boulder conditions were labeled heavy when the zone exceeded 15 ft, medium when the zone ranged between 5 and 15 ft, and light where less than 5 ft thick.

The results of the boring program were examined and evaluated in many conferences and informal discussions among the designers and reviewers. Pile types were studied in light of the added exploration information. Experience remained the only tool available to assess the choices. Steel H-piles continued as the selected type. The added information on cobbles led to inclusion of tip reinforcement in the selected foundation.

Design loads were also reevaluated because of increased foundation information. Calculations that used static formulas and the limited soil shear data yielded a new set of capacity estimates. These data were combined with the estimates that used remote (Arkansas) tests to arrive at values for this design stage. A two-phase testing program was developed. The first phase was designed as an overwater, quickly completed driving test to assess the practicality of requiring that the piles penetrate to rock. The second phase, which was for the determination of acceptable loadings, would be accomplished during initial construction of the dam and would follow the format developed during the survey report stage.

The first phase consisted of driving the favored H-piling with a series of three impact hammers and different tip reinforcements. Three locations where heavy, moderate, and light boulders could be expected were chosen for the tests. Tension tests (overwater) were added shortly before driving started. The tension results were not available for this stage of design but were used to evaluate and adjust the allowable loads for later detailed design stages. The driving results supported the original H-pile decision for the dam. Results showed that where medium or light cobbles were present, H-piles protected by tip reinforcement could be driven to rock. Details of this testing program can be found elsewhere (5).

ROLE OF CONSULTANTS

It was during the general design stage that several internationally known consultants were retained to review the progress to date. Among these was one expert in foundation design. This individual provided an invaluable overview. He noted that, while much detailed blow count and shear-testing information was available, no cogent geologic history had been established. He recommended that the focus of the exploration program be adjusted to provide an improved understanding of the overall geology. This improved geologic knowledge would, in turn, yield greater appreciation of detailed engineering requirements.

Geologically oriented profiles were developed for the total area. Multiple exploration methods, including electric logging and overwater seismic evaluation of the overburden, were used. Figure 6 shows one of these profiles. The profile depicts the geologic history of the Mississippi River at this location. At the top of the profile is the recent alluvium. Then the Wisconsin glaciation is represented by an outwash zone. In some areas, the two are intermingled to provide an alluvial-outwash zone. To this point in depth, the normal picture of a river valley filled with stream flow sediments is present. The underlying zone is composed of a heterogeneous mixture of sand, gravel, boulders, and clay till. The till can be found in both the lower and upper portions of this zone. Cobbles and boulders are scattered intermittently throughout. The deposit has both alluvial and morainic characteristics. It has been labeled ice contact material of the Illinoian Age. A patch of older Kansan alluvium and outwash smeared with a lense of the Illinoian clay till completes the picture. Engineering classifications of the soils found in each of these geologic zones are presented on Figure 5.

The added exploration required to develop the profiles yielded a bonus. Penetration resistance graphs were developed that compared 3- and 1.375-in-diameter spoon resistances in geologically similar materials. A discussion of these comparisons is presented by Moore (6).

DETAILED DESIGN STAGE

At Lock and Dam No. 26, the detailed design is

Figure 6. Geologic section (dam).

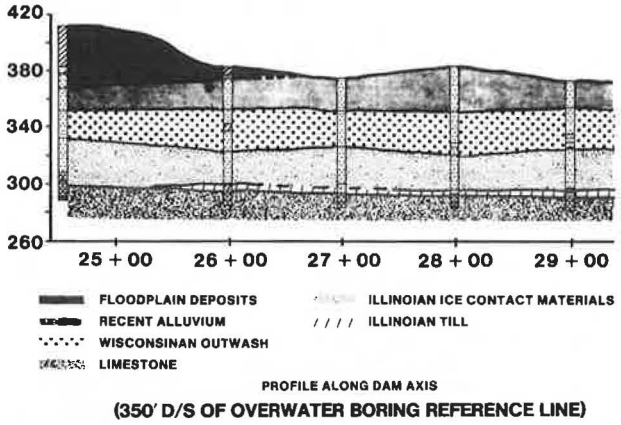

Figure 7. Overwater boring locations: detailed design memorandum.

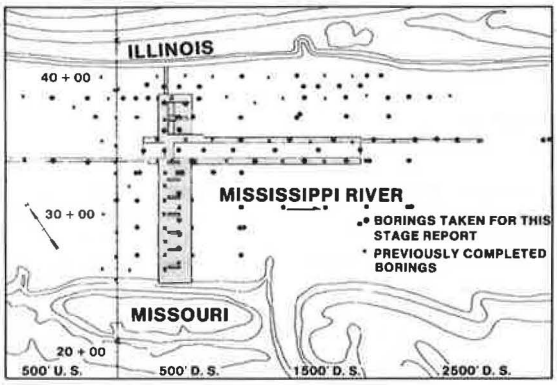

presented in two reports--one for the dam and one for the lock. The report for the dam is complete. The lock memorandum is currently being prepared. Additional explorations include 85 borings, two large-scale pumping tests, overwater geophysical surveys, and dredge sampling of the river bottom soils. Figure 7 shows the added borings. The added explorations confirm the previously developed geologic sections.

The previous load capacity evaluation tools were static formulas, soil data, and remote test results. For the first time, factual test information was available from the actual site. The load testing accomplished in the overwater pile test program was used in developing the tension capacities for the dam.

Explorations at pile-founded Lock and Dam No. 24, which is about 40 miles upstream of the No. 26 site, revealed extensive voids under this structure. Some voids were also found during drilling for a stability evaluation of existing Dam No. 26. There was concern that earthquake or other vibrations could cause possible soil settlements beneath the new structure and create a similar void. The coefficient of horizontal subgrade reaction was effectively reduced to zero with a resulting increase in the number of piling.

The detailed design memorandum outlined a conceptual pile-testing program similar to that for the preceding stages. It was to be accomplished within the cofferdam during the first phase of construction. The testing was to include an evaluation of the hammer and resistance curves and load results. These relations would control the construction effort for the dam.

At this point, all design for the replacement structure ceased in response to litigation contesting the project. During litigation, there was a major testing program to evaluate methods available to rehabilitate the existing structure. This included chemical-grouting assessments, evaluating rock anchorage, and predicting and measuring lateral movements associated with driving piles near a loaded structure. An overview of this program was prepared by Lacroix, Perez, and Fieldhammer (7). In 1979, the final bars to the design and construction effort were lifted--a hiatus of 5 years.

CONSTRUCTION

After the restriction on design was lifted, the plans and specifications were completed by using the same soil information but also by applying the latest formulas together with the remote and overwater site test results. The pile load test program was expanded to include an evaluation of the accuracy of quick tests similar to those described by Fellenius (8).

ANALYSIS OF DESIGN PROCEDURE

It remains to be established whether any design (numerical) deficiencies or excesses exist. The initial choice (survey report) of pile type and penetration was arbitrary and experienced-based only. The initial capacities were determined through experience and application of remote (Arkansas) test results. The final choice (detailed design) of pile type was again experienced-based but supplemented by extensive explorations and on-site driving tests. The final capacities, as used in the detailed design, were determined through experience, soil testing and calculations, and limited overwater test results. Horizontal capacities were discounted because of unknowns related to the permanence of the soil support. As the construction phase begins, the assurance of capacities and constructibility are still the subject of future testing. The table below summarizes this history:

Stage	Basis for Design
Survey	Experience
General	Experience, remote tests, limited calculations
Detail	Experience, remote tests, driving tests at site, limited tension tests at site
Construction	Experience, driving tests, detailed load tests, production load testing

These procedures can be simplified further into conservative design and testing. Under a conservative design would be found calculations that used soil parameters, testing and performance at other structures, and that facet of engineering labeled experience. Testing would include all the steps from inclusion of results from limited site tests through detailed capacity testing and construction proof testing.

At Lock and Dam No. 26, both testing and conservative design have been used in developing the current plans. The decisions regarding timing and extent of testing were made by using nonquantified evaluations. The decisions tended to follow a direction that said "get as much foundation information as you need but at a minimum cost for the testing." The effect of test extent and timing on construction costs was not given formal consideration. Certainly, the responsible engineers were aware of these relations and included them in their thought processes, but no formal evaluation was developed. This lack of a formalized analysis is

Figure 8. Decision analysis: pile tests.

ACTIONS

a_1 — Capacities chosen from Experience.

a_2 — Capacities chosen from Tests.

a_3 — Negotiate Contract.

STATES

θ_1 — Experience gives valid Capacities.

θ_2 — Tests give valid Capacities.

PAY OFF MATRIX

STATES	ACTIONS a_1	a_2	a_3
θ_1	0	−100^k	−50^k
θ_2	−500^k	0	−50^k

considered a serious deficiency and may have allowed testing to be uneconomically delayed or unnecessarily included in the selected options. Had an analysis been developed for Lock and Dam No. 26, the questions regarding need, timing, and extent of pile testing could have been resolved logically and with consideration for total costs.

RECOMMENDATIONS

The choice of whether testing or conservative design is proper for one project is not necessarily valid for another. The design engineer must use his or her experience in early planning as to the best route through these choices. This may not be an engineering decision, but it certainly lies within the professional responsibilities of the engineer. It is to the benefit of the profession that the engineer recognize and translate these actions into a management decision format for his or her client.

The use of decision-analysis techniques is one means of combining available solutions and expected results into such a management decision format. Tummala (9) provides a good description of this method of analysis as applied to engineering decisions. Tummala describes the logical combination of "actions" and "states of nature" with attendant "payoffs". A simplified payoff matrix for pile load testing is shown in Figure 8. This very simple matrix is completely hypothetical. It illustrates three actions combined with two states. Position θ_2, a_1 means that capacities were chosen from experience, but that only tests give correct capacities. The engineer estimates that in such a case it could cost the owner $500 000 to correct the situation during construction of this hypothetical project. Other positions in the matrix are developed in a similar manner. Other states and actions could be introduced with timing of the testing and extent of testing included among them. Various techniques are available to allow logical selection of the most desirable course of action. In one case, risks can be minimized. Conversely, potential savings can be maximized. Other, more complex choices are available. All of these actions are described in Tummala (9).

A formalized evaluation of the need, timing, and economics of pile testing is strongly recommended for any project where such testing appears warranted. In addition, until the driving and testing of production piling are complete, conservatism must govern design thinking. Conservatism does not preclude a design that, after testing, can be adjusted to the higher or lower capacities revealed by the testing. Conservatism does not preclude use of up-to-date procedures for analysis of both pile capacity and load distribution. Whether conservatism is approached in an arbitrary choice of a factor of safety or in a very thorough evaluation of soil and rock parameters that use the most advanced techniques is immaterial. What is essential is that it be present in the design prior to completion of the testing of the driven production pile.

Analysis of the selection and design procedures at Lock and Dam No. 26 (replacement) has revealed a management deficiency, notably the lack of a formal decision analysis relative to pile testing. Four basic approaches to capacity prediction were outlined previously. These were experience, remote testing, calculations by using soils data, and on-site testing. The procedure used in developing capacities at various stages of design for Lock and Dam No. 26 (replacement) were examined and classified. The extensive explorations, iterative design stages, multiple review levels, and the examples provided by existing structures would seem to indicate that a large degree of conservatism has been incorporated into the chosen pile capacities. It will be interesting to ascertain that degree when the planned pile tests are completed.

REFERENCES

1. L. White and E.A. Prentis. Cofferdams. Columbia Univ. Press, New York, 1950.
2. S.B. Feagin. Performance of Pile Foundations of Navigation Locks and Dams on the Upper Mississippi River. Proc., Second International Conference on Soil Mechanics and Foundation Engineering, Vol. 4, June 21-30, 1948, pp. 98-106.
3. C.I. Mansur and A.H. Hunter. Pile Tests--Arkansas River Project. Journal of the Soil Mechanics and Foundations Division, ASCE, Vol. 96, No. SM5, Sept. 1970, pp. 1545-1582.
4. M. Alizadeh and M.T. Davisson. Lateral Load Tests on Piles. Journal of the Soil Mechanics and Foundations Division, ASCE, Vol. 96, No. SM5, Sept. 1970, pp. 1583-1604.
5. B.H. Moore. Pile Driving Tests and Problems on the Mississippi River. In PILETIPS, APF Corp., Saddlebrook, NJ, March 1976.
6. B.H. Moore. Highlights--Foundation Exploration Design--Locks and Dam No. 26 (Replacement). Proc., Foundations for Dams, ASCE, March 17-21, 1974, pp. 11-36.
7. Y. Lacroix, J.Y. Perez, and E.L. Fieldhammer. Overview of Foundation Investigation and Test Program: Phase IV Report, Vol. 1. U.S. Department of Commerce, Rept. AD-A076090, July 1979.
8. B.H. Fellenius. Test Loading of Piles and New Proof Testing Procedure. Journal of the Geotechnical Engineering Division, ASCE, Vol. 101, No. GT9, Sept. 1975, pp. 855-869.
9. V.M.R. Tummala. Decision Analysis with Business Applications. Educational Publishers, New York, 1973.

Field Measurement of Swept Cast-in-Place Piles

WILLIAM F. LOFTUS

The age-old dilemma of not knowing the condition or direction of a cast-in-place pile that undergoes sweep during driving may be on the verge of being solved. By using a simple method of an inverted flashlight on a measuring tape, the sweep may be plotted within reasonable limits. If one knows and can plot the slope of the top portion (i.e., the depth where full circumferential light ceases), the depth where no light can be seen from the top, and, finally, the overall depth of the pile, an acceptable prediction of final tip displacement can be made. This method, called the integrity OK (INTOK) method, eliminates the use of expensive and time-consuming equipment and the extra labor previously required to determine the slope and direction of the unseen portion of a driven cast-in-place pile.

In a recently completed foundation project, some 17 000, 10.75x0.188-in-wall 50-ton cast-in-place piles were driven to support a 100 million gal/day secondary sewage treatment plant in Cleveland, Ohio. The joint venture of Gibbons-Grable Company of Canton, Ohio, and Richard Goettle Construction Company of Cincinnati overcame the problems and successfully installed 210 miles of piling at an average speed of 0.25 mph by using Link-Belt 520 double-acting diesel hammers (26 300 ft-lbf). The piles were divided equally between plumb and batter (1 horizontal to 3 vertical) and averaged approximately 65 ft in length.

The soil profile consists of random and rather unstable loose sand and silt deposits that vary in depths of up to 40 ft. The underlying bearing stratum, which is a firm stiffer-with-depth clay layer, is in an almost level condition; the top of this layer has minimal elevation changes throughout the site.

Several straight plumb piles had initially been tested under the subject contract, and 10 others had also been tested under a previous contract (the latter was the one on which the design and specifications had been prepared). The drawings and specifications of previously built structures revealed that some 30 other load tests had been performed years before. Based on these tests and the boring and laboratory data, a 50-ton design had been recommended by using an adhesion value of 0.9 ton/ft^2 of embedded pile surface area and tip resistance computed on the basis of 11.5 tons/ft^2 of pile tip area. These values then dictated the length of penetration into the clay for each of the piles of the project.

Because the wall thickness of the pipe was not critical, the less-expensive 10.75x0.188-in-wall tube piles were ordered (half had already been delivered to the site or to storage); the waste was kept to a minimum. However, with the lighter wall, the probability of sweep and collapse became fearful anticipations. The sweep became immediately apparent when the bottoms of virtually none of the first 100 piles could be seen after driving.

Because all parties would gain from the less-expensive foundation, the initial requirements of having to see the bottom of the pile after driving and that zero loss of cross section be maintained had to be reanalyzed. Thus, William F. Loftus Associates, Inc., was commissioned by the contractor (with the support of the owner, the Cleveland District; the engineer, Malcom Pirnie, Inc.; and the geotechnical firm, Mueser, Rutledge, Johnston and DeSimone) to evaluate the situation, to devise an early production-oriented sweep-detection system, and to recommend conditions of acceptance for these swept cast-in-place piles.

A swept pile is one that departs from its original altitude line in a gradually increasing amount with the depth of the pile. This amount varies in each pile sweep and begins to be of concern if this rate of departure increases too rapidly. Inclinometers (developed by Slope Indicator, Inc., of Seattle, Washington, which consist of upper and lower pendulums swinging in the north-south direction and the other swinging east-west) were used to measure the sweep. The slope can be measured merely by digitally measuring the distance from the instrument line to the plumb pendulum. Eighty of the driven piles that were already noted as swept by the inspector were measured by using this device.

In an effort to determine the carrying capacities of these piles, one pile with a 7.3 percent sweep was load tested in the same manner that all other previous piles had been tested--namely, that the load was incrementally applied in 50, 75, 100, 125, 175, and 200 percentiles of the design load. These loads were generally held until settlement under the increment was less than 0.001 ft in a 2-h period and held for 48 h, and then until the settlement was less than 0.001 ft over a 4-h period. Because telltales for measuring tip movement were not installed, some cycling was done at certain increments throughout the test.

The movement of the pile both in full load and zero load conditions indicated that completely tolerable settlements had occurred. No consideration was given to the possible combinations of resistance to movement, as shown in Figures 1 and 2. (As an aside, further study should be given to the possibility that sweeps in cohesive soils actually increase the capacity of the pile.)

Having satisfied all parties that a maximum sweep of 7 percent (total off-alignment tip displacement) was acceptable, the next task was to develop a quick method for determining these values.

ANALYSIS

It became apparent that (a) the slope of the upper portion of the pile, (b) the point where the sweep starts, and (c) an idea of the abruptness or gentleness of the sweep were important in the study. Thus, William F. Loftus Associates developed the Integrity OK (INTOK) method. After the initial slope of the pile was recorded, an inverted six-cell flashlight, which was firmly attached to a steel tape, was lowered down the pile. The following data were then recorded:

1. Point B--This is the depth beyond which full circumferential light is no longer visible from the top. For batter piles, it is critical to note if the sweep coincides with batter direction or, if not, the approximate clock-oriented deviation (e.g., assume 12 o'clock for batter direction and record the hour closest to the sweep direction). In all cases of batter piles, the flashlight will ride the low side of the pile.
2. Point C--This is the depth beyond which no light can be seen from the top of the pile.
3. Point D--This is the overall length of the pile.

Having all of the above data is fine, but what hap-

Figure 1. Swept pile.

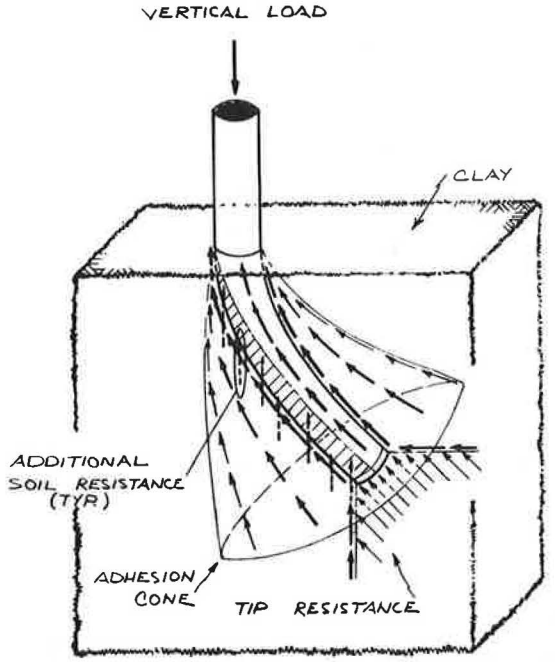

Figure 2. Straight pile.

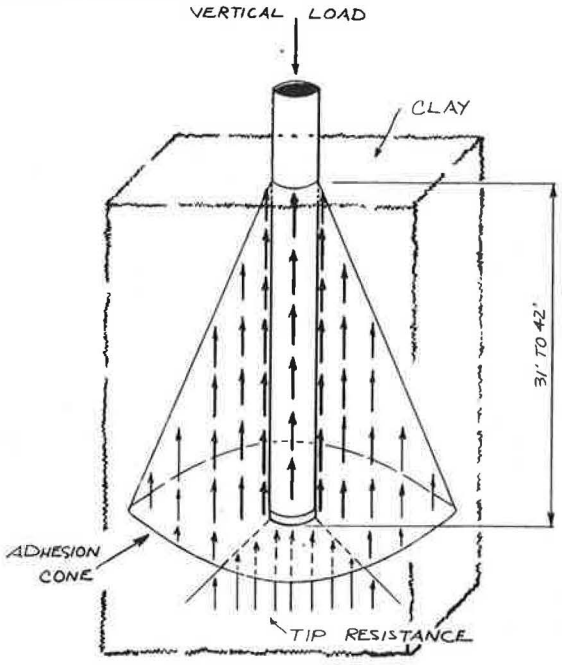

pens to the sweep direction in the unseen, darkened portion of the pile?

The comparison with the slope indicator shows that the pile will continue in a circular path, either (a) keeping its cross-sectional area intact and remaining dry or going beyond its elastic limit; (b) "crimping" and rupturing itself into a "wet", rejected condition; or (c) the pile will straighten out and continue to a "tangential" alignment after its initial directional change.

Regardless of the interpretation (tangential or circular), the following conclusions can be made about the displacements prior to entering the darkened portion of the pile:

1. For plumb piles when point B is recorded, the displacement from axial alignment at the depth is always one diameter. When point C is recorded, the displacement from axial alignment increases to something less than two diameters. Geometrically, it can be proved that this value will be two or more diameters, only if the distance from the top of the pile to point B equals or is less than the distance from point B to point C, which, from a practical point of view, never happens. For field and conservative purposes, however, the use of two diameters displacement of point C seems prudent.
2. For batter piles when point B is recorded, the displacement from axial alignment at the depth is one diameter only when the sweep is in the direction of the batter (12 o'clock). For piles where the sweep is at right angles to the batter (9 o'clock and 3 o'clock), this displacement is one-half a diameter. For piles where the sweep is opposite the batter (6 o'clock), this displacement is very close to zero. This condition is extremely rare.
3. For batter piles when point C is recorded, the total displacement from axial alignment at the depth is two diameters for 12 o'clock piles. For 3 o'clock and 9 o'clock piles, the total displacement at point C is 1.5 diameters. For 6 o'clock piles, the total displacement approaches zero at point C.

Sketches that show these measurements are included in Figures 3-5. All of the above points should be plotted for general understanding in accordance with Figure 6. Distances such as BC, CD, and BD can be plotted as in Figures 7 and 8 for displacement (sweep) predictions.

JOB SITE PROCEDURE

After the pile is driven and the dust has settled enough inside the pipe, the inspector who just recorded the driving looks down the pile. If he or she cannot see the bottom either with a mirror reflecting the sun or with a flashlight, the pile is marked for further inspection. Either later or at that moment the INTOK inspector is summoned, he or she measures the pile by recording the data (as outlined on the INTOK sheet) to be checked against the curves for an immediate determination of acceptability. If the pile is rejected, a replacement can be installed without sequence interruption.

INTOK CHECK

The INTOK check is completed in the following manner:

1. Check slope of pile below hammer-distorted area (±2 ft) to 5 ft below the top of the pile. In addition, repeat procedure at the 30-ft mark for plumb piles. If sweep is apparent at 30 ft, raise plumb bob to the 25-ft mark, 20-ft mark, etc., as required and record reading. All readings will be taken by using a lowered light or a sun-and-mirror combination. Record direction of bottom of sloped portion. The slope at 5 ft (30 ft) is point A.
2. Lower the inverted light (attached to a tape) down the pile. Record distance from the top of the pile to a point beyond which circumferential light is no longer visible. Record direction toward which light is no longer visible (plan batter direction is 12 o'clock). The start of lost light is point B.
3. Continue lowering light to a point where the light can no longer be seen from any point on the circumference of the top of the pile. Record this

Figure 3. Sweep of plumb pile.

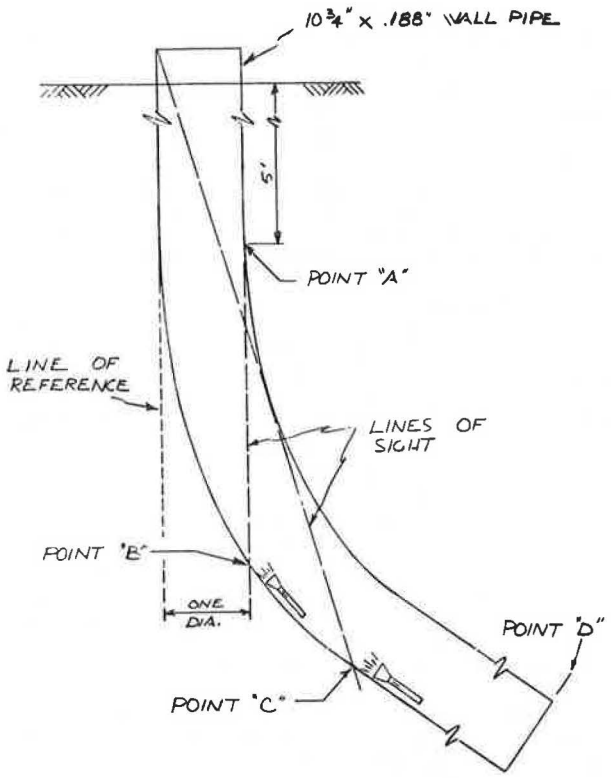

Figure 4. Sweep of 12 o'clock batter pile.

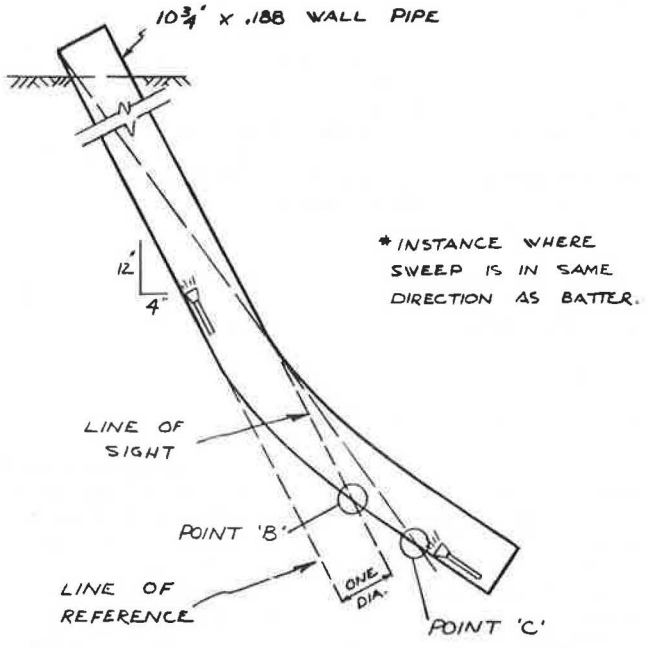

depth. Confirm continuity of direction. Completion of lost light is point C.

4. Continue lowering the light to the bottom of the pile and record sounded depth of pile. Sounded depth of pile will be shorter than driven length of pile by bottom plate thickness and by flashlight length. This is point D.

The above procedures can be performed in any order.

Figure 5. Sweep of 6 o'clock batter pile.

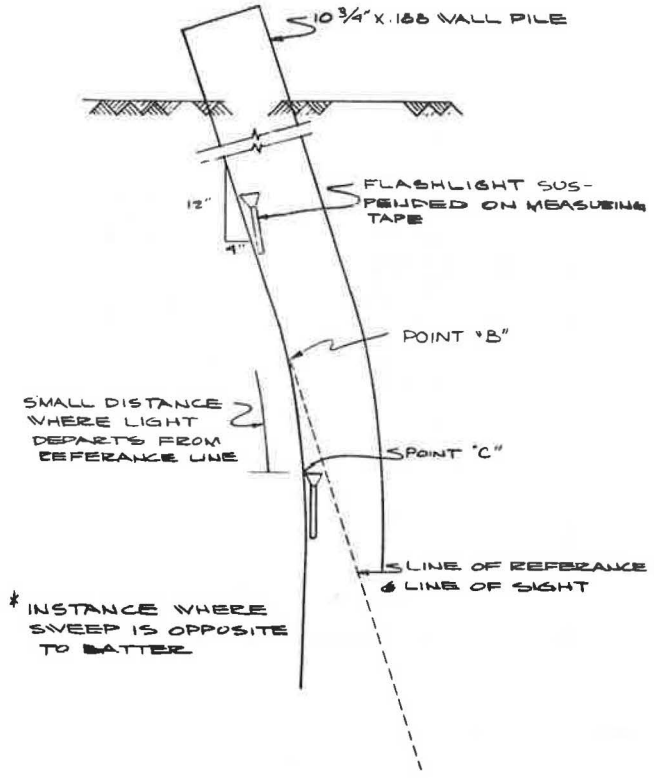

CONCLUSIONS

Although this is not a precise method of determining sweep in a driven pile (or caisson for that matter), it is nonetheless a good field approach toward telling the inspector if the sweep is large or small. For example, if a BC distance is very large and its corresponding CD distance is small, pile sweep is gradual and most probably not troublesome, regardless of total displacement. If the BC distance is very small and CD large, most probably this is a troublesome pile and almost an on-the-spot rejection. These are extremes, and if they are known immediately, production may not have to be interrupted.

When the in-between cases are encountered, the curves must be relied on. In addition, other tools are available, such as a wooden ball that has a diameter 0.5 in less than that of the pipe lowered throughout its length, thus assuring no collapse; a length of inflexible tubing precalculated in its length through which an unacceptable dogleg will prohibit passage; or the use of a pile scan device that actually measures the specific cross-sectional area at the constricted depth (this pile scan is from William F. Loftus Associates).

Another aid that requires interpretation and expertise by the inspector is the length of the reflected light beam of the flashlight itself. Consider a small BC and a large CD distance that normally may result in a rejection. What might alter the inspectors decision if he or she could see the reflection of the flashlight on the wall of the pipe throughout the entire CD distance? He or she may accept the pile after all, and properly so. Indiscriminate rejection is never the job of the good and knowledgeable inspector.

Some parameters that were used for pile acceptance at the Cleveland site are as follows:

1. If point C occurs within a distance of 15 ft

Figure 6. Sample plot of INTOK data with typical accuracy.

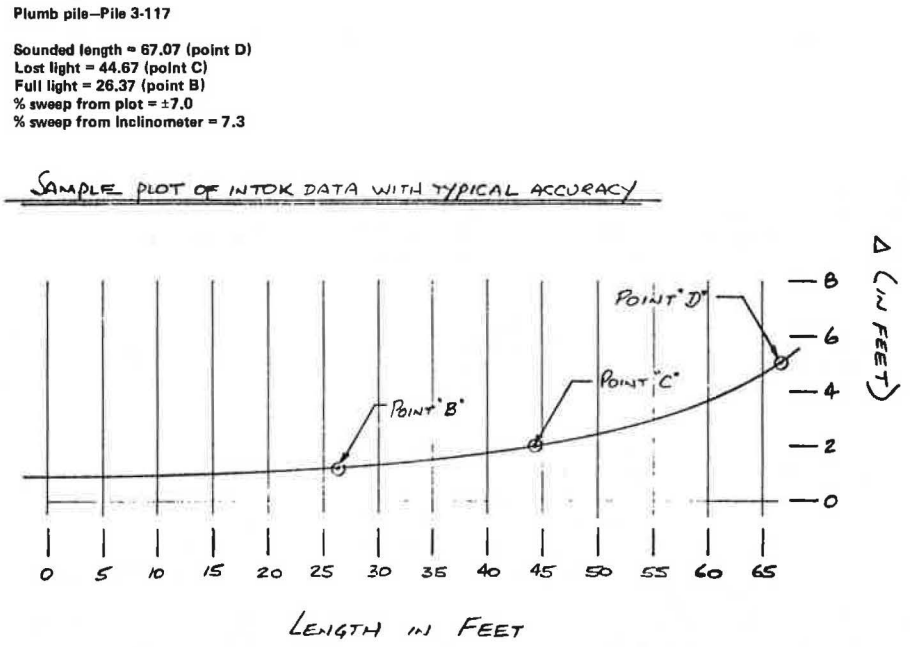

Figure 7. Typical sweep comparison between tangential and circular analyses.

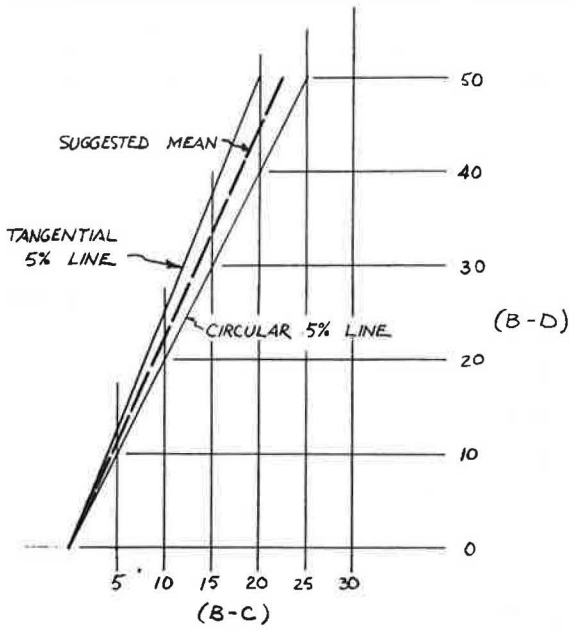

Figure 8. Summary of suggested means for all percent sweeps (tangential and circular analyses).

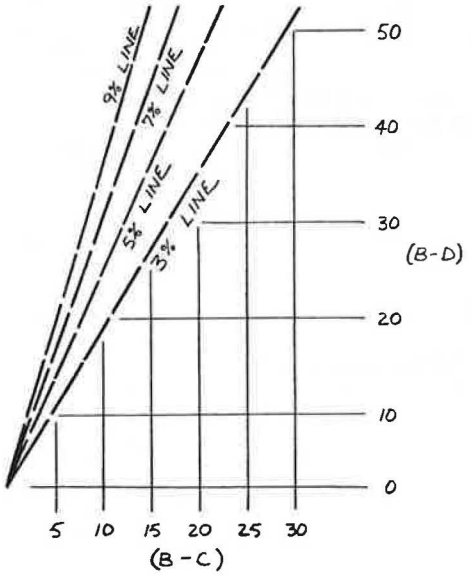

from the bottom of the pile and point B occurs within a distance of 45 ft from the top of the pile, the pile is acceptable with regard to sweep, provided that no shorter radius of curvature occurs in the unseen portion of the pile and that the top 5 ft of the pile is within a 2 percent tolerance of the out-of-plumbness criterion.

2. If the minimum distance between points B and C (as described in 1) occurs below 45 ft and the plumbness is within the 2 percent tolerance, this pile is acceptable.

3. All piles not covered by the above parameters will be plotted and analyzed further.

The all-important benefit of the INTOK method is that one person can inspect 30 to 40 piles in the same 8-h shift that two persons can inspect in 6-8 h with the use of the inclinometer. Once the data are taken, those values are simply plotted on the graphs (such as Figure 6) and the percentage of sweep is known. Production driving may then proceed with minimal delay.

Notice: The Transportation Research Board does not endorse products or manufacturers. Trade and manufacturers' names appear in this paper because they are considered essential to its object.

Uplift Capacity of Rectangular Foundations in Sand

BRAJA M. DAS AND ANDREW D. JONES

Laboratory model test results for the net ultimate uplift capacity of rectangular foundations in sand are presented. The length-to-width ratios of the rectangular foundations were varied from 1 to 5. Tests were conducted in loose, medium, and dense sands. For square foundations, the critical embedment ratio increases with the degree of compaction of sand and is approximately the same as that proposed by Meyerhof and Adams. For a given degree of sand compaction, the critical embedment ratio increases with the length-to-width ratio of the foundation. A procedure for the estimation of the uplift factor, and thus the net ultimate pullout load for deep foundations, is presented.

During the past 15-20 years, a number of studies, both experimental and theoretical, have been carried out for the determination of the ultimate uplift capacity of anchors and foundations in cohesionless soils [e.g., Baker and Kondner (1), Balla (2), Esquivel-Diaz (3), Meyerhof and Adams (4), Sutherland (5), and Vesić (6)]. An excellent review of these works is given by Vesić (6). Most of the experimental studies mentioned above, either the small-scale laboratory model tests or the large-scale field tests, have been made on horizontal circular anchors and foundations that have the vertical uplifting force being applied through a rigid shaft attached at the center. The purpose of this paper is to present some laboratory model test results for the ultimate uplift capacity of horizontal foundations (Figure 1) that have the uplifting force being applied centrally through a rigid shaft. Some of the preliminary results of this study were presented by Das and Seeley (7). To the best of our knowledge, no other detailed experimental study on this subject is currently available in the literature. Results of a similar study in saturated medium and stiff clays have been presented by Das (8,9).

THEORETICAL EXPRESSION FOR ULTIMATE UPLIFT CAPACITY

A review of existing literature shows that a number of theoretical expressions for the ultimate foundation uplift capacity of axially symmetric cases (circular) have been proposed by investigators like Balla (2), Vesić (6), and Mariupol'skii (10). However, the only analytical expression currently available for the determination of the ultimate uplift capacity of rectangular foundations is given by Meyerhof and Adams (4). For foundations at shallow depths, their relation can be expressed as follows:

$$Q_u = \gamma D^2(2SB + L - B)K_u \tan\phi + W + W_a \quad (1)$$

where

Q_u = gross ultimate uplift capacity,
γ = unit weight of soil,
D = depth of embedment,
S = shape factor,
B = width of foundation,
L = length of foundation,
K_u = uplift coefficient,
ϕ = soil friction angle,
W = effective weight of soil immediately above the foundation, and
W_a = effective weight of the foundation.

As proposed by Meyerhof and Adams, the theoretical values of the uplift coefficient (K_u) for various friction angles of sand are shown in Figure 2 (4). For shallow foundations, the shape factor (S) increases linearly (4) with the embedment ratio (D/B), i.e.,

$$S = 1 + m(D/B) \quad (2)$$

where m is the shape-factor coefficient.

The variation of m with ϕ is shown in Figure 3 (4). It needs to be pointed out that the values of m suggested by Meyerhof and Adams were ϕ = 20°, 25°, 30°, 35°, 40°, and 45°. In order to interpolate the values for intermediate friction angles, we have joined the points by a line.

Although Equation 1 was proposed about 12 years ago, adequate experimental work has not been undertaken to verify it. It appears that the above relation (Equation 1) may be expressed in a more convenient form, i.e., in terms of a nondimensional uplift factor (N_q). This can be done in the following manner.

For an uplift capacity test, the net ultimate uplift load may be given by the expression:

$$Q_o = Q_u - W_a \quad (3)$$

where Q_o is the net ultimate uplift load. Also, the expression for W in Equation 1 is of the form:

$$W = D\,B\,L\,\gamma \quad (4)$$

The uplift factor may be defined as

$$N_q = Q_o/(\gamma\,A\,D) \quad (5)$$

where A is the area of the foundation = B x L.

A combination of Equations 1-5 and some rearrangement yields the following:

$$N_q = (D/B)K_u \tan\phi \left\{[1 + 2m(D/B)]\,(B/L) + 1\right\} + 1 \quad (6)$$

In general, for a given foundation, N_q increases with the embedment ratio D/B (general shear failure in soil) up to a certain maximum value, and after that it remains constant (local shear failure in soil). The embedment ratio at which the uplift factor (N_q) reaches a maximum value is referred to

Figure 1. Parameter for ultimate uplift capacity of rectangular foundations.

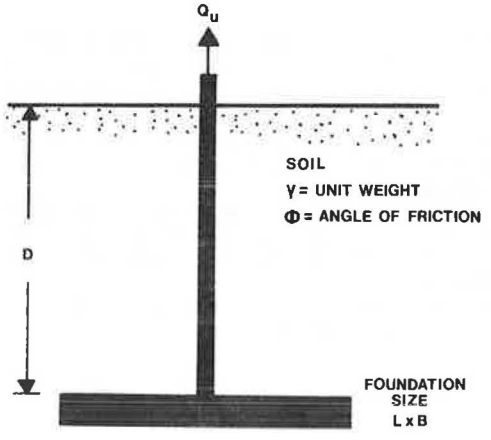

Figure 2. Theoretical value of uplift coefficient.

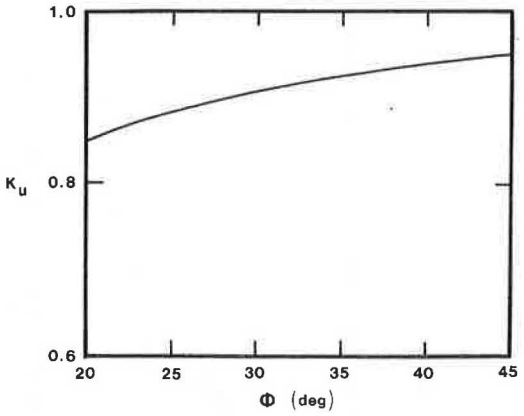

Figure 3. Variation of shape-factor coefficient with angle of friction of soil.

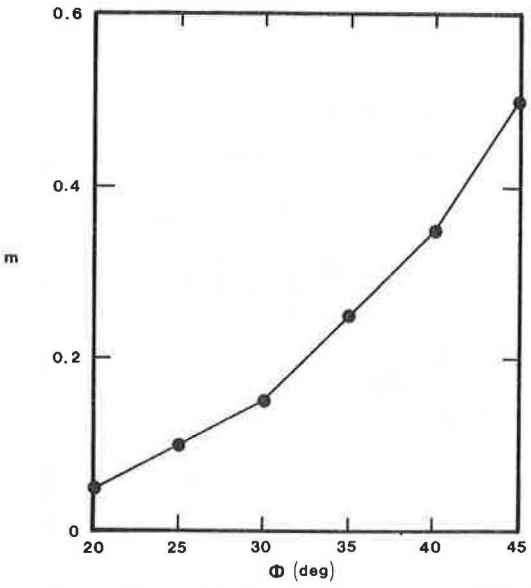

Figure 4. Variation of critical embedment ratio for circular or square foundations.

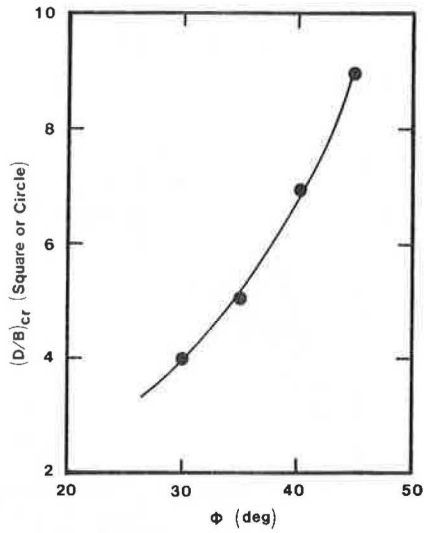

here as the critical embedment ratio $(D/B)_{cr}$. Foundations with $D/B \leq (D/B)_{cr}$ are referred to as shallow foundations, and those with $D/B > (D/B)_{cr}$ are called deep foundations.

Figure 4 shows the values of critical embedment ratios for circular foundations as recommended by Meyerhof and Adams. They were obtained after observation of several model tests. It may be assumed that similar values will be applicable for square foundations.

LABORATORY MODEL TESTS

Laboratory model tests for the uplift capacity of horizontal foundations were conducted in a box that measured 0.6x0.6x0.6 m. A silica sand was used for these tests. The grain-size distribution of the sand is shown in Figure 5.

Four model aluminum plates, which measured 50.8x50.8 mm, 50.8x101.6 mm, 50.8x152.4 mm, and 50.8x254 mm, were used for the tests. This gave length-to-width ratios (L/B) of 1, 2, 3, and 5, respectively. All of the aluminum plates were 3.18 mm thick.

For conducting the model tests, sand was compacted in layers of 25.4 mm thickness in the box for the desired height. Uplifting force to the plates was applied through a 6.35-mm-diameter steel rod attached rigidly at the center of each plate. The rod was connected to a lever arm that was fixed to the side of the test box. Step loads were applied at the other end of the lever arm. The lever-arm ratio was 1:10.

Three series of tests were conducted by changing the density of compaction of sand. The average unit weight of compaction for each series and the corresponding angle of friction, as determined from standard triaxial tests, are given in the table below:

Series	Nature of Compaction	Relative Density (%)	Unit Weight (kN/m^3)	Friction Angle (°)
1	Loose	21.7	14.81	31
2	Medium	47.6	15.79	34
3	Dense	72.9	16.88	40.5

For a given series, the ultimate uplift load for each plate was obtained for embedment ratios that varied from 1 to 10.

LABORATORY MODEL TEST RESULTS AND INTERPRETATION

The laboratory experimental results for the net ultimate uplift loads (Q_o) for the three series of tests are given in Figures 6, 7, and 8. By using these experimental values of net ultimate load and Equation 5, the experimental values of the uplift factor for all tests at various embedment ratios have been calculated and are shown by solid lines in Figures 9, 10, and 11. Note that the broken lines shown in these figures are calculated theoretical variations of the uplift factors based on Equation 6 and will be discussed later in this paper. As expected, for a given plate in a given series, the value of N_q increased with embedment ratio up to a certain maximum value and remained constant thereafter, thereby showing deep foundation behavior. From the best-fit experimental curves, the critical embedment ratios have been determined and are also shown in Figures 9, 10, and 11. Based on this, it may be seen that the critical embedment ratio for the square plates increased from about 4.8 in loose sand (series 1) to about 6.5 in the case of dense sand (series 3). With some variation that has to be expected, these are in good agreement with the sug-

Figure 5. Grain-size distribution of sand used in model tests.

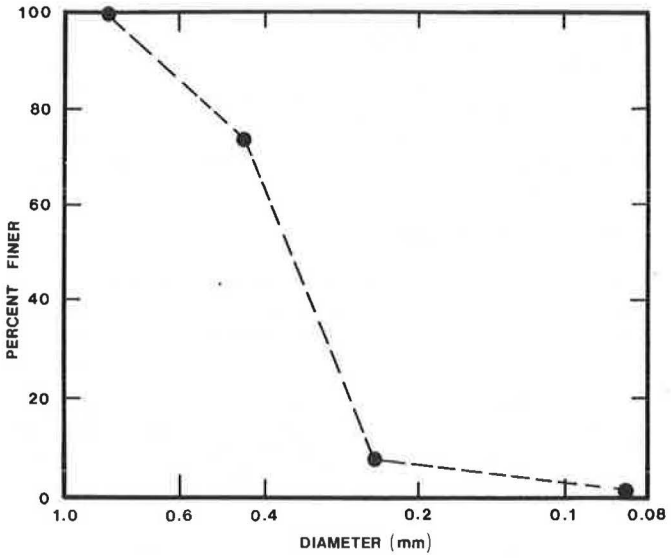

Figure 6. Plot of net ultimate uplift load versus embedment ratio (series 1).

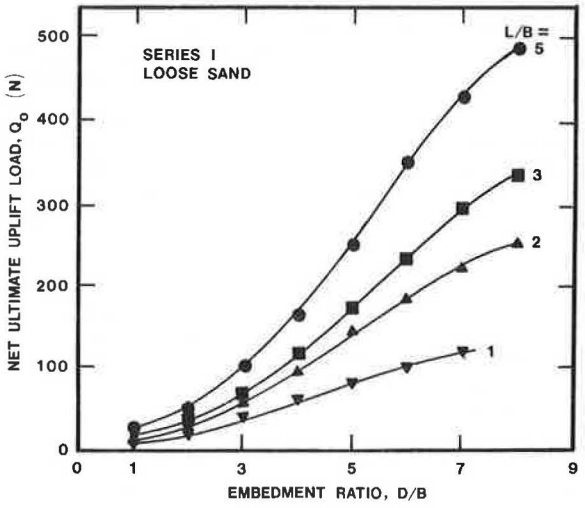

Figure 7. Plot of net ultimate uplift load versus embedment ratio (series 2).

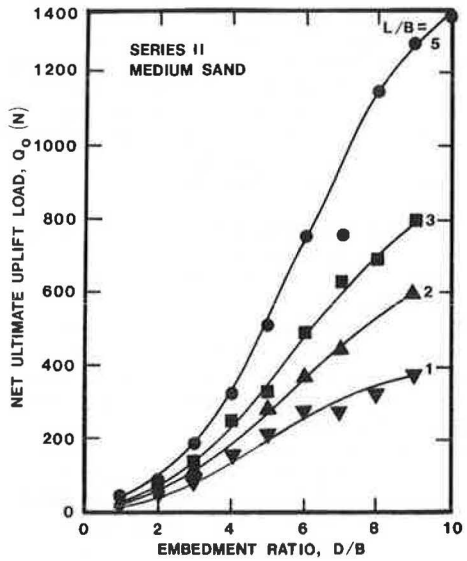

Figure 8. Plot of net ultimate uplift load versus embedment ratio (series 3).

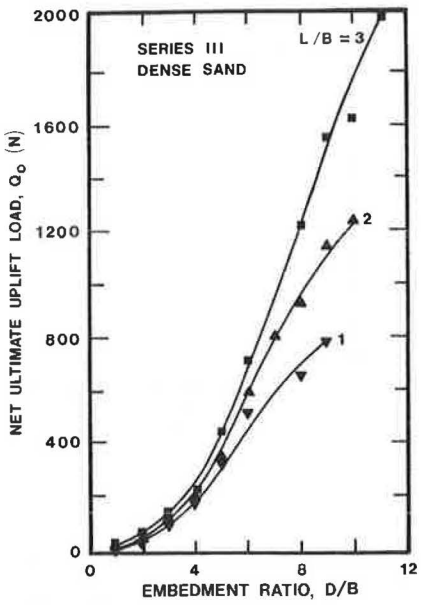

Figure 9. Plot of N_q versus embedment ratio (series 1).

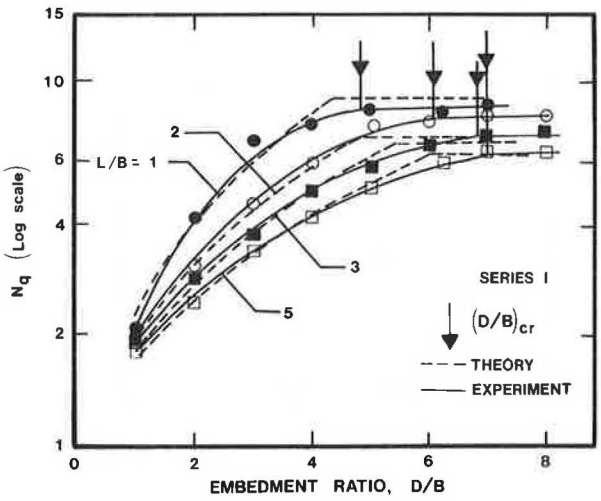

Figure 10. Plot of N_q versus embedment ratio (series 2).

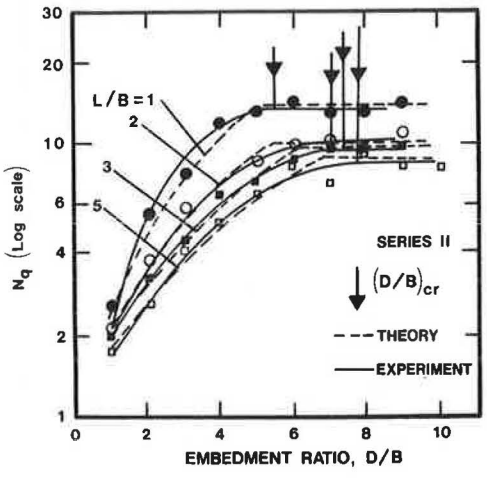

Figure 11. Plot of N_q versus embedment ratio (series 3).

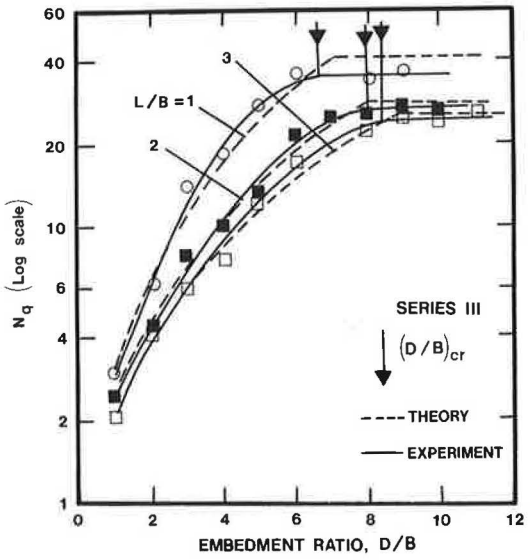

Figure 12. Variation of critical embedment ratio with plate size.

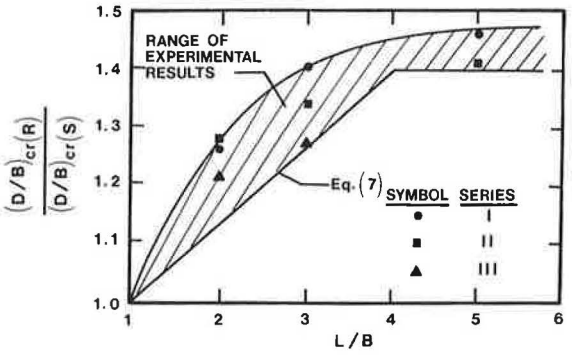

gested values that are shown in Figure 4. However, one important factor that needs to be pointed out is that, for a given series of tests, the critical embedment ratio generally increased with the length-to-width ratio of the plate. Figure 12 shows the variation of the ratio of the critical embedment ratio of rectangular plates $[(D/B)_{cr(R)}]$ to that for square plates $[(D/B)_{cr(S)}]$. Although this shows the general trend, the limited number of experimental data points and their wide scattering make it difficult to draw a definite conclusion. However, a conservative estimate may be given by the following equation:

$$(D/B)_{cr(R)} = (D/B)_{cr(S)}[0.133(L/B) + 0.867] \leq 1.4\,(D/B)_{cr(S)} \quad (7)$$

In order to compare the experimental uplift factors with theory, the following procedure has been adopted:

1. By using the soil friction angle (ϕ), the critical embedment ratio for square foundations $[(D/B)_{cr(S)}]$ was determined from Figure 4.
2. By using the value for $(D/B)_{cr(S)}$ determined in step 1 and Equation 7, the critical embedment ratio of rectangular foundations was determined.
3. For $D/B \leq (D/B)_{cr(R)}$ (as determined in step 2), the uplift factor (N_q) at various embedment ratios was calculated from Equation 6 as follows:

$$N_q = (D/B)\,K_u \tan\phi \left\{[1 + 2m(D/B)_R](B/L) + 1\right\} + 1 \quad (8)$$

4. For $D/B \geq (D/B)_{cr(R)}$ (as determined in step 2), N_q was calculated as follows:

$$N_q = (D/B)_{cr(R)}\,K_u \tan\phi \left\{[1 + 2m(D/B)_{cr(R)}](B/L) + 1\right\} + 1 \quad (9)$$

The uplift factors, as determined from steps 3 and 4, have been plotted in Figures 9, 10, and 11. The comparison shows a generally good agreement between experiment and theory for shallow foundation conditions $[D/B < (D/B)_{cr}]$. For deep foundation conditions, the theoretical uplift factor sometimes overestimates the experimental values up to a maximum of about 10 percent. However, for a preliminary estimation of the ultimate capacity, this appears to be generally satisfactory.

CONCLUSIONS

Based on the model test results for the ultimate uplift capacity of foundations reported herein, the following conclusions can be drawn:

1. The critical embedment ratio of foundations increases with the degree of compaction of sand. The general range of the values of $(D/B)_{cr(S)}$ observed in this test program is generally consistent with that recommended by Meyerhof and Adams (4).
2. The degree of compaction of soil remaining constant, for horizontal foundations the critical embedment ratio increases with the increase of the length-to-width ratio of the plate. A conservative equation for $(D/B)_{cr(R)}$ has been proposed (Equation 7).
3. The uplift factor for shallow foundations derived from the basic equation of Meyerhof and Adams (4) compares reasonably well with the experimental results.
4. A procedure for obtaining the uplift factor and thus the net ultimate load for deep rectangular foundations has been proposed.

REFERENCES

1. W.H. Baker and R.L. Kondner. Pullout Load Capacity of a Circular Earth Anchor Buried in Sand. HRB, Highway Research Record 108, 1966, pp. 1-10.
2. A. Balla. The Resistance to Breaking-Out of Mushroom Foundations for Pylons. Proc., 5th International Conference on Soil Mechanics and Foundation Engineering, Vol. 1, 1961, pp. 569-576.
3. R.F. Esquivel-Diaz. Pullout Resistance of Deeply Buried Anchors in Sand. Duke Univ., Durham, NC, MS thesis, 1967.
4. G.G. Meyerhof and J.I. Adams. The Ultimate Uplift Capacity of Foundations. Canadian Geotechnical Journal, Vol. 5, No. 4, Nov. 1968, pp. 225-244.
5. H.B. Sutherland. Model Studies for Shaft Raising Through Cohesionless Soils. Proc., 6th International Conference on Soil Mechanics and Foundation Engineering, Vol. 11, 1965, pp. 410-513.
6. A.S. Vesić. Breakout Resistance of Objects Embedded in Ocean Bottom. Journal of the Soil Mechanics and Foundations Division, ASCE, Vol. 97, No. SM9, 1971, pp. 1183-1205.
7. B.M. Das and G.R. Seeley. Breakout Resistance of Shallow Horizontal Anchors. Journal of the Geotechnical Engineering Division, ASCE, Vol. 101, No. GT9, Sept. 1975, pp. 999-1003.
8. B.M. Das. Model Tests for Uplift Capacity of Foundations in Clay. Soils and Foundations:

The Japanese Society of Soil Mechanics and Foundation Engineering, Vol. 18, No. 2, June 1978, pp. 17-24.

9. B.M. Das. A Procedure for Estimation of Ultimate Uplift Capacity of Foundations in Clay. In Soils and Foundations, The Japanese Society of Soil Mechanics and Foundation Engineering, Vol. 20, No. 1, March 1980, pp. 77-82.
10. L.G. Mariupol'skii. The Bearing Capacity of Anchor Foundations. Soil Mechanics and Foundation Engineering, Vol. 3, No. 1, Jan.-Feb. 1965, pp. 14-18.